Local Black Hole Demographics

Jenny Greene (Princeton)

Table 1 Star formation in disks and nuclei of galaxies

Property	Spiral disks	Circumnuclear regions
Radius	1–30 kpc	0.2–2 kpc
Star formation rate (SFR)	0–20 $M_\odot$ year^{-1}	0–1000 $M_\odot$ year^{-1}
Bolometric luminosity	10^6–10^{11} $L_\odot$	10^6–10^{13} $L_\odot$
Gas mass	10^8–10^{11} $M_\odot$	10^6–10^{11} $M_\odot$
Star formation time scale	1–50 Gyr	0.1–1 Gyr
Gas density	1–100 $M_\odot$ pc^{-2}	10^2–10^5 $M_\odot$ pc^{-2}
Optical depth (0.5 μm)	0–2	1–1000
SFR density	0–0.1 $M_\odot$ year^{-1} kpc^{-2}	1–1000 $M_\odot$ year^{-1} kpc^{-2}
Dominant mode	steady state	steady state + burst
Type dependence?	strong	weak/none
Bar dependence?	weak/none	strong
Spiral structure dependence?	weak/none	weak/none
Interactions dependence?	moderate	strong
Cluster dependence?	moderate/weak	?
Redshift dependence?	strong	?

Kennicutt 1998

Calzetti et al. 2005

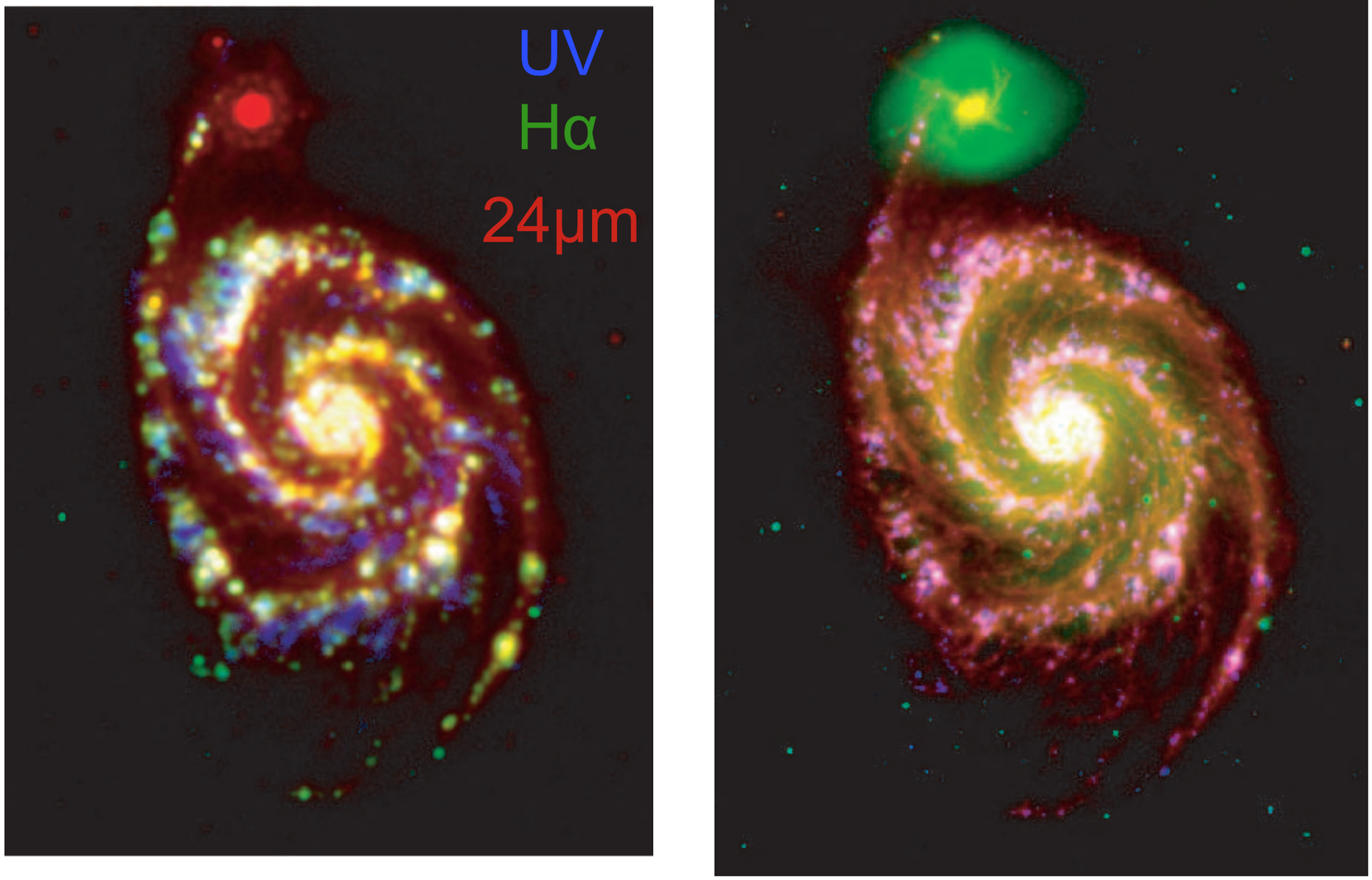

FIG. 1.—Two three-color composites of M51. *Left*: FUV (*blue*), continuum-subtracted Hα (*green*), and 24 μm dust (*red*) emission of the galaxy pair. The FUV and FIR images, from *GALEX* and *Spitzer*, respectively, have closely matched resolution ($\approx 6''$), while the resolution of the ground-based Hα image has been degraded to match that of the two space-borne images. *Right*: Continuum-subtracted Hα (*blue*), 3.6 μm stellar continuum (*green*), and 8 μm dust (*red*) emission of the galaxy pair. This second image exploits the higher angular resolution of the IRAC images (about $2''$ FWHM) to provide higher level of detail. The stellar continuum emission traces evolved (old) stellar populations. In this figure, a foreground star appears pure green. North is up, and east is to the left. The size of the pictures is $\sim 8.'6 \times 11.'8$.

Star formation rate indicator 1: direct UV emission from young stars. Note that we are tracing the YOUNG stars, so an IMF (initial mass function) is needed to calculate TOTAL star formation rate. Very dust sensitive.

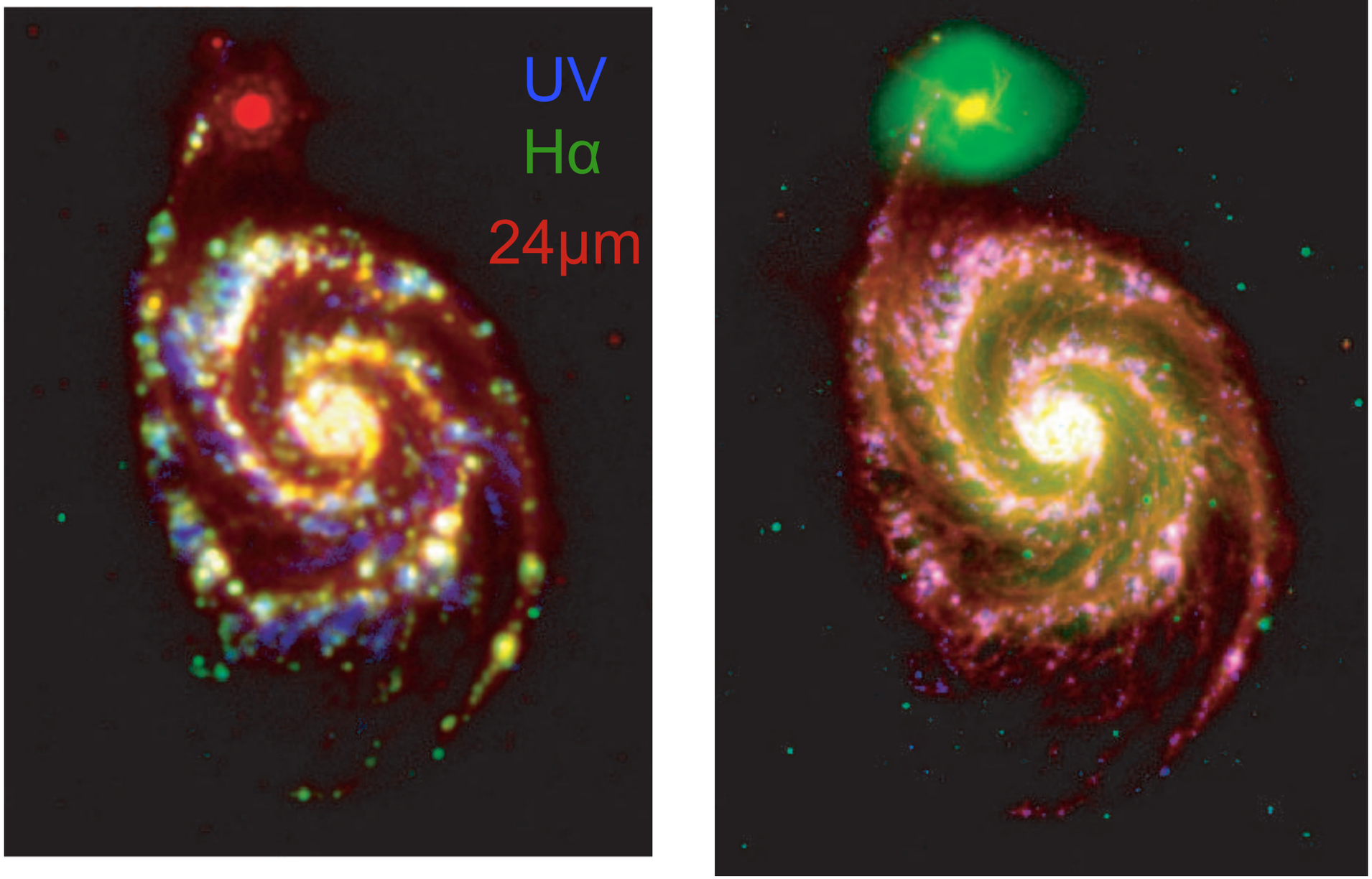

FIG. 1.—Two three-color composites of M51. *Left*: FUV (*blue*), continuum-subtracted Hα (*green*), and 24 μm dust (*red*) emission of the galaxy pair. The FUV and FIR images, from *GALEX* and *Spitzer*, respectively, have closely matched resolution ($\approx 6''$), while the resolution of the ground-based Hα image has been degraded to match that of the two space-borne images. *Right*: Continuum-subtracted Hα (*blue*), 3.6 μm stellar continuum (*green*), and 8 μm dust (*red*) emission of the galaxy pair. This second image exploits the higher angular resolution of the IRAC images (about $2''$ FWHM) to provide higher level of detail. The stellar continuum emission traces evolved (old) stellar populations. In this figure, a foreground star appears pure green. North is up, and east is to the left. The size of the pictures is $\sim 8.'6 \times 11.'8$.

Star formation rate indicator 2: Hα emission. UV light photo-ionizes bubbles (HII regions). (Relatively) Insensitive to dust, so a robust indicator of SFR. Also good because directly counts photo-ionizing photons with very few assumptions.

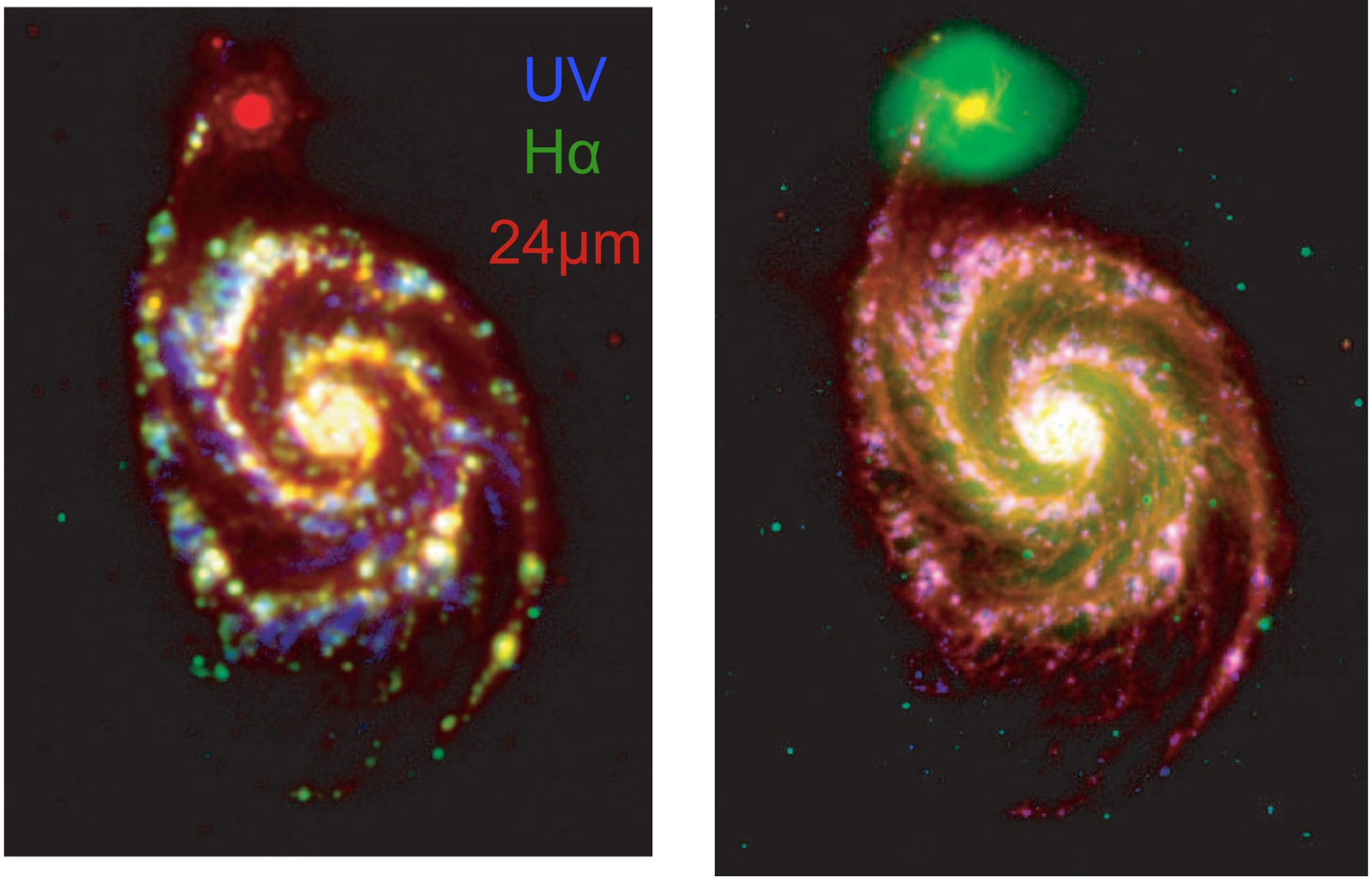

FIG. 1.—Two three-color composites of M51. *Left*: FUV (*blue*), continuum-subtracted Hα (*green*), and 24 μm dust (*red*) emission of the galaxy pair. The FUV and FIR images, from *GALEX* and *Spitzer*, respectively, have closely matched resolution ($\approx 6''$), while the resolution of the ground-based Hα image has been degraded to match that of the two space-borne images. *Right*: Continuum-subtracted Hα (*blue*), 3.6 μm stellar continuum (*green*), and 8 μm dust (*red*) emission of the galaxy pair. This second image exploits the higher angular resolution of the IRAC images (about $2''$ FWHM) to provide higher level of detail. The stellar continuum emission traces evolved (old) stellar populations. In this figure, a foreground star appears pure green. North is up, and east is to the left. The size of the pictures is $\sim 8.'6 \times 11.'8$.

Star formation rate indicator 3: Reprocessed dust emission (24 μm or redder).

Problem is: need a satellite, and resolution is not great. But with *Spitzer, Herschel, ALMA* this is a powerful alternative.

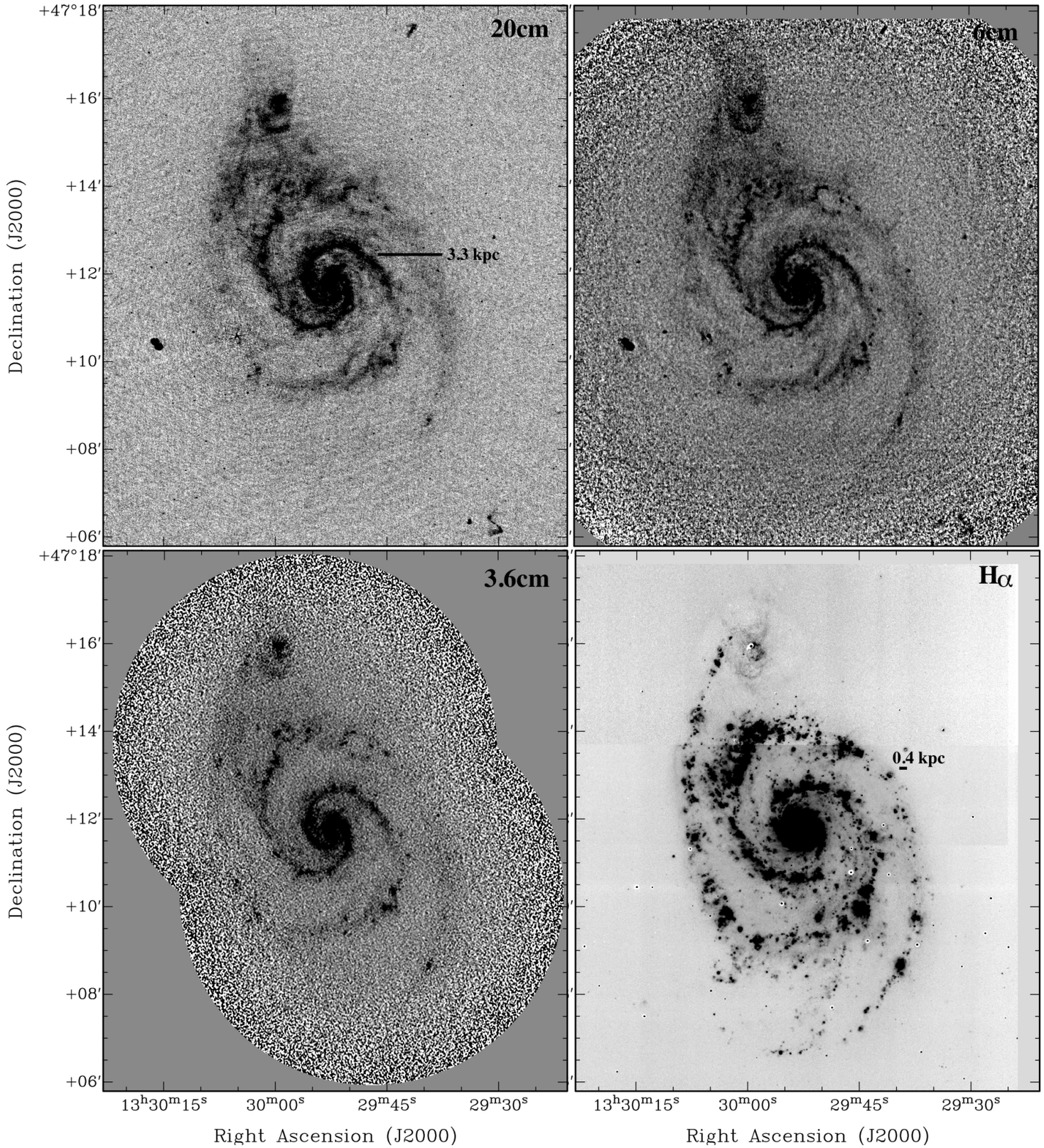

Radio continuum correlates with SFR through thermal brehmsstrahlung (free-free) radiation and CR acceleration in SNe leading to synchrotron radiation.

From Dumas et al. 2011.

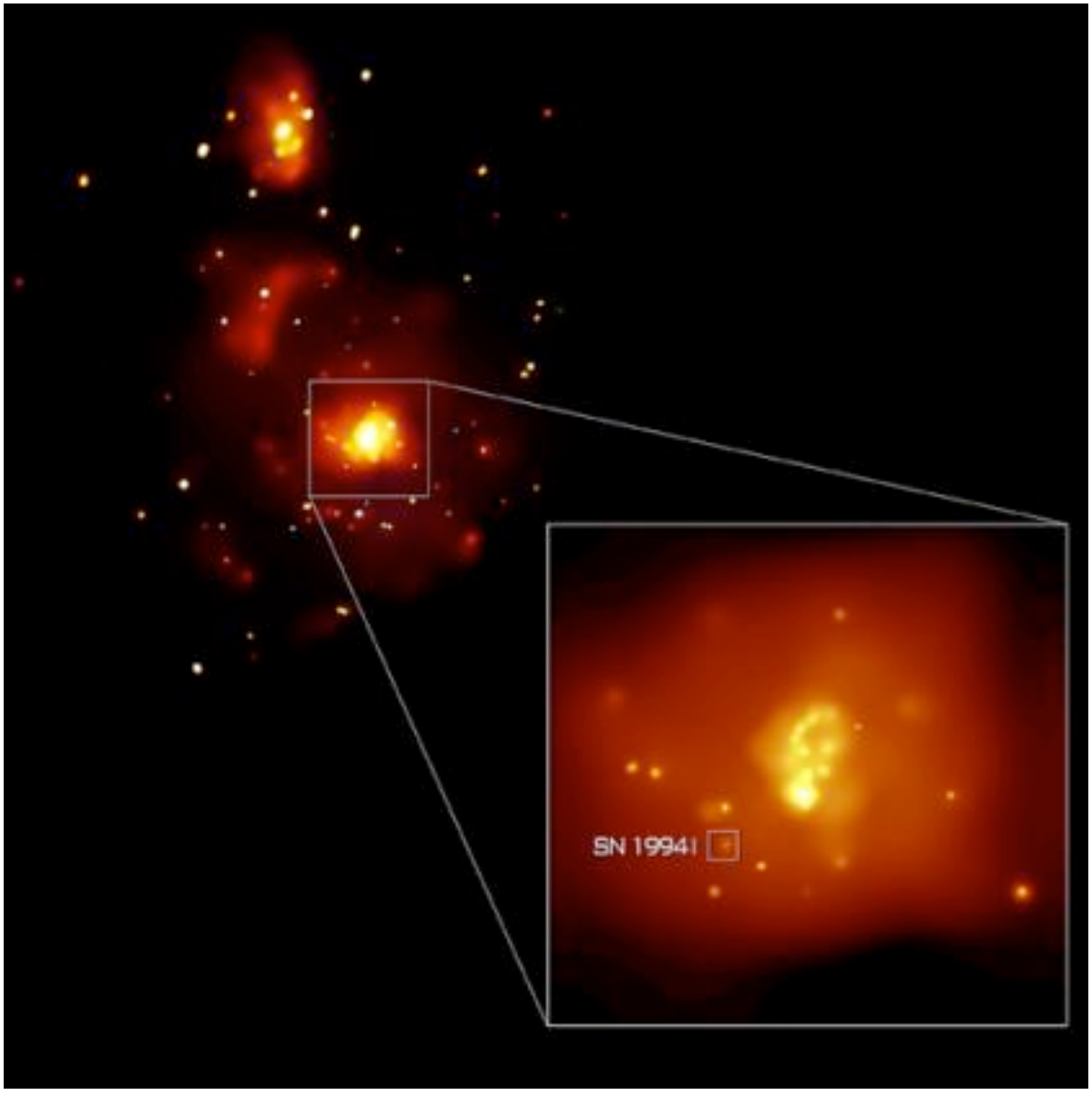

X-rays also correlate with SF. X-rays in starburst galaxies dominated by SN remnants and high-mass X-ray binaries.

Star Formation Rate Tracers

1 Ultraviolet continuum emission from hot stars

2 Balmer and other recombination emission lines

3 Infrared thermal emission (reradiated starlight)

4 Radio continuum emission (free-free and non-thermal)

5 CO emission from molecular clouds

6 Integrated constraints from total optical luminosity.

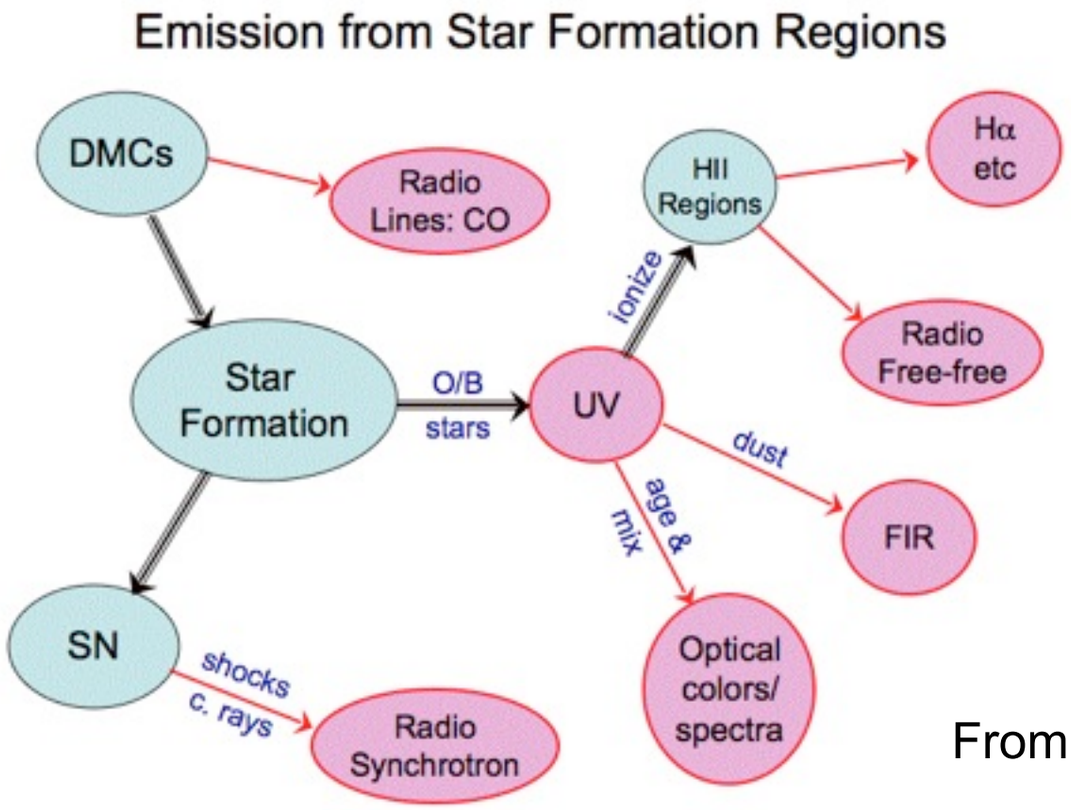

From Whittle lectures

THE ASTROPHYSICAL JOURNAL

AN INTERNATIONAL REVIEW OF SPECTROSCOPY AND ASTRONOMICAL PHYSICS

VOLUME 129 MARCH 1959 NUMBER 2

THE RATE OF STAR FORMATION

MAARTEN SCHMIDT*

Mount Wilson and Palomar Observatories

Carnegie Institution of Washington, California Institute of Technology

Received October 29, 1958

$\Sigma_{SFR} \alpha \Sigma_{gas}^{N}$

ABSTRACT

It is assumed that the rate of star formation for population I varies with a power n of the density of interstellar gas and that the initial luminosity function is time-independent. Direct evidence on the value of n is found in the relative distribution, perpendicular to the galactic plane, of gas and young objects. For various values of n, computations were made of the initial luminosity function, the rate of star formation, the exchange of gas between stars and interstellar medium, the number of white dwarfs and their luminosity function, and the abundance of helium. It is concluded, from a comparison of the results with observational data, that n is around 2. The present rate of star formation, then, is five times slower than the average rate. The interstellar gas, of which the surface density on the galactic plane was taken to be 11 $\mathfrak{M}\odot$ per square parsec, loses 1.4 $\mathfrak{M}\odot/pc^2$ per 10^9 years by the formation of stars but gains about one-third of this by ejection of gas from evolving stars. The present helium abundance of the interstellar gas may be explained if a star has burned, on the average, 53 per cent of its original hydrogen into helium at the time that ejection takes place. The ejected material was assumed to have a composition equal to the average composition of the star. The effect of star formation on the gas density in the galactic system and other galaxies is briefly discussed.

Connection between Gas and Star Formation

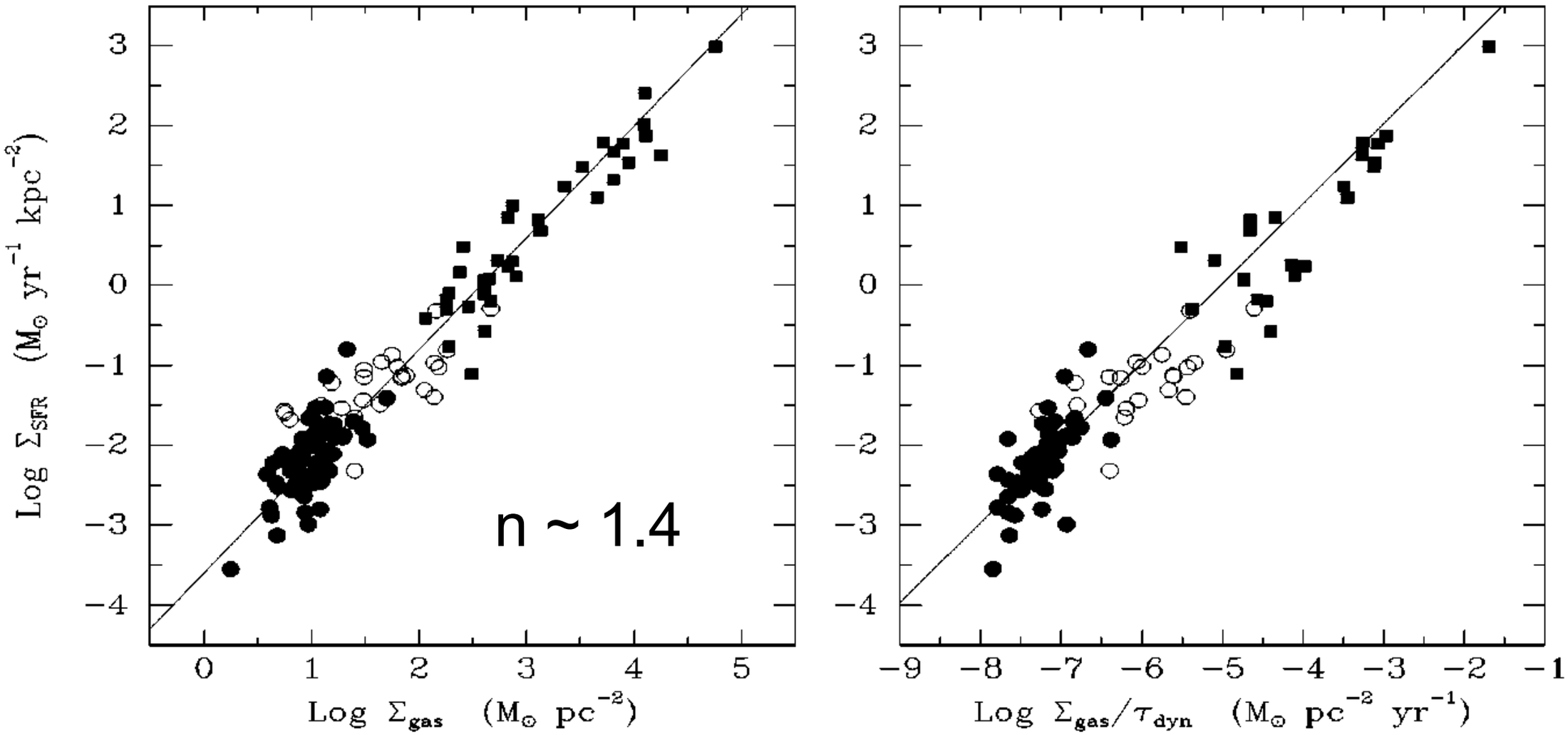

Figure 9 (*Left*) The global Schmidt law in galaxies. *Solid points* denote the normal spirals in Figure 5, *squares* denote the circumnuclear starbursts in Figure 7. The *open circles* show the SFRs and gas densities of the central regions of the normal disks. (*Right*) The same SFR data but plotted against the ratio of the gas density to the average orbital time in the disk. Both plots are adapted from Kennicutt (1998).

Kennicutt 1998
Looks at surface density of molecular+atomic gas. Derives a 'Schmidt (1959)' power-law relation between Σ_{SFR} and Σ_{gas}

Spatially Resolved

THE ASTROPHYSICAL JOURNAL, 704:842–862, 2009 October 10

THE SPATIALLY RESOLVED STAR FORMATION LAW FROM INTEGRAL FIELD SPECTROSCOPY: VIRUS-P OBSERVATIONS OF NGC 5194

GUILLERMO A. BLANC, AMANDA HEIDERMAN, KARL GEBHARDT, NEAL J. EVANS II, AND JOSHUA ADAMS
Astronomy Department, University of Texas at Austin, Austin, TX 78712, USA
Received 2009 June 4; accepted 2009 August 31; published 2009 September 25

ABSTRACT

We investigate the relation between the star formation rate (SFR) surface density (Σ_{SFR}) and the mass surface density of gas (Σ_{gas}) in NGC 5194 (a.k.a. M51a, Whirlpool Galaxy). Visible Integral field Replicable Unit Spectrograph Prototype (VIRUS-P) integral field spectroscopy of the central 4.1 $\times$ 4.1 kpc^2 of the galaxy is used to measure Hα, Hβ, [O III]λ5007, [N II]$\lambda\lambda$6548,6584, and [S II]$\lambda\lambda$6717,6731 emission line fluxes for 735 regions $\sim$170 pc in diameter. We use the Balmer decrement to calculate nebular dust extinctions, and correct the observed fluxes in order to accurately measure Σ_{SFR} in each region. Archival H I 21 cm and CO maps with spatial resolution similar to that of VIRUS-P are used to measure the atomic and molecular gas surface density for each region. We present a new method for fitting the star formation law (SFL), which includes the intrinsic scatter in the relation as a free parameter, allows the inclusion of non-detections in both Σ_{gas} and Σ_{SFR}, and is free of the systematics involved in performing linear regressions over incomplete data in logarithmic space. After rejecting regions whose nebular spectrum is affected by the central active galactic nucleus in NGC 5194, we use the [S II]/Hα ratio to separate spectroscopically the contribution from the diffuse ionized gas (DIG) in the galaxy, which has a different temperature and ionization state from those of H II regions in the disk. The DIG only accounts for 11% of the total Hα luminosity integrated over the whole central region, but on local scales it can account for up to a 100% of the Hα emission, especially in the inter-arm regions. After removing the DIG contribution from the Hα fluxes, we measure a slope $N = 0.82 \pm 0.05$, and an intrinsic scatter $\epsilon = 0.43 \pm 0.02$ dex for the molecular gas SFL. We also measure a typical depletion timescale $\tau = \Sigma_{H\,I+H_2}/\Sigma_{SFR} \approx 2$ Gyr, in good agreement with recent measurements by Bigiel et al. The atomic gas density shows no correlation with the SFR, and the total gas SFL in the sampled density range closely follows the molecular gas SFL. Integral field spectroscopy allows a much cleaner measurement of Hα emission line fluxes than narrow-band imaging, since it is free of the systematics introduced by continuum subtraction, underlying photospheric absorption, and contamination by the [N II] doublet. We assess the validity of different corrections usually applied in narrow-band measurements to overcome these issues and find that while systematics are introduced by these corrections, they are only dominant in the low surface brightness regime. The disagreement with the previous measurement of a super-linear molecular SFL by Kennicutt et al. is most likely due to differences in the fitting method. Our results support the recent evidence for a low, and close to constant, star formation efficiency (SFE $= \tau^{-1}$) in the molecular component of the interstellar medium. The data show an excellent agreement with the recently proposed model of the SFL by Krumholz et al. The large intrinsic scatter observed may imply the existence of other parameters, beyond the availability of gas, which are important in setting the SFR.

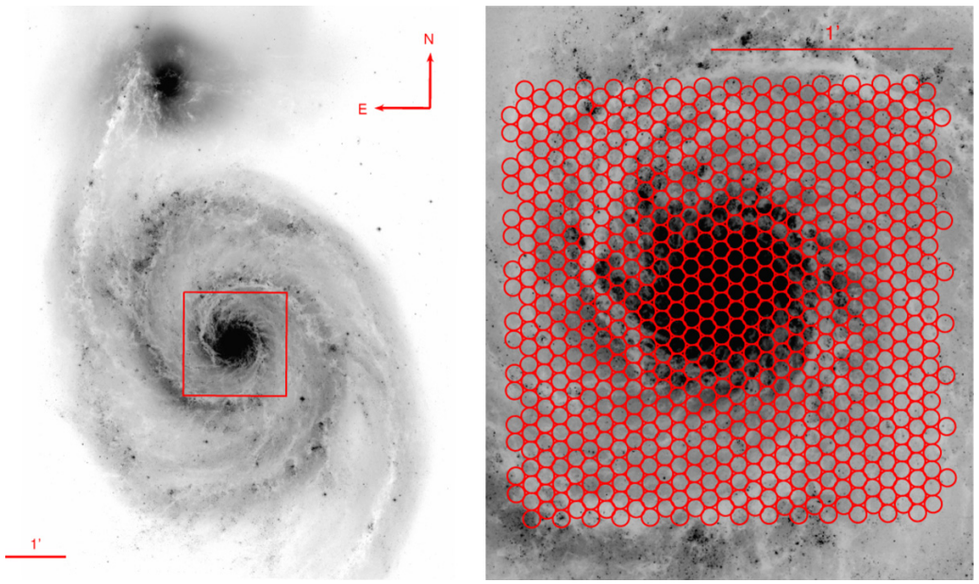

Figure 1. Left: *HST*+ACS *V*-band image of NGC5194 and its companion NGC 5195 (Mutchler et al. 2005). The central 4.1 × 4.1 kpc^2 region sampled by the 1.′7 × 1.′7 VIRUS-P field of view is marked in red. Right: map of the 738 regions sampled by VIRUS-P in the three dither positions. Each region has a diameter of 4.″3 corresponding to ∼170 pc at the distance of NGC5194.

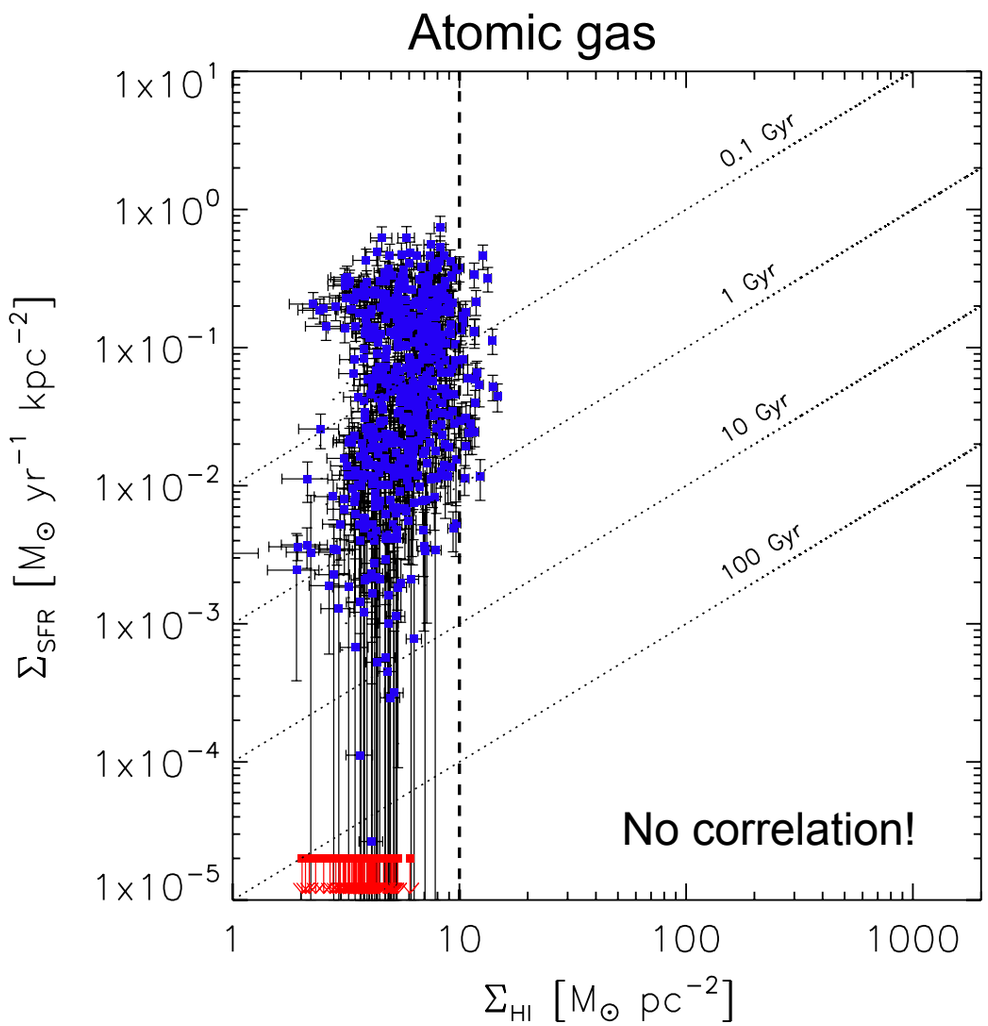

Figure 11. Atomic gas surface density vs. SFR surface density for the 718 regions unaffected by AGN contamination. Upper limits in Σ_{SFR} correspond to regions with $C_{\rm H\,II} = 0$. The vertical dashed line marks the H I to H_2 transition threshold at 10 $M_\odot$ pc^{-2}. The diagonal dotted lines correspond to constant depletion timescales $\tau = {\rm SFE}^{-1}$ of 0.1, 1, 10, and 100 Gyr.

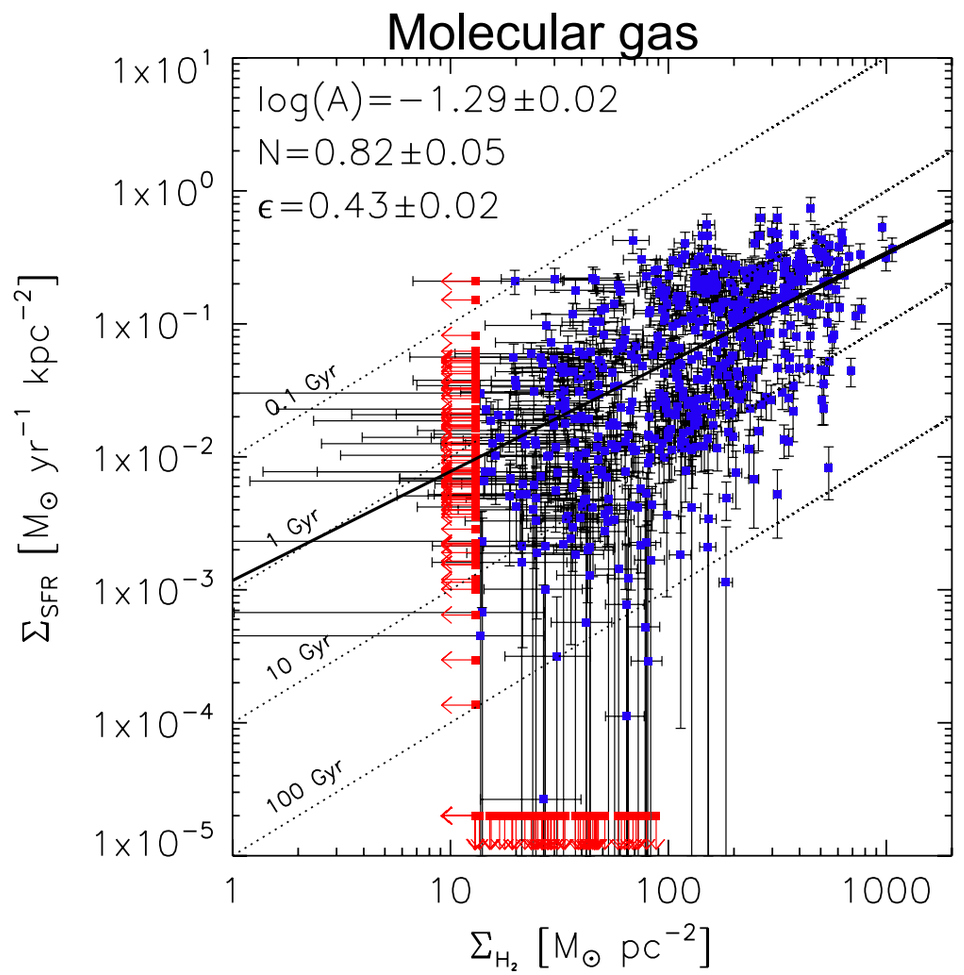

Figure 12. Molecular gas surface density vs. SFR surface density for the 718 regions unaffected by AGN contamination. Upper limits in Σ_{SFR} correspond to regions with $C_{\rm H\,II} = 0$. Upper limits in Σ_{H_2} correspond to regions with non-detection in CO at the 1σ level. The diagonal dotted lines correspond to constant depletion timescales $\tau = {\rm SFE}^{-1}$ of 0.1, 1, 10, and 100 Gyr. Also shown is the best-fitted power law from the MC method (black solid line), and the best-fitted parameters.

THE STAR FORMATION LAW IN ATOMIC AND MOLECULAR GAS

The Astrophysical Journal, 699:850–856, 2009 July 1

Mark R. Krumholz[1], Christopher F. McKee[2], and Jason Tumlinson[3]
[1] Department of Astronomy and Astrophysics, University of California, Santa Cruz, CA 95060, USA; krumholz@ucolick.org
[2] Departments of Physics and Astronomy, University of California, Berkeley, CA 94720-7304, USA; cmckee@astro.berkeley.edu
[3] Space Telescope Science Institute, Baltimore, MD 21218, USA; tumlinson@stsci.edu

Received 2009 March 20; accepted 2009 April 29; published 2009 June 15

ABSTRACT

We propose a simple theoretical model for star formation in which the local star formation rate (SFR) in a galaxy is determined by three factors. First, the interplay between the interstellar radiation field and molecular self-shielding determines what fraction of the gas is in molecular form and thus eligible to form stars. Second, internal feedback determines the properties of the molecular clouds that form, which are nearly independent of galaxy properties until the galactic interstellar medium (ISM) pressure becomes comparable to the internal giant molecular cloud (GMC) pressure. Above this limit, galactic ISM pressure determines molecular gas properties. Third, the turbulence driven by feedback processes in GMCs makes star formation slow, allowing a small fraction of the gas to be converted to stars per free-fall time within the molecular clouds. We combine analytic estimates for each of these steps to formulate a single star formation law, and show that the predicted correlation between SFR, metallicity, and surface densities of atomic, molecular, and total gas agree well with observations.

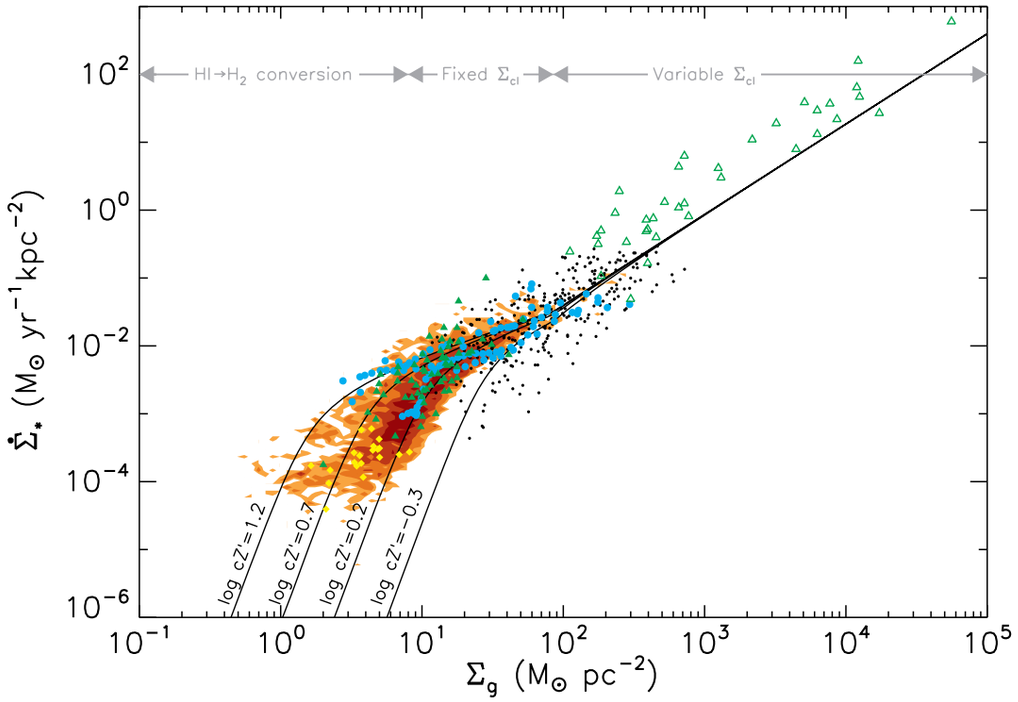

Figure 2. SFR surface density $\dot{\Sigma}_*$ as a function of total gas surface density Σ_g. Lines and contours are the same as in Figure 1. Other points are a compilation of literature data from B08. We show individual apertures in M51 (black dots; Kennicutt et al. 2007), azimuthal averages (blue circles) in NGC4736 and NGC5055 (Wong & Blitz 2002), NGC6946 (Crosthwaite & Turner 2007), and M51 (Schuster et al. 2007), and global averages for starbursts (open green triangles; Kennicutt 1998), normal spirals (filled green triangles; Kennicutt 1998), and low surface brightness galaxies (yellow diamonds; Wyder et al. 2009). The gray arrows and labels indicate schematically the dominant physical process responsible for setting the slope in each region.

We have shown that the observed relationship between the SFR and the atomic and molecular content of galaxies can be explained by a simple model, whose elements are summarized by the regions labeled in Figure 2. First, self-shielding of hydrogen determines the amount of gas in molecular form. This imposes a characteristic gas surface density of $\sim 10/cZ'\ M_\odot$ pc^{-2} for the transition from atomic to molecular, where c is the factor by which the gas surface density is increased due to clumping unresolved by the observations and Z' is the metallicity relative to solar. Second, once molecules do form, molecular clouds reach a surface density of roughly 85 $M_\odot$ pc^{-2} independent of galactic environment. This behavior can be understood as arising from the fact that molecular clouds are overpressured relative to their surroundings, so they must be regulated by internal processes, most likely H II regions (Matzner 2002; Krumholz et al. 2006), that do not depend on metallicity or other large-scale galaxy properties. The constant surface density imposes a roughly constant volume density and free-fall time on all molecular gas. The exception to this is galaxies where the mean galactic surface density is $\gtrsim 100\ M_\odot$ pc^{-2}, in which the ambient pressure is high enough to force GMC densities to rise along with galactic surface density in order to keep the clouds in pressure balance. Third, once formed molecular clouds convert themselves into stars at a nearly universal rate of $\sim$1% of the mass per free-fall time as a result of turbulent regulation. Together these effects produce a total

The Astrophysical Journal, 721:975–994, 2010 October 1 doi:10.1088/0004-637X/721/2/97

REGULATION OF STAR FORMATION RATES IN MULTIPHASE GALACTIC DISKS: A THERMAL/DYNAMICAL EQUILIBRIUM MODEL

Eve C. Ostriker[1], Christopher F. McKee[2,3], and Adam K. Leroy[4,5]
[1] Department of Astronomy, University of Maryland, College Park, MD 20742, USA; ostriker@astro.umd.edu
[2] Departments of Physics and Astronomy, University of California, Berkeley, CA 94720, USA; cmckee@astro.berkeley.edu
[3] LERMA-LRA, Ecole Normale Superieure, 24 rue Lhomond, 75005 Paris, France
[4] National Radio Astronomy Observatory, 520 Edgemont Road, Charlottesville, VA 22903, USA; aleroy@nrao.edu
Received 2010 March 11; accepted 2010 July 30; published 2010 September 3

ABSTRACT

We develop a model for the regulation of galactic star formation rates $\Sigma_{\rm SFR}$ in disk galaxies, in which interstellar medium (ISM) heating by stellar UV plays a key role. By requiring that thermal and (vertical) dynamical equilibrium are simultaneously satisfied within the diffuse gas, and that stars form at a rate proportional to the mass of the self-gravitating component, we obtain a prediction for $\Sigma_{\rm SFR}$ as a function of the total gaseous surface density Σ and the midplane density of stars+dark matter $\rho_{\rm sd}$. The physical basis of this relationship is that the thermal pressure in the diffuse ISM, which is proportional to the UV heating rate and therefore to $\Sigma_{\rm SFR}$, must adjust until it matches the midplane pressure value set by the vertical gravitational field. Our model applies to regions where $\Sigma \lesssim 100\,M_\odot$ pc^{-2}. In low-$\Sigma_{\rm SFR}$ (outer-galaxy) regions where diffuse gas dominates, the theory predicts that $\Sigma_{\rm SFR} \propto \Sigma\sqrt{\rho_{\rm sd}}$. The decrease of thermal equilibrium pressure when $\Sigma_{\rm SFR}$ is low implies, consistent with observations, that star formation can extend (with declining efficiency) to large radii in galaxies, rather than having a sharp cutoff at a fixed value of Σ. The main parameters entering our model are the ratio of thermal pressure to total pressure in the diffuse ISM, the fraction of diffuse gas that is in the warm phase, and the star formation timescale in self-gravitating clouds; all of these are (at least in principle) direct observables. At low surface density, our model depends on the ratio of the mean midplane FUV intensity (or thermal pressure in the diffuse gas) to the star formation rate, which we set based on solar-neighborhood values. We compare our results to recent observations, showing good agreement overall for azimuthally averaged data in a set of spiral galaxies. For the large flocculent spiral galaxies NGC 7331 and NGC 5055, the correspondence between theory and observation is remarkably close.

Local Black Hole Demographics

Jenny Greene (Princeton)

Active Galactic Nuclei

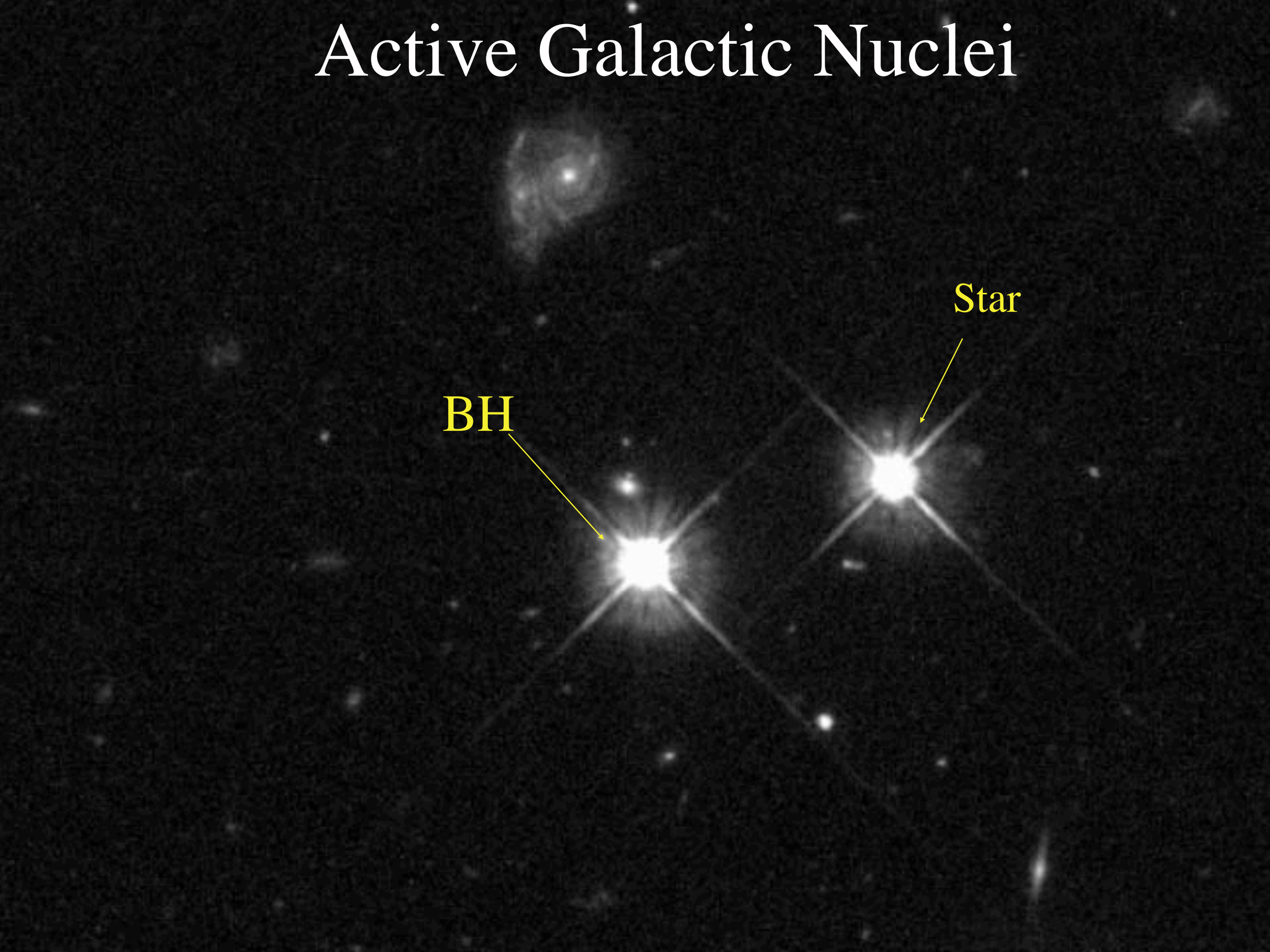

A Sense of Scale

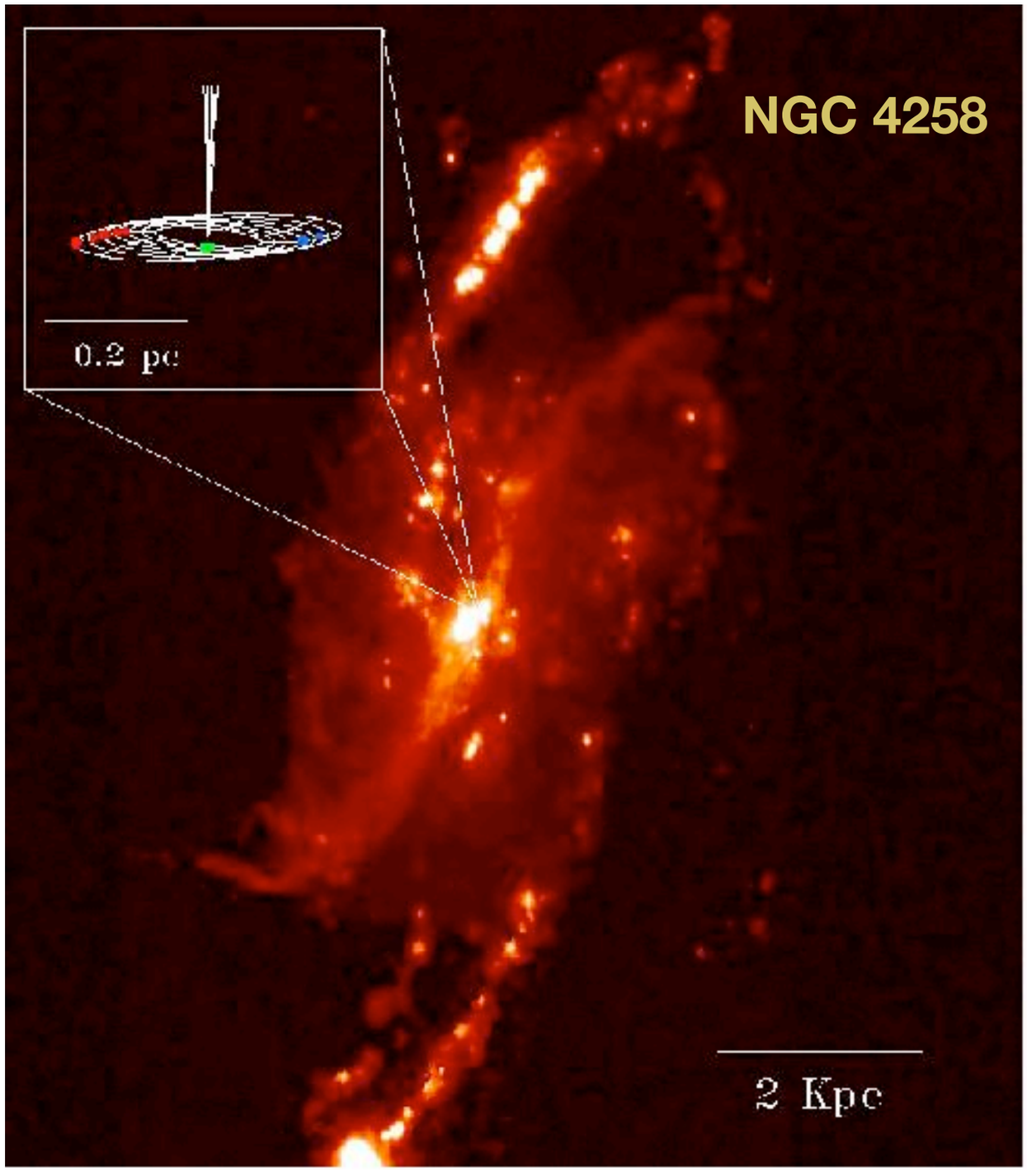

A Sense of Scale

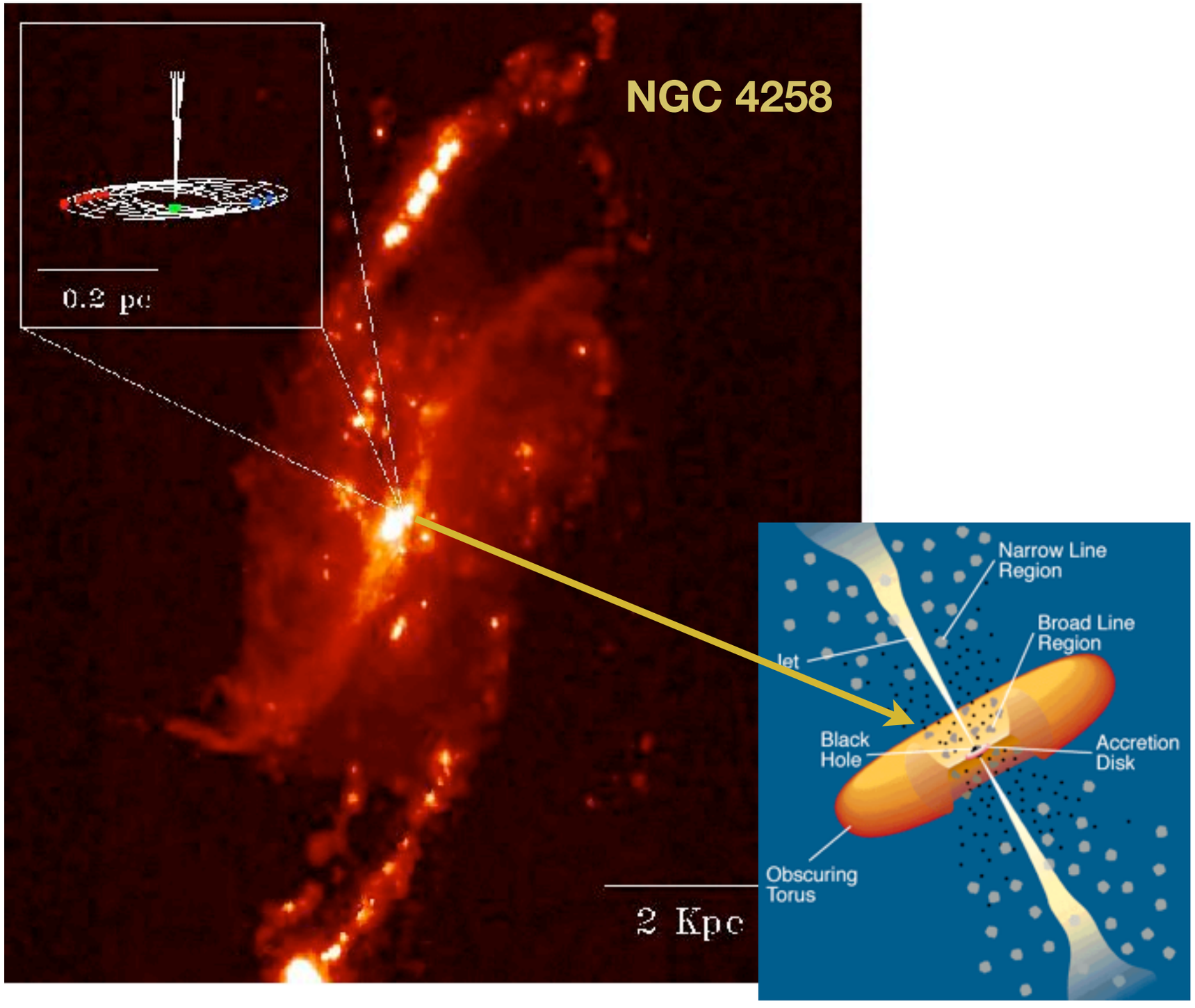

A Sense of Scale

narrow-line regions
~100pc scales

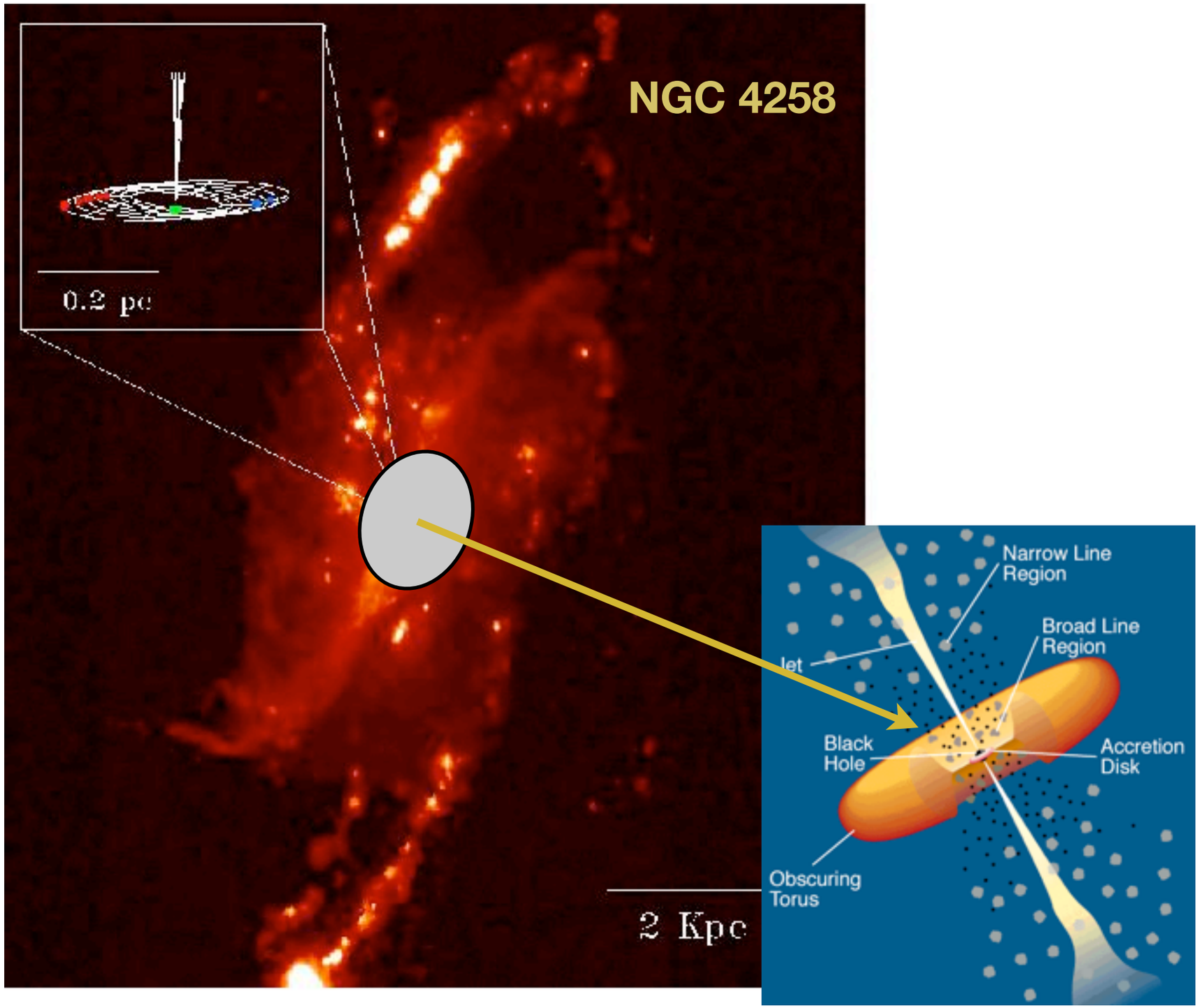

A Sense of Scale

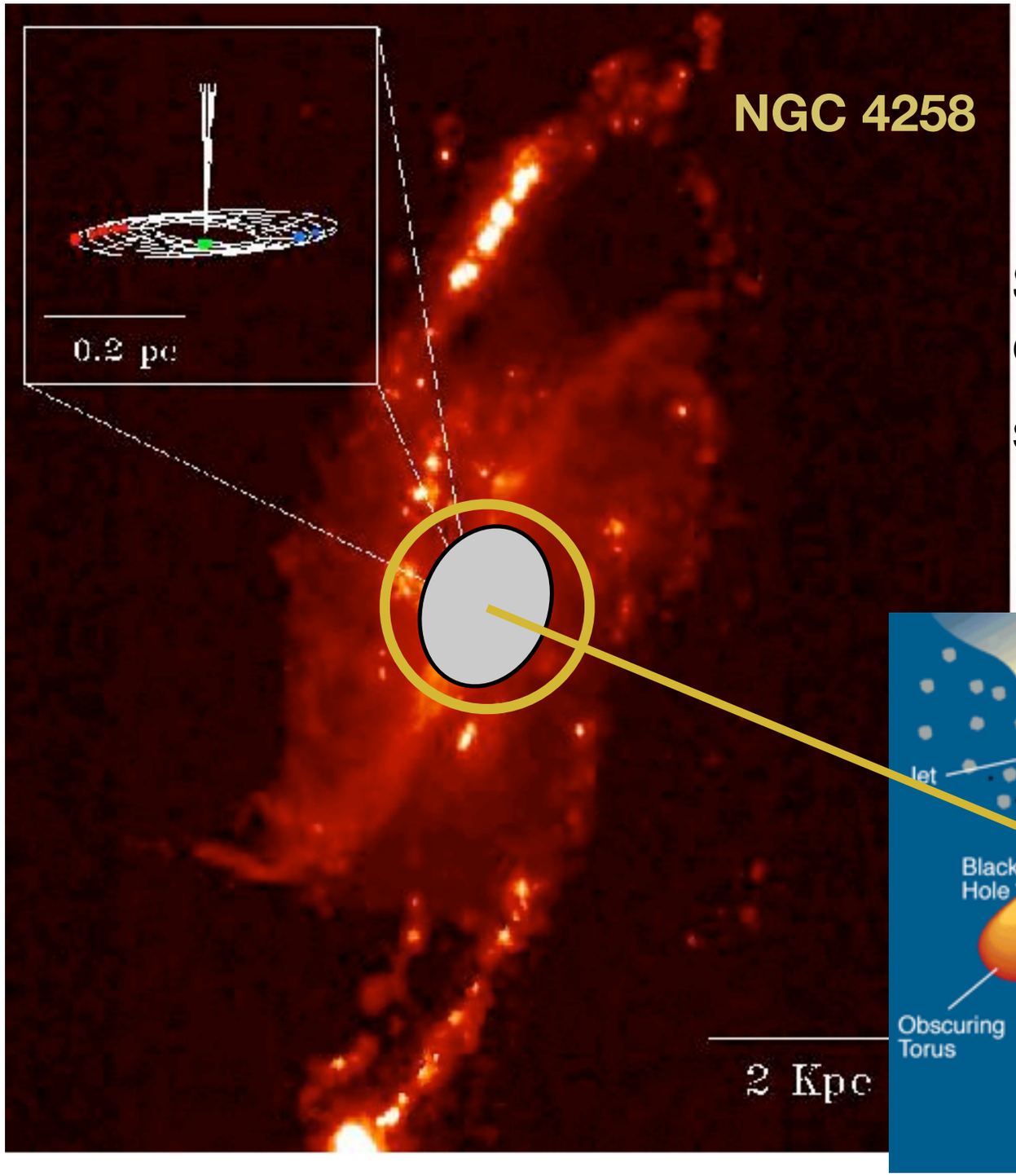

Stellar velocity dispersions ($\sigma_\star$) on kpc scales (R_e)

narrow-line regions ~100pc scales

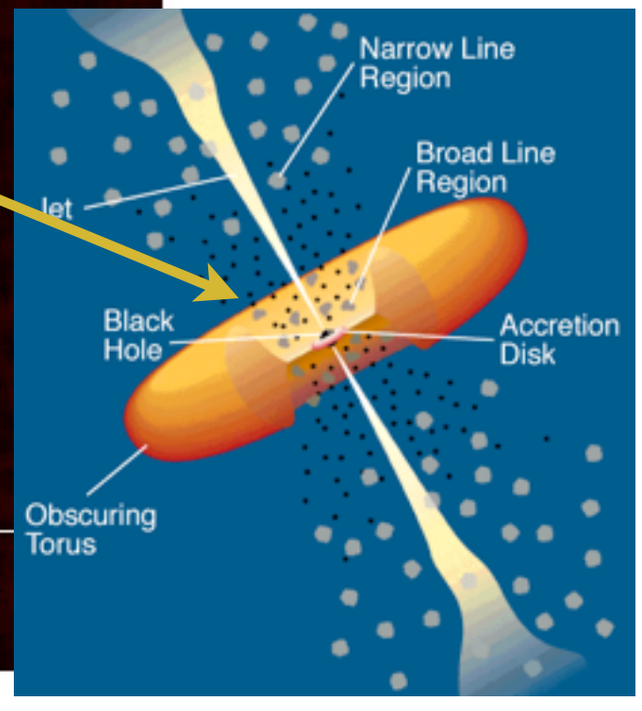

Outline

Using nuclear activity to study BHs

Using dynamics to study BHs

Scaling relations

Outstanding questions

Outline

Using nuclear activity to study BHs

Using dynamics to study BHs

} BHs are ubiquitous at the centers of massive galaxies

Scaling relations

Outstanding questions

Nuclear Activity (I): Optical Spectra

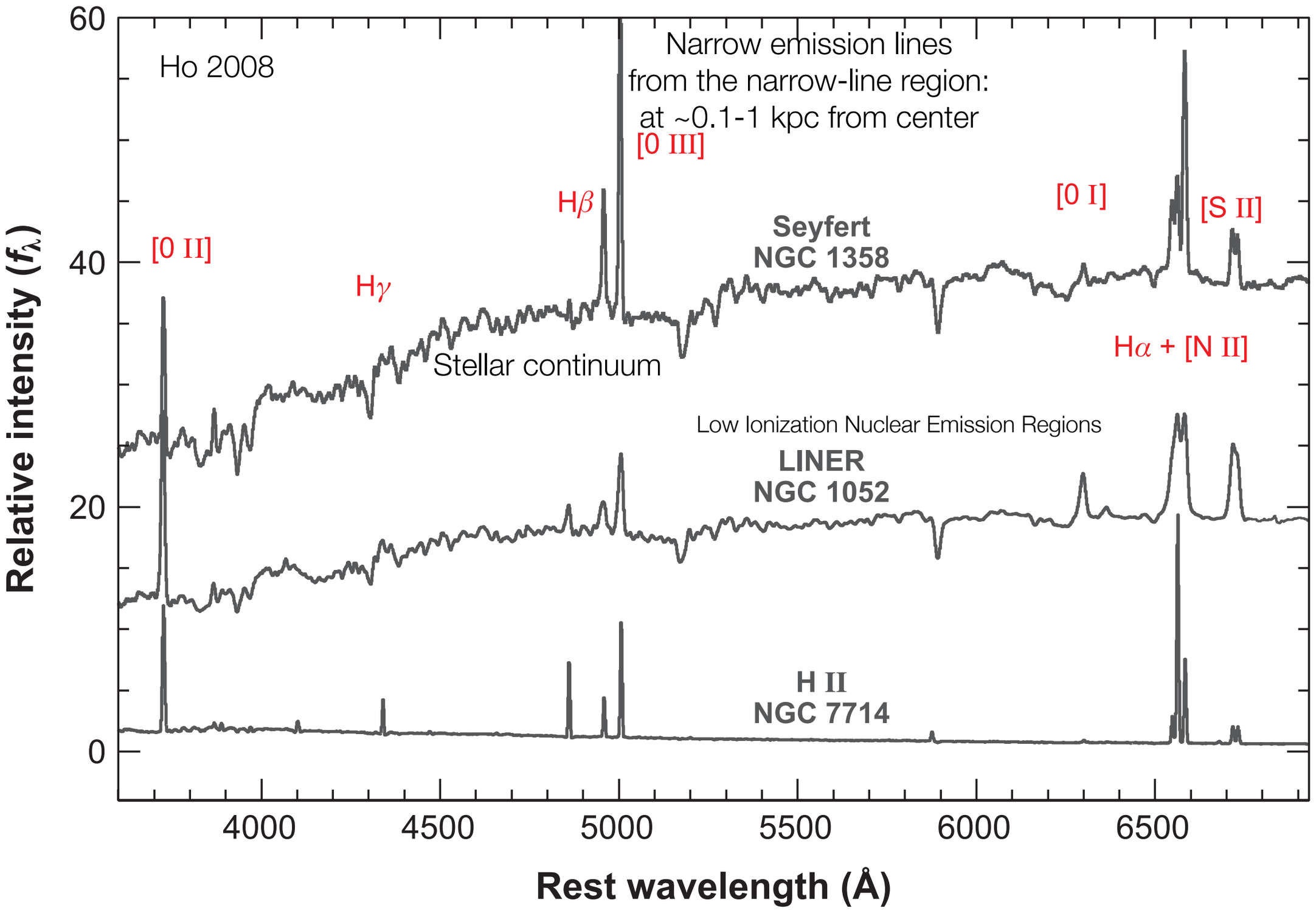

Nuclear Activity (I): Optical Spectra

Note the major difference between AGN and HII galaxies is the strength of the low ionization lines

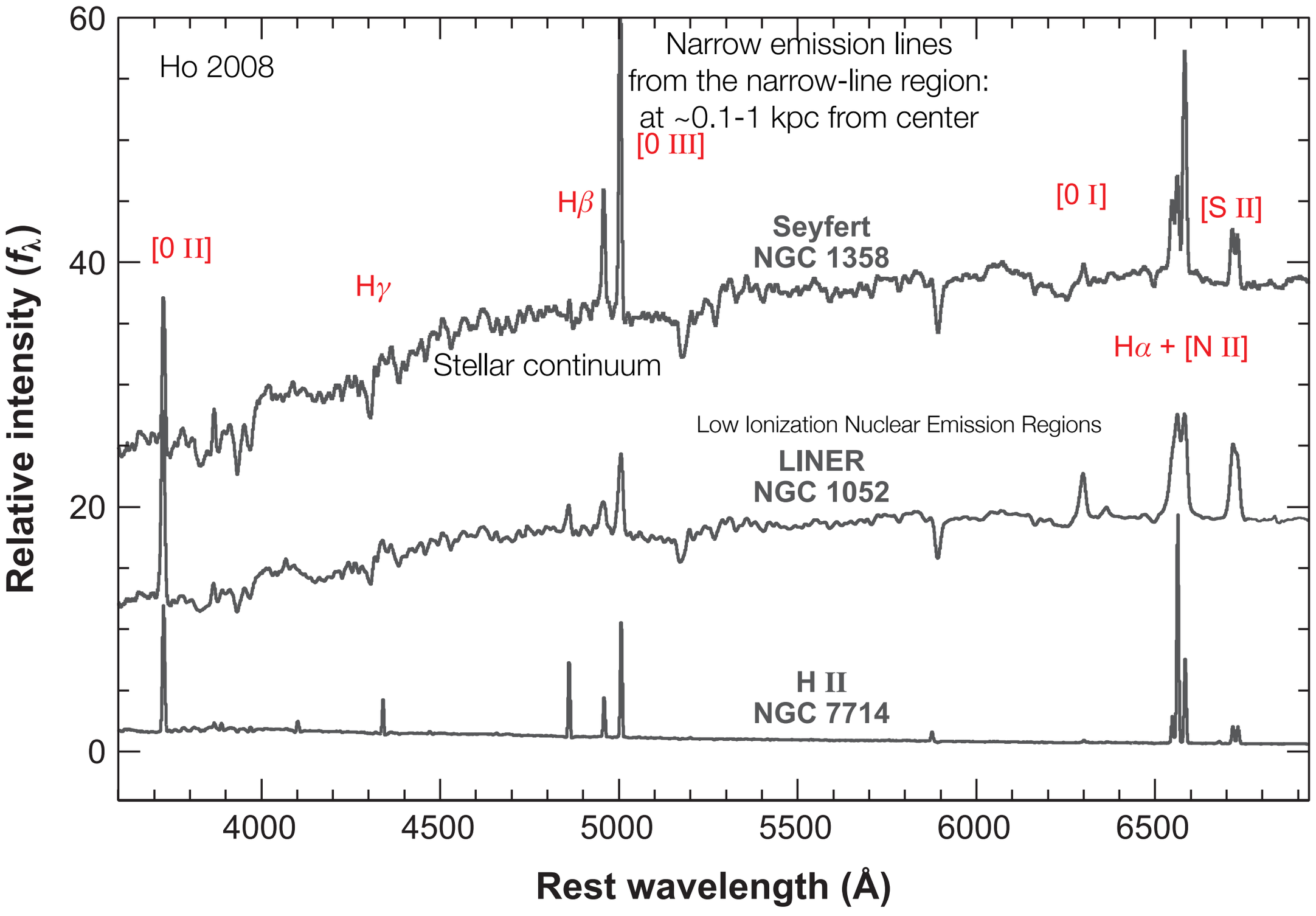

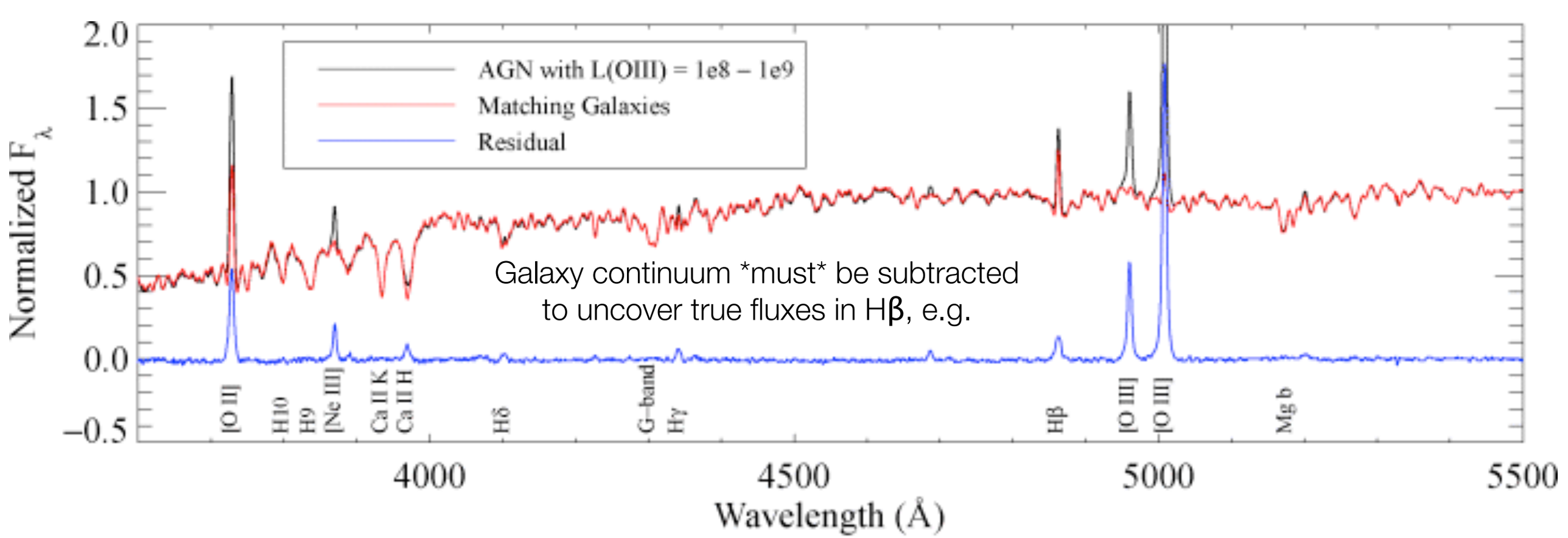

Kauffmann et al. 2003

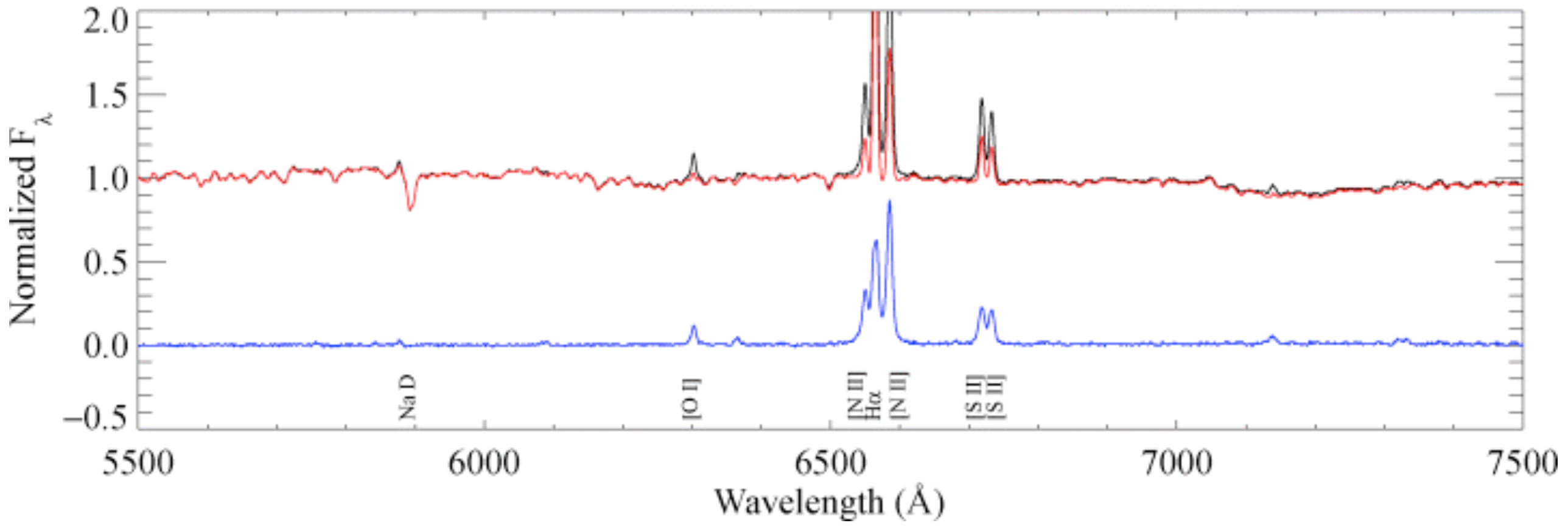

We use the so-called "BPT" diagram

PUBLICATIONS OF THE
ASTRONOMICAL SOCIETY OF THE PACIFIC

Vol. 93 February 1981 No. 551

CLASSIFICATION PARAMETERS FOR THE EMISSION-LINE SPECTRA OF EXTRAGALACTIC OBJECTS

J. A. BALDWIN AND M. M. PHILLIPS
Cerro Tololo Inter-American Observatory,* Casilla 603, La Serena, Chile

AND

ROBERTO TERLEVICH
Institute of Astronomy, Madingley Road, Cambridge, England CB3 0HA

Received 1980 August 21

An investigation is made of the merits of various emission-line intensity ratios for classifying the spectra of extragalactic objects. It is shown empirically that several combinations of easily-measured lines can be used to separate objects into one of four categories according to the principal excitation mechanism: normal H II regions, planetary nebulae, objects photoionized by a power-law continuum, and objects excited by shock-wave heating. A two-dimensional quantitative classification scheme is suggested.

What is the excitation mechanism?

Photoionization by O stars (HII galaxies, star-forming galaxies, etc)

Photoionization by a power-law continuum -- typified by a wide range of ionization states

PNe -- photoionization by evolved star

Shock heating

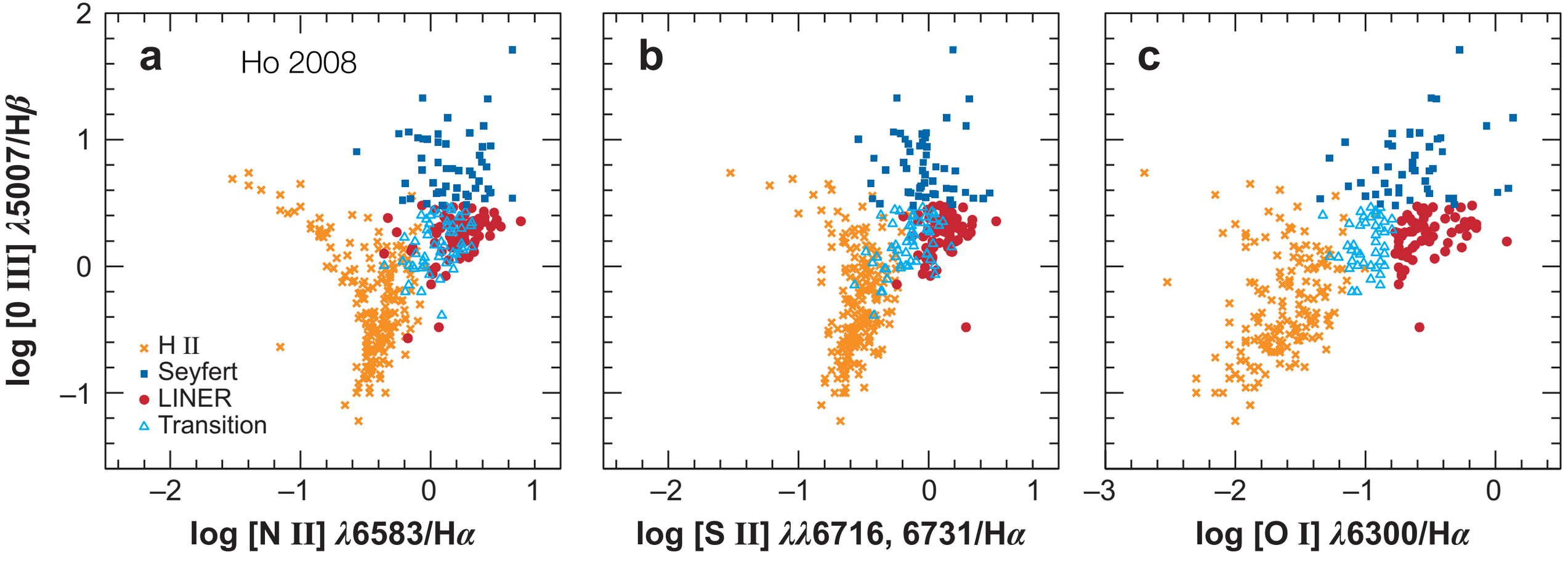

Use strong, ubiquitous lines ([OIII] 4363/[OIII] 5007 is sensitive to temp...but impossible to measure): Veilleux & Osterbrock 1987

Uses rest-frame optical lines: perfect for low-z demographics

Lines are close together = importance of reddening minimized

Kauffmann et al. 2003

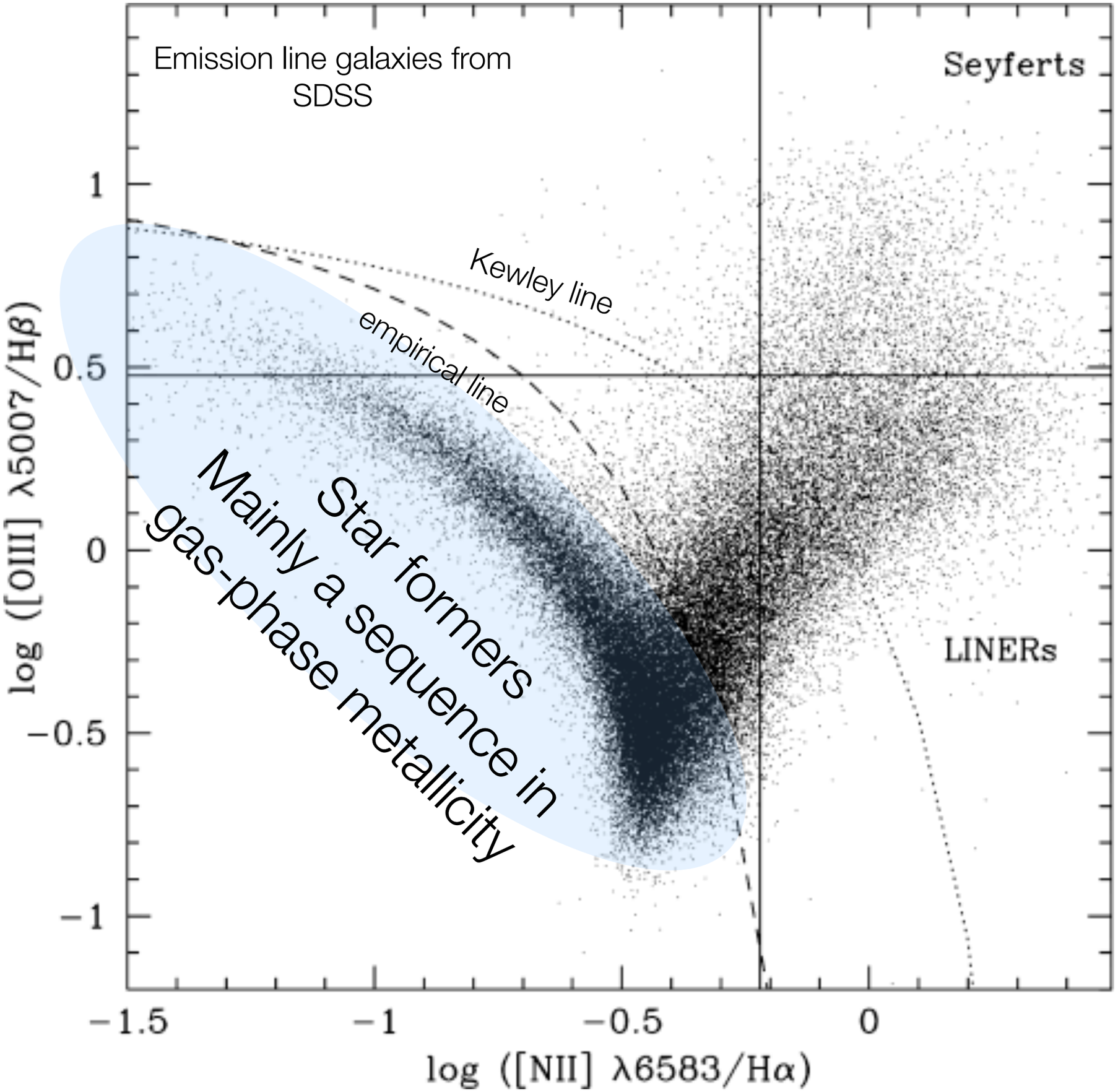

Detailed Photoionization Models

Range of assumptions
for the metallicity and density
of the gas

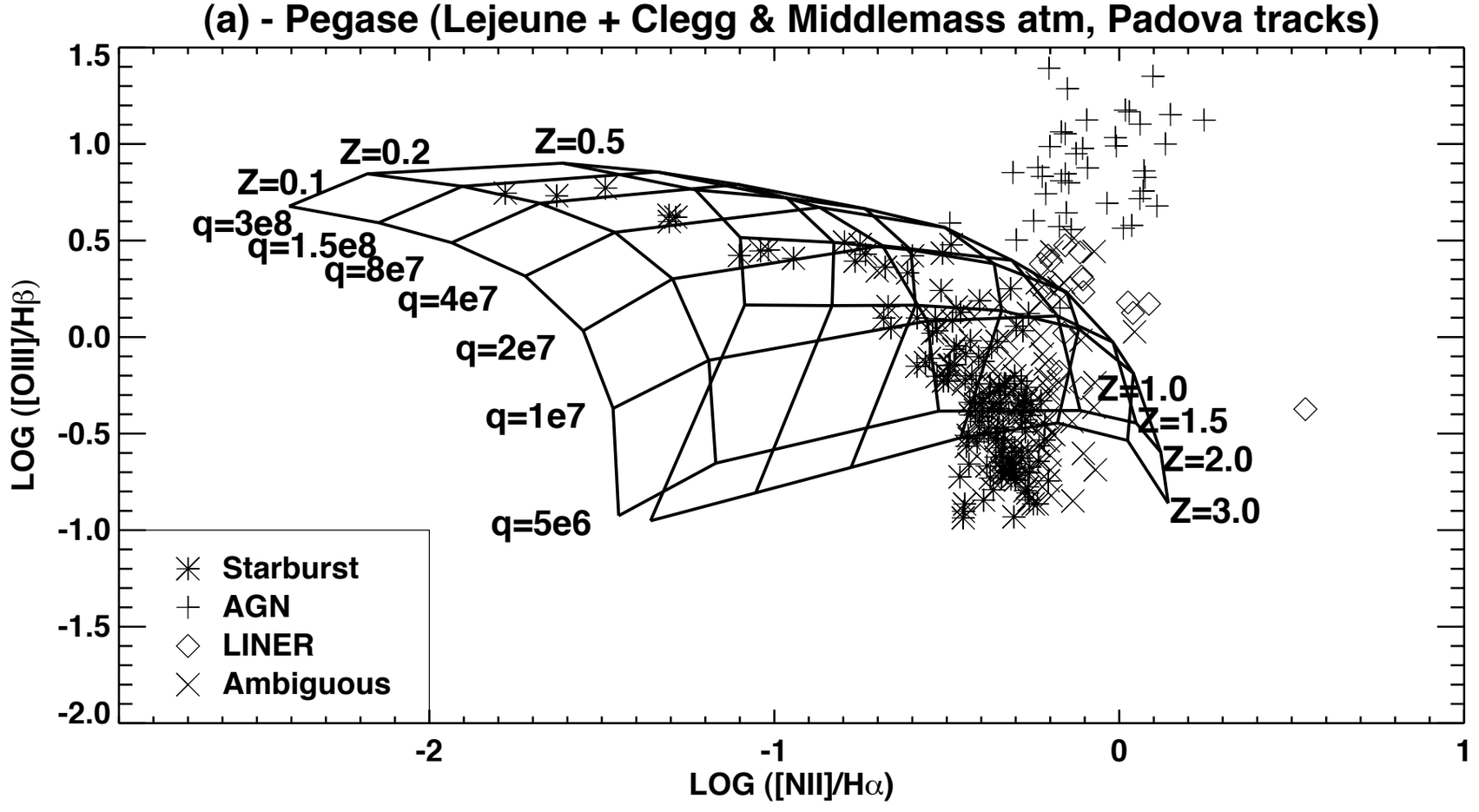

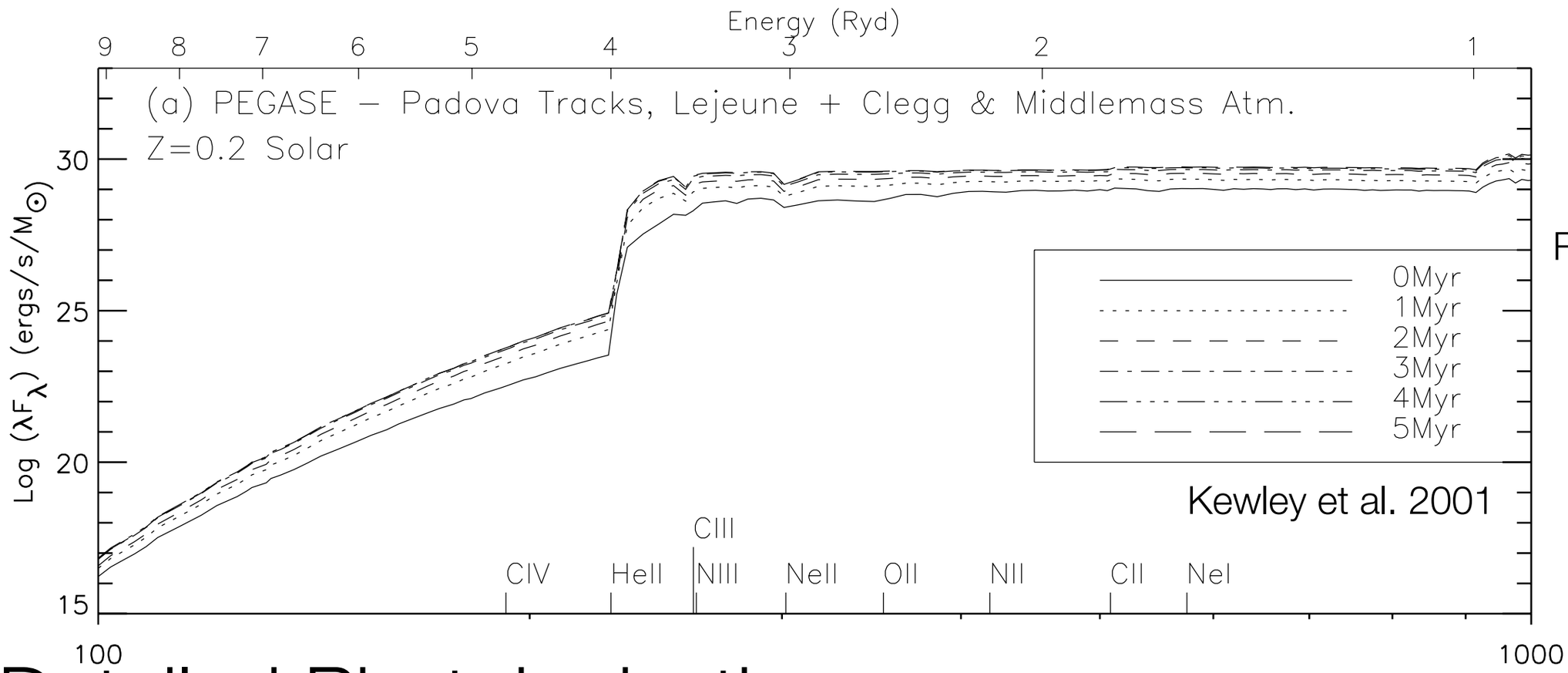

Range of assumptions
for the shape of the
ionizing continuum

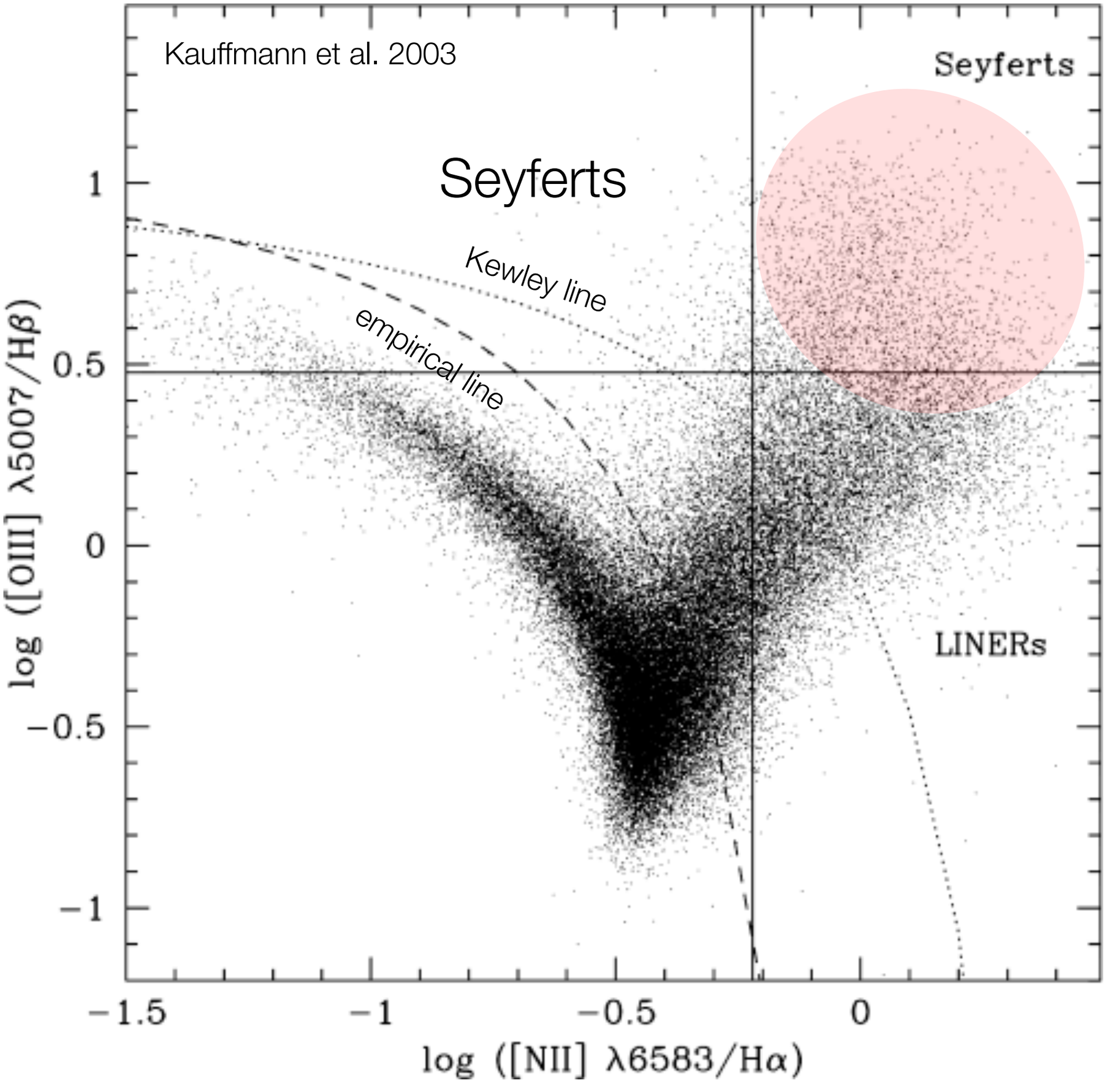
Kauffmann et al. 2003
Seyferts
Seyferts
Kewley line
empirical line
LINERs
1
0.5
0
−0.5
−1
−1.5
−1
−0.5
0
log ([OIII] λ5007/Hβ)
log ([NII] λ6583/Hα)

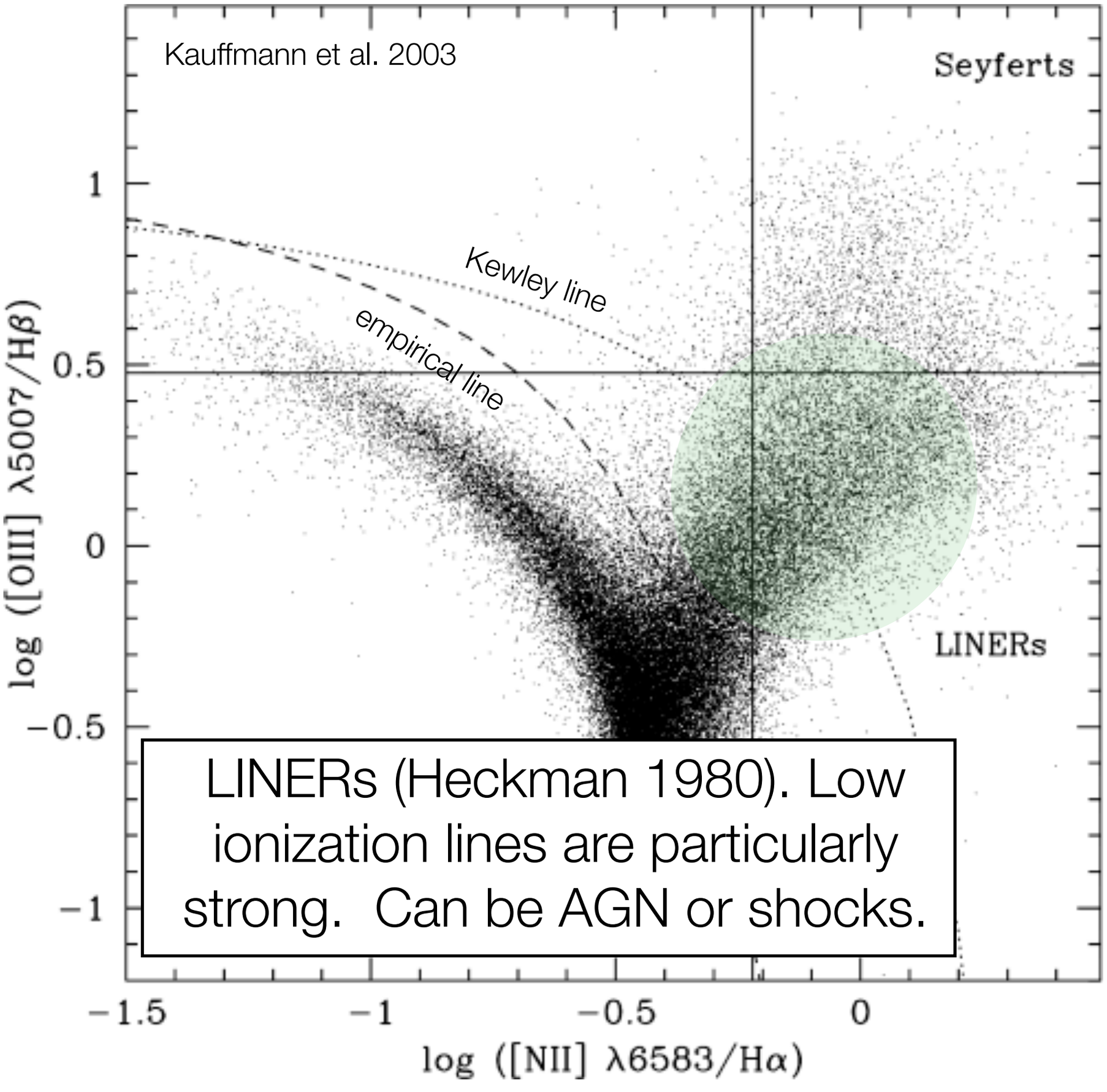

LINERs (Heckman 1980). Low ionization lines are particularly strong. Can be AGN or shocks.

Digression: What powers LINERs?

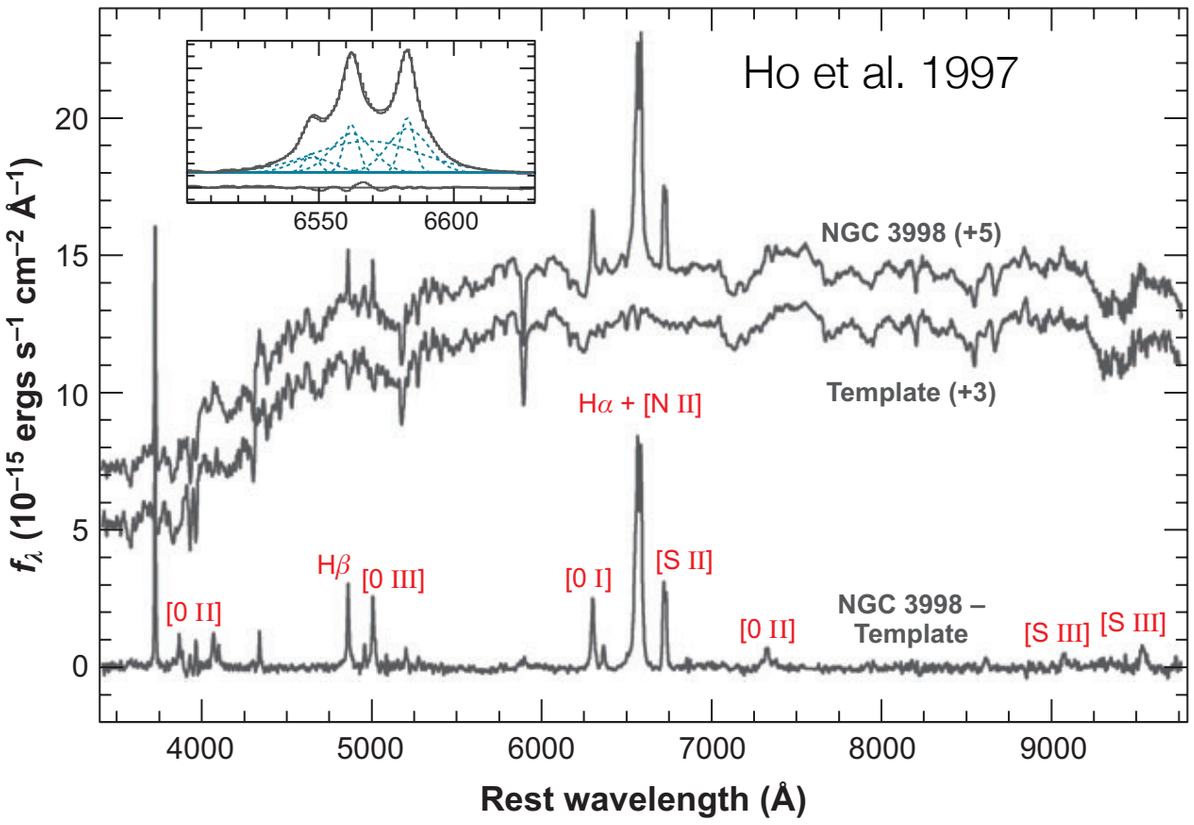

Large aperture on a ULIRG: Shocks

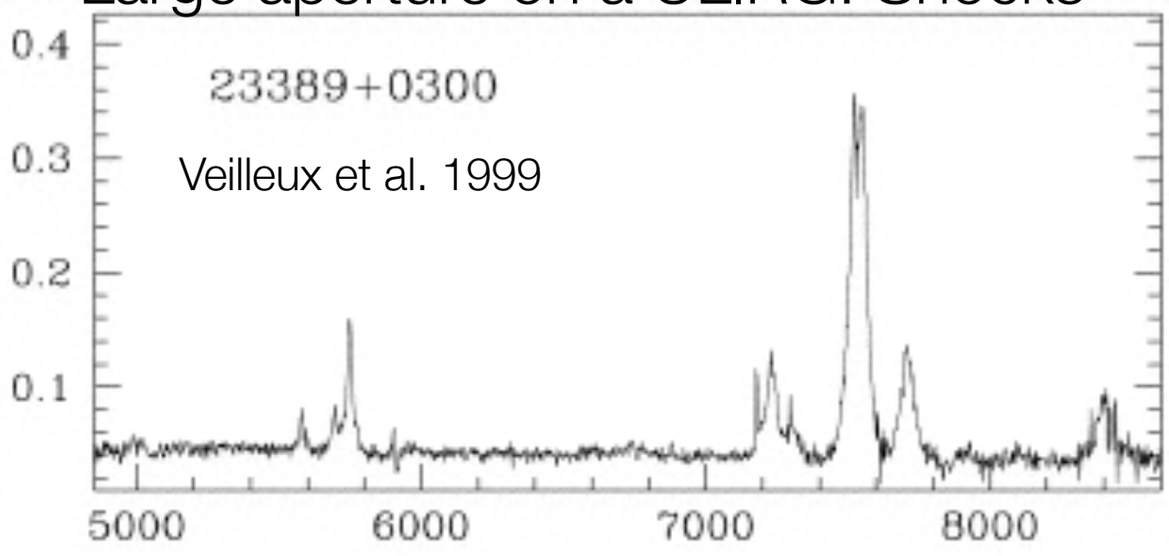

Answer: It depends. But there is no doubt that LINER emission from the very center of nearby massive ellipticals is correlated with accretion. See Eracleous et al. 2010 for detailed analysis of power source of LINERs.

Black Hole Demographics

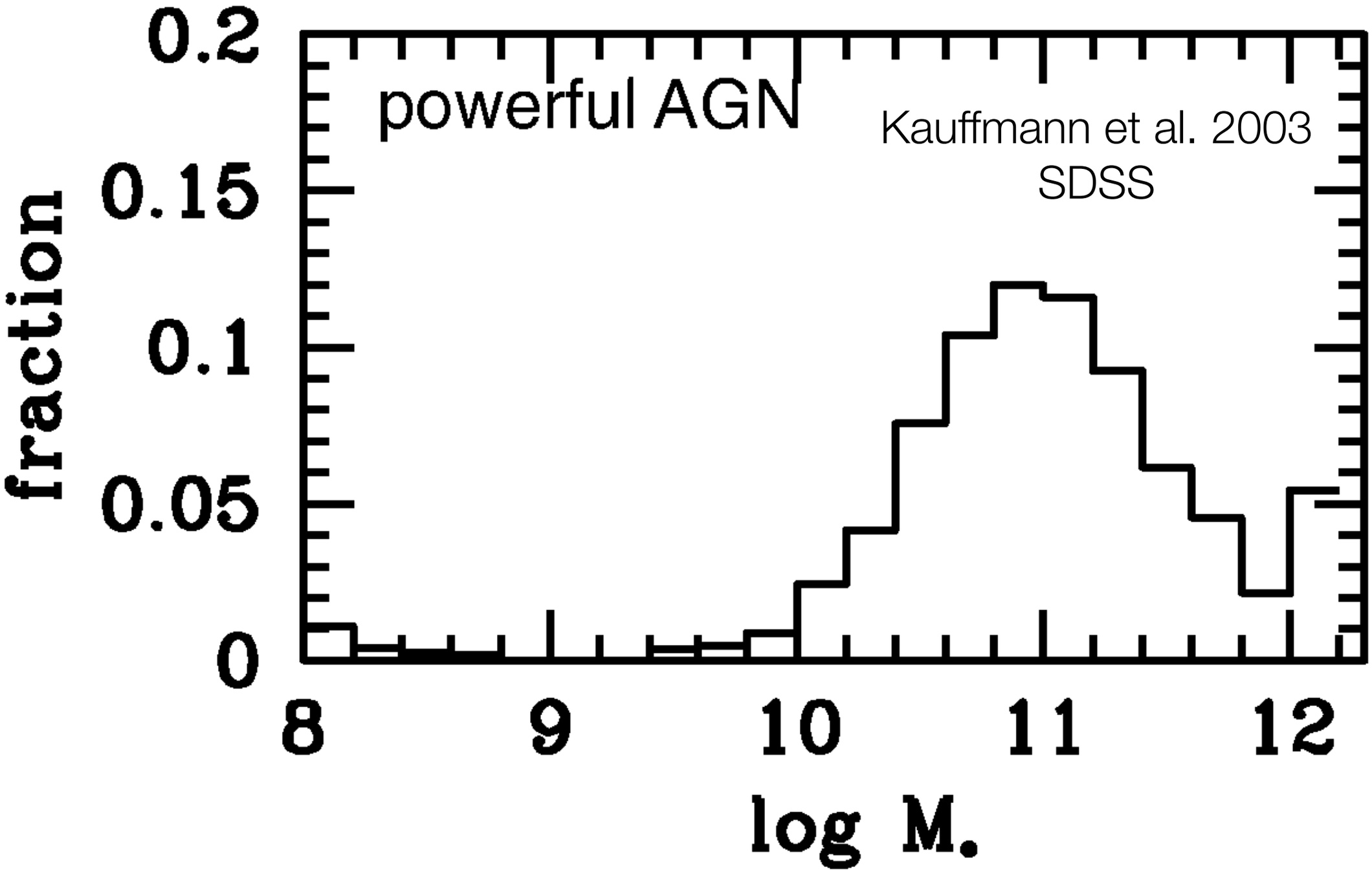

Point 1: Accreting black holes are found in massive, bulge-dominated galaxies

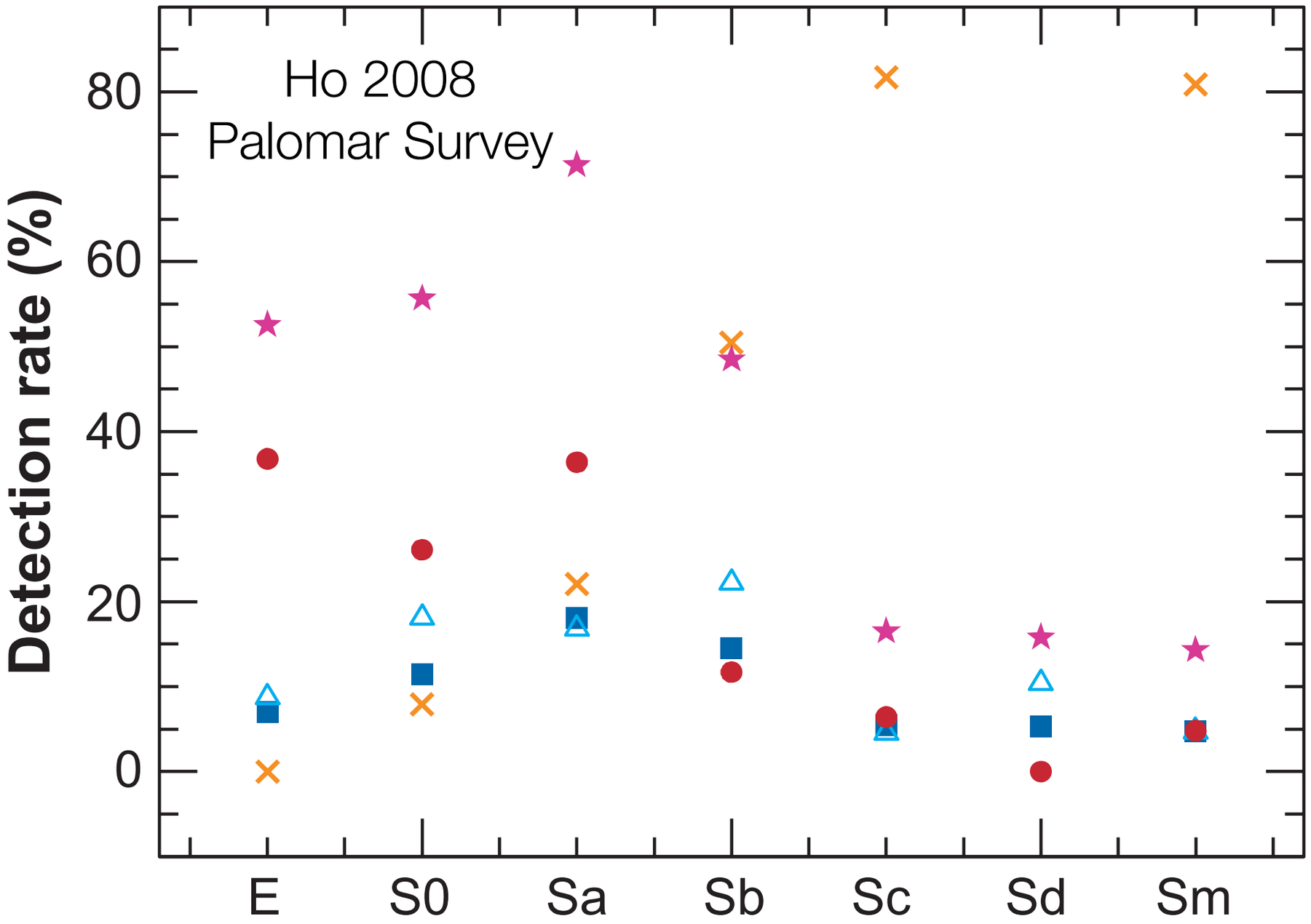

Point 2: If you look hard enough you find that virtually ALL massive, bulge-dominated galaxies contain (very weakly) accreting supermassive black holes

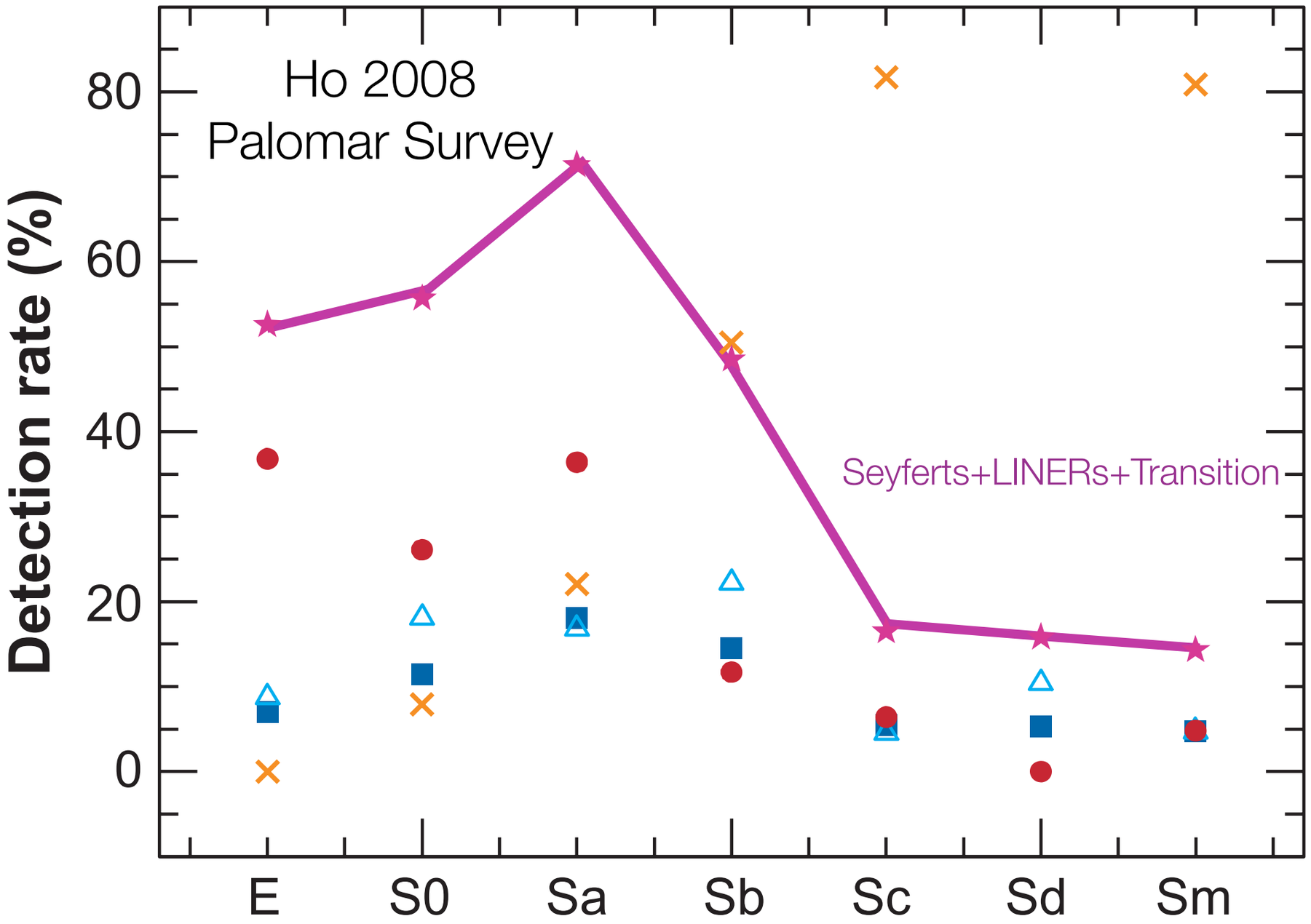

Point 2: If you look hard enough you find that virtually ALL massive, bulge-dominated galaxies contain (very weakly) accreting supermassive black holes

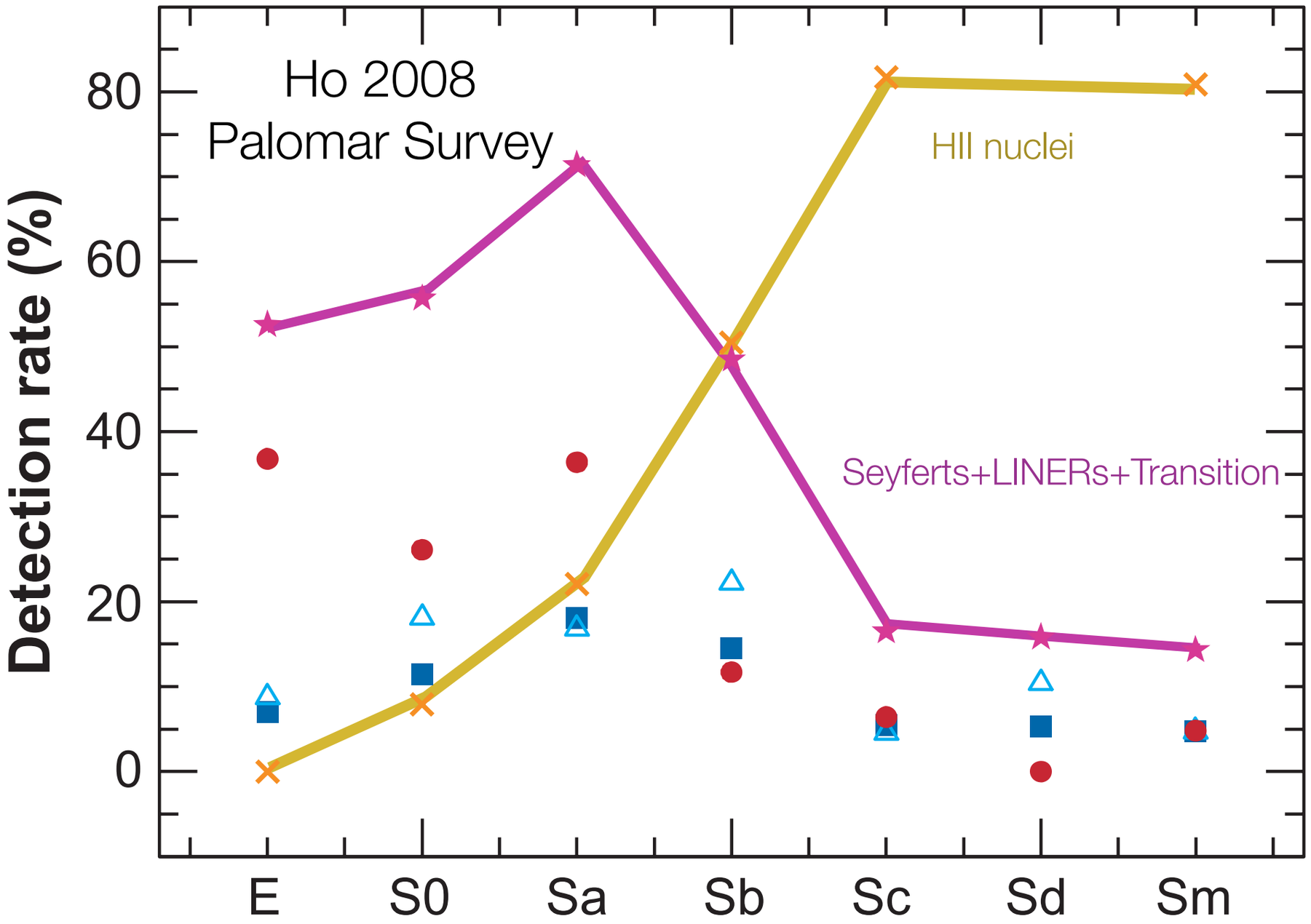

Point 2: If you look hard enough you find that virtually ALL massive, bulge-dominated galaxies contain (very weakly) accreting supermassive black holes

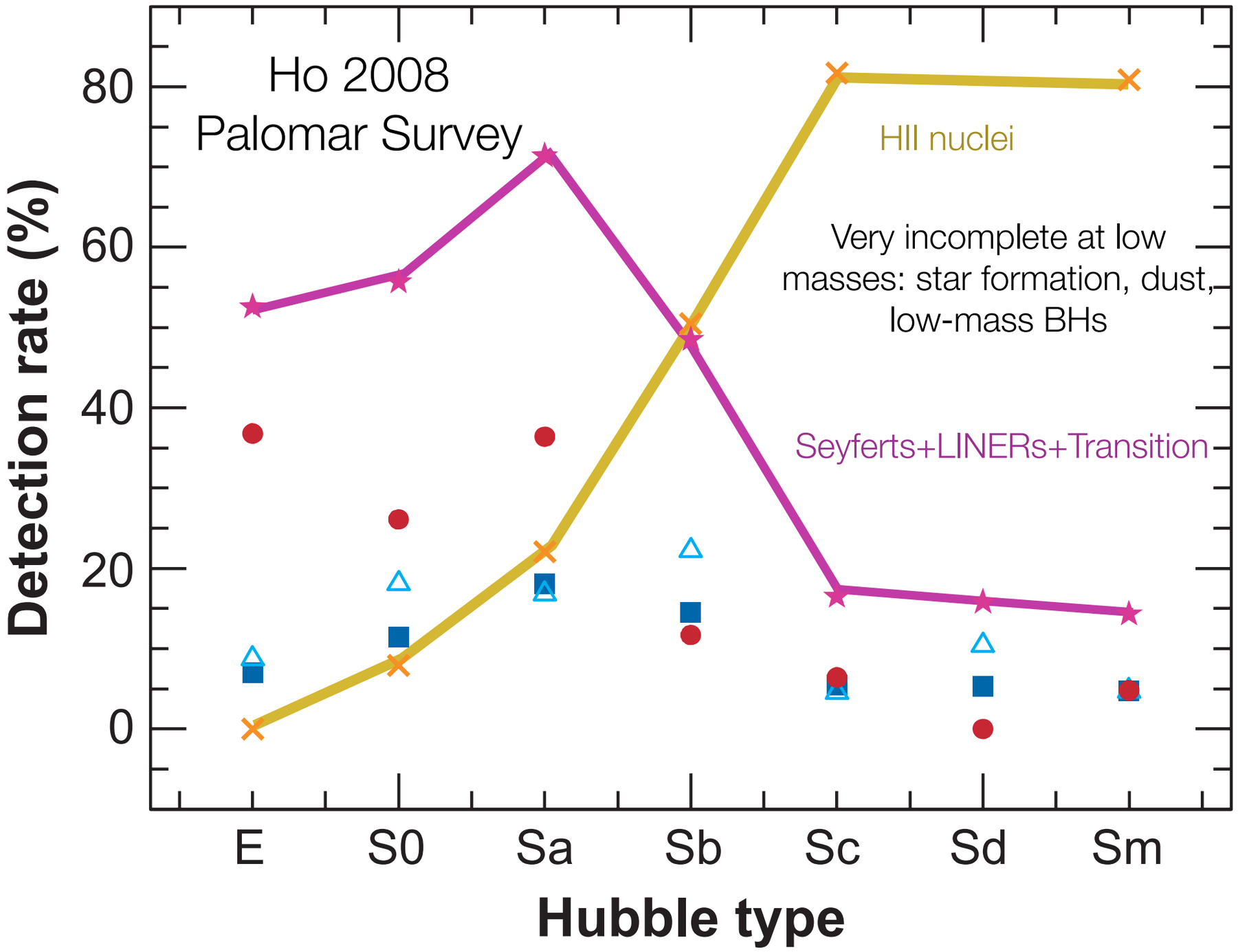

Point 2: If you look hard enough you find that virtually ALL massive, bulge-dominated galaxies contain (very weakly) accreting supermassive black holes

Other ways to find local active galaxies

Also Broad Emission Lines

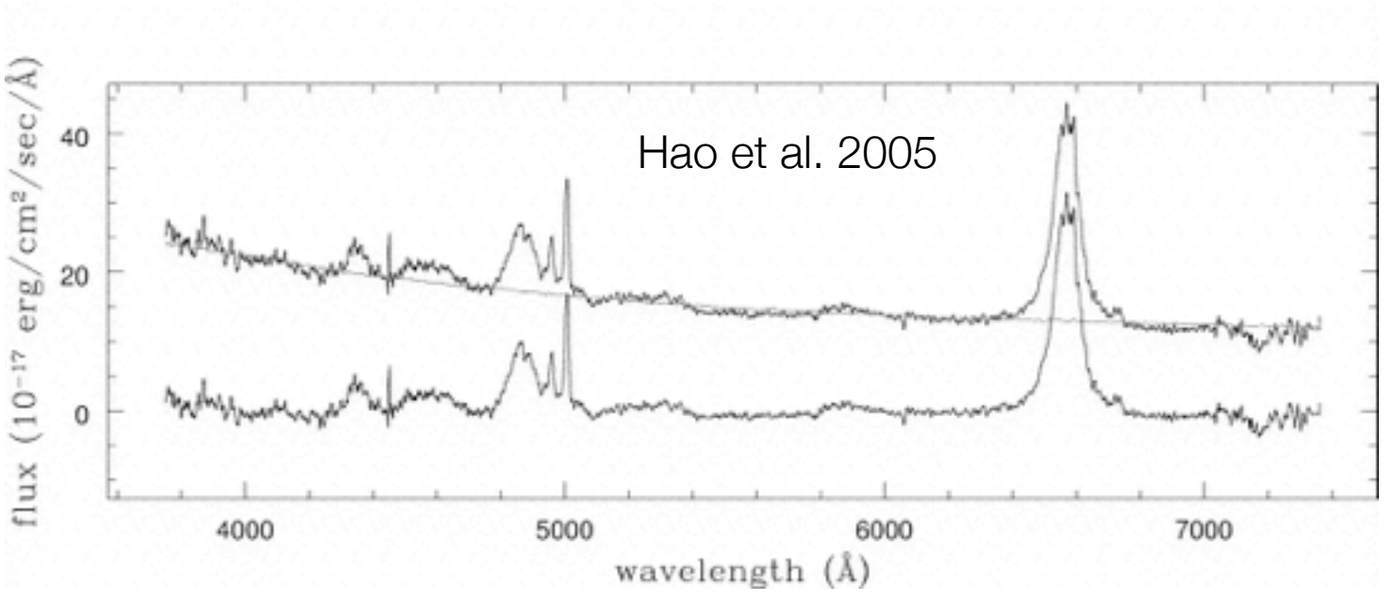

Schulze & Wiszotski 2009

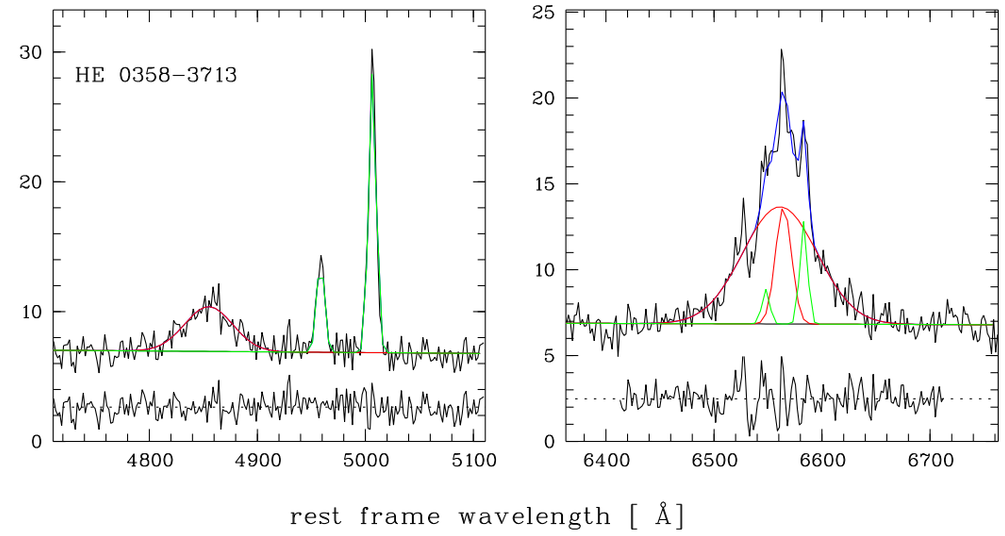

Greene & Ho 2004

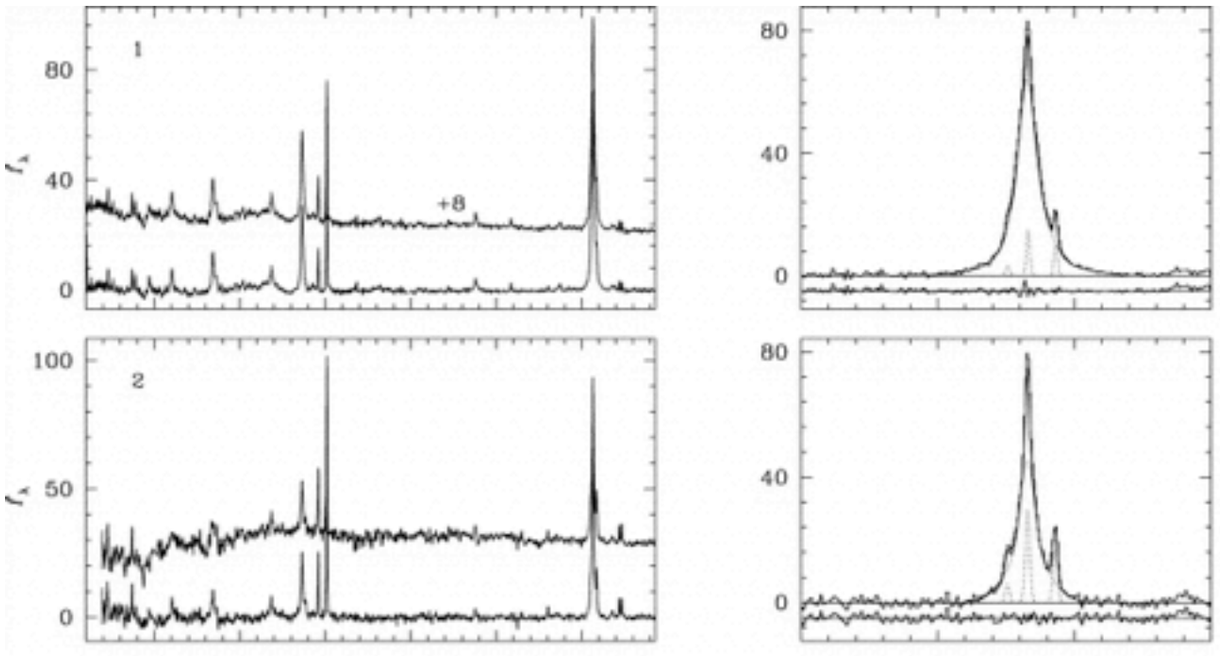

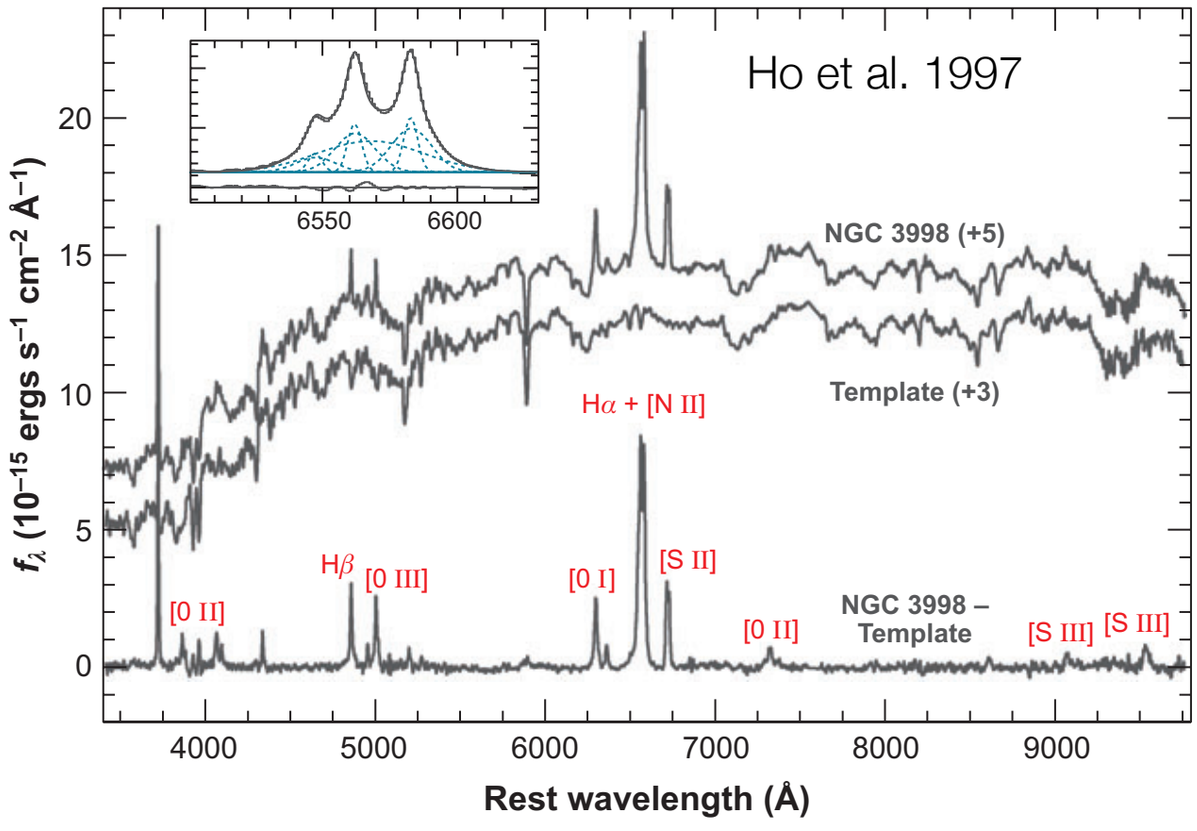

Nuclear Acitivity (II): X-ray/Radio Emission

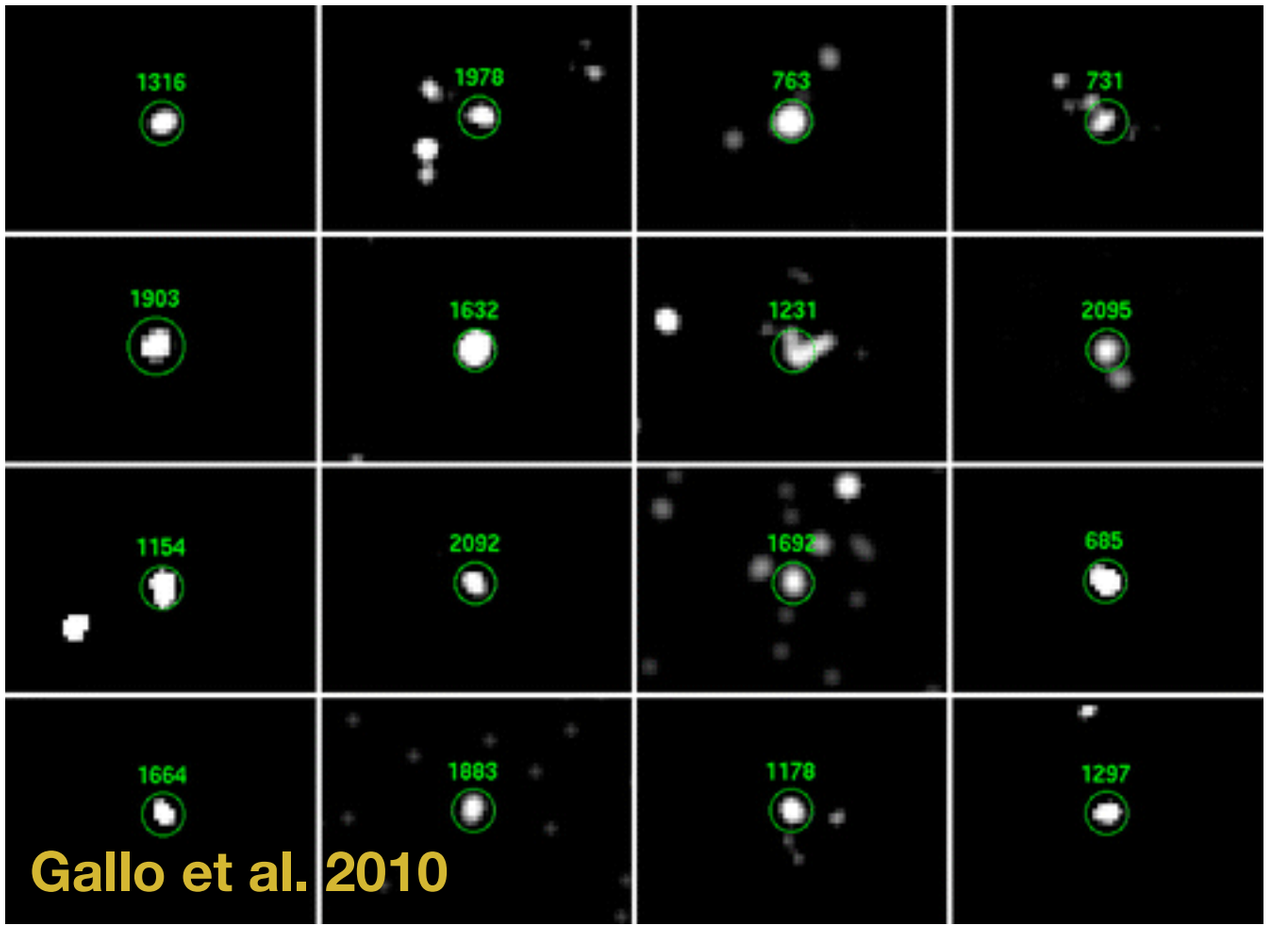

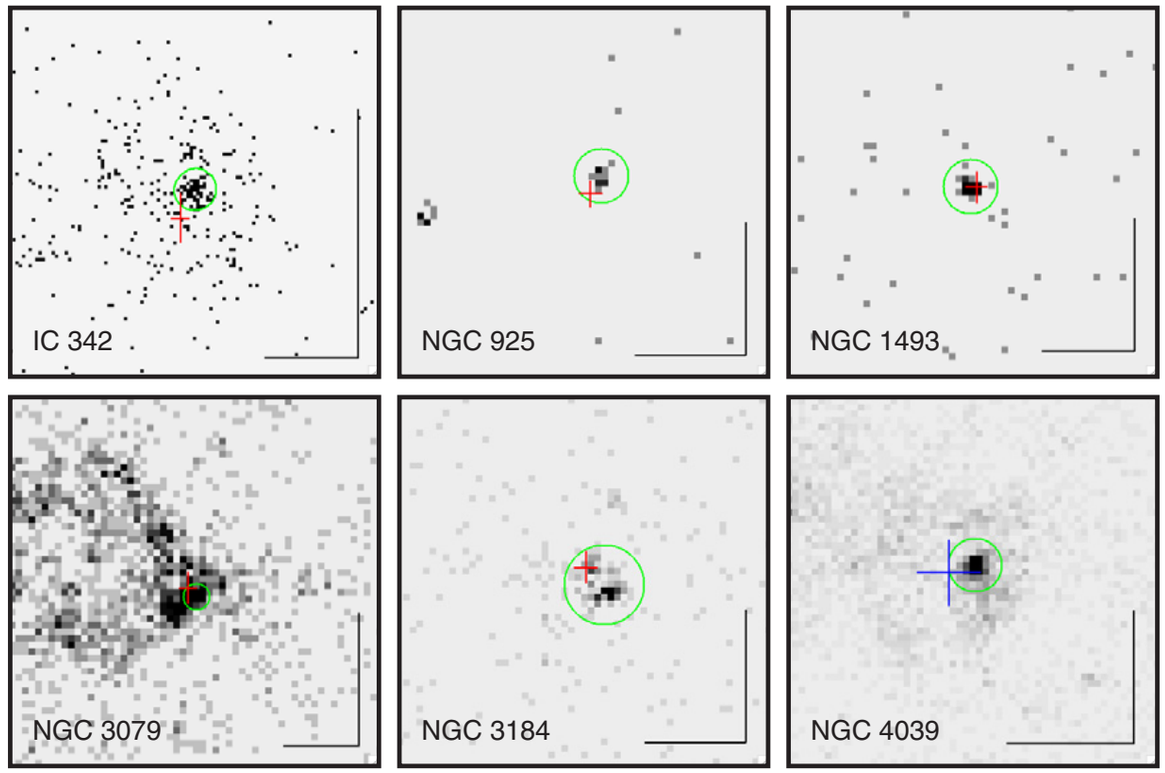

Very important to: (a) Confirm the targets identified in the optical, particularly the LINERs, (b) Search in targets with high star formation rates, high dust obscuration, weak BHs. At even higher energies, lots of work with Swift/BAT survey that I will not cover.

Nuclear Activity (III): MIR

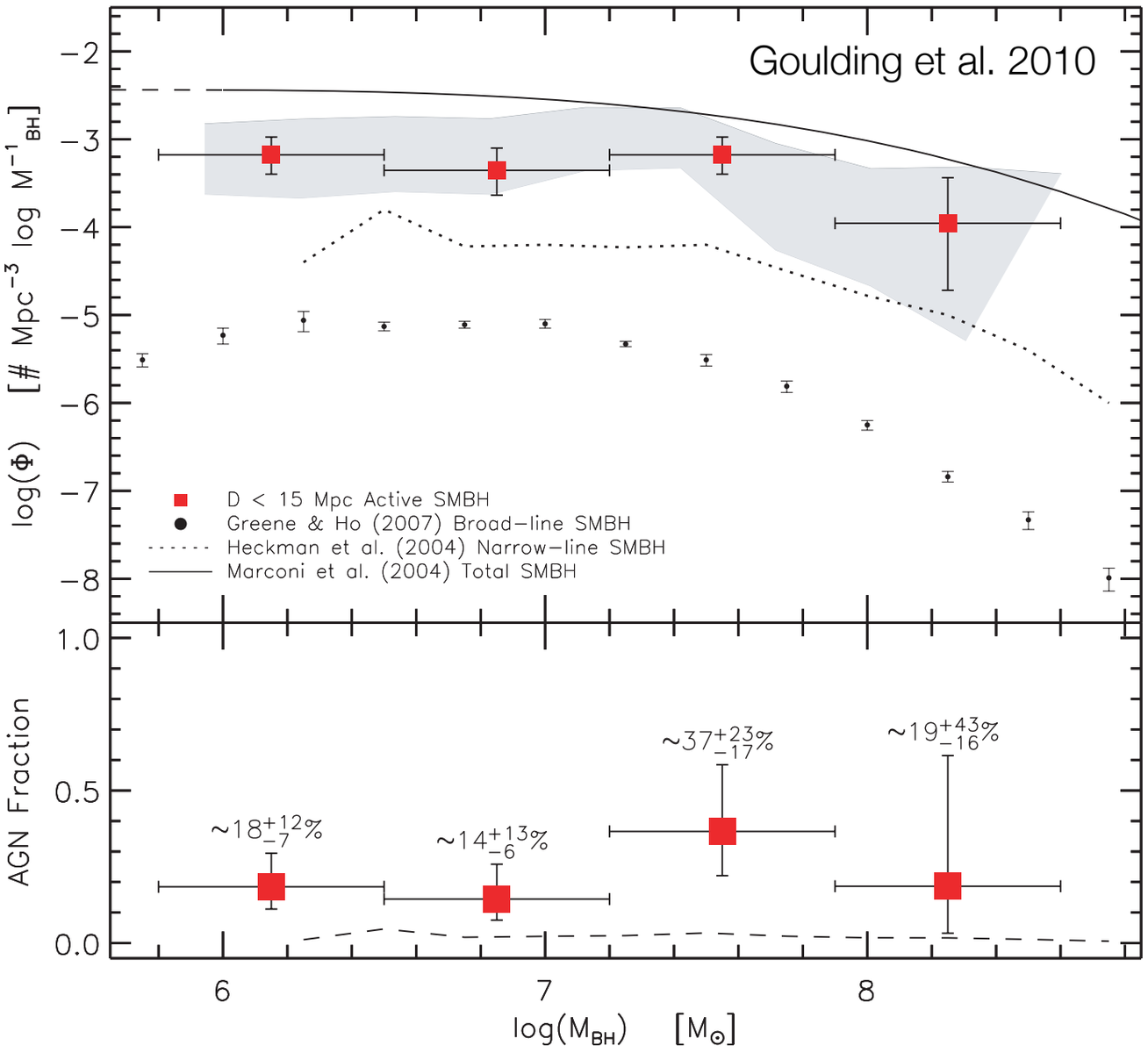

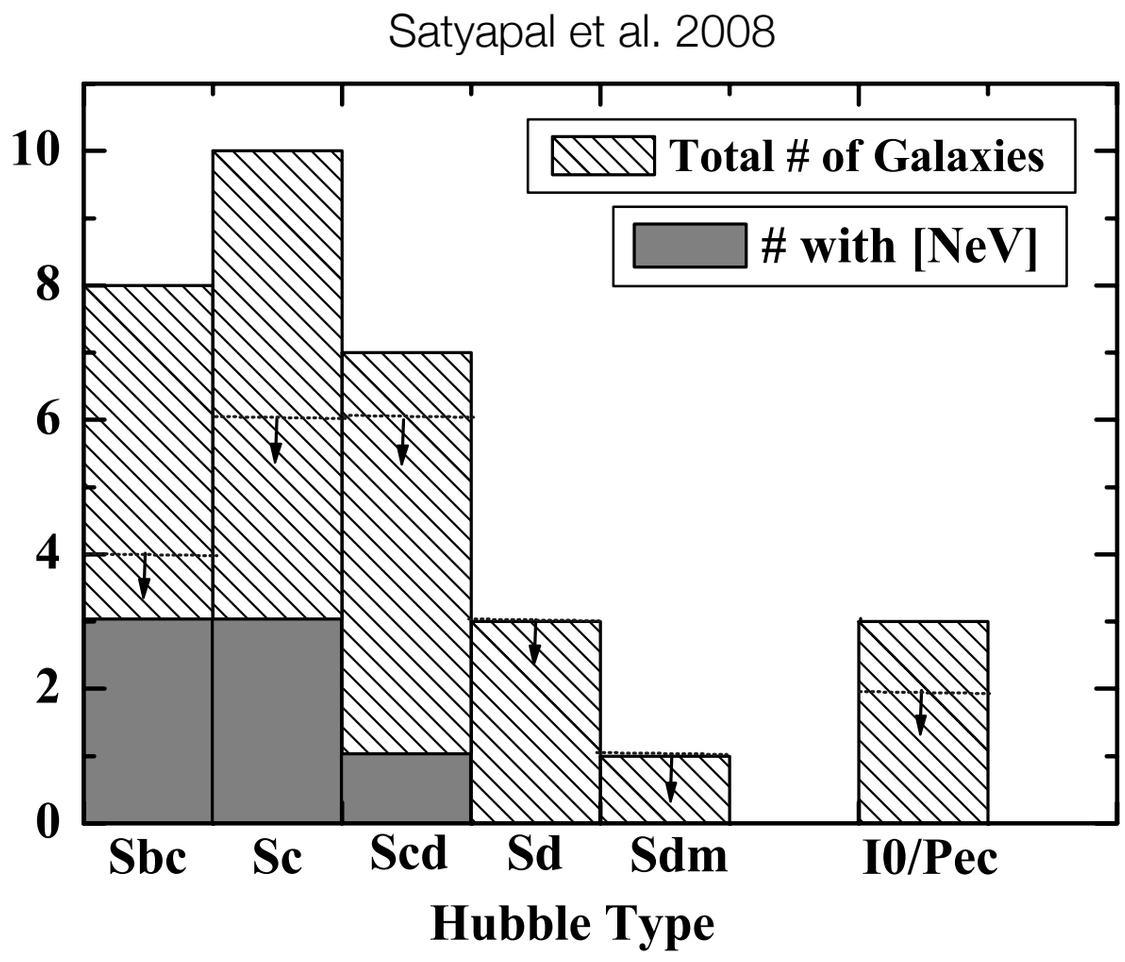

Using [NeV]λ14.3, 15.1 μm lines as indicator of an AGN. Stay tuned for results from Hershel and WISE...

Demographics from Dynamics

M ~ 4,000,000 Suns

M ~ 4,000,000 Suns

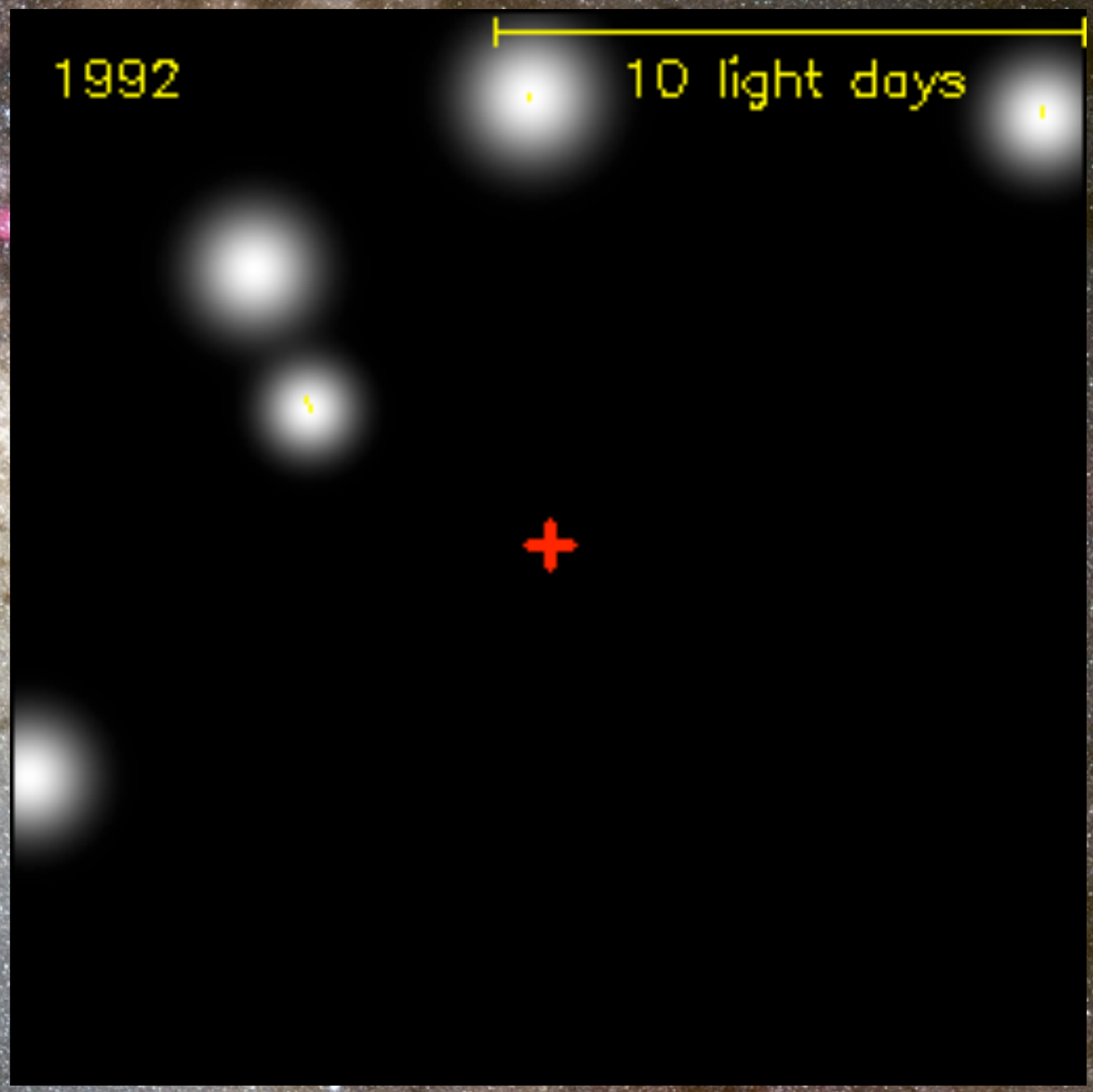

Dynamics

Def of gravitational sphere of influence

$$r_{\rm G} = 0.11 \left(\frac{M_\bullet}{10^8 M_\odot} \right) \left(\frac{200\ {\rm km\ s^{-1}}}{\sigma_\star} \right)^2 \left(\frac{20\ {\rm Mpc}}{D} \right) \ {\rm arcsec.}$$

Required HST to achieve (although now we can also achieve with IFU+AO)

In addition to stellar dynamical modeling, it is also possible to model gas disks (when they exist)

Finally, in special cases we can use very compact masing disks

THE ASTROPHYSICAL JOURNAL, 221:721–730, 1978 May 1

EVIDENCE FOR A SUPERMASSIVE OBJECT IN THE NUCLEUS OF THE GALAXY M87 FROM SIT AND CCD AREA PHOTOMETRY

PETER J YOUNG, JAMES A. WESTPHAL, JEROME KRISTIAN, AND CHRISTOPHER P. WILSON
Hale Observatories, California Institute of Technology, Carnegie Institution of Washington

AND

FREDERICK P. LANDAUER
Space Photography Section, Jet Propulsion Laboratory
Received 1977 June 10; accepted 1977 October 7

ABSTRACT

Two-dimensional SIT and CCD detectors have been used to measure the surface brightness of the peculiar elliptical radio galaxy M87. Measurements were made in three broad-band colors (B, V, and R) to a distance of 80″ from the nucleus, with 1″ spatial resolution and photometric accuracy of the order of 1%.

The data are given in some detail and are compared with earlier photographic results. The most obvious feature of the data is a bright, barely resolved central luminosity spike, which is not seen in similar data on other nearby normal ellipticals. Also, attempts to fit isothermal or King models away from the nuclear spike show additional excess luminosity in the central regions of the galaxy ($r < 10''$), which cannot be fitted by such a model.

A model-independent dynamical analysis, using the photometric data combined with spectrographic results by Sargent *et al.*, shows that the nucleus of M87 contains a compact mass of low luminosity, with $M = 5 \times 10^9\ M_\odot$, $r < 100$ pc, and $M/\mathscr{L} > 60$. All of the existing data is well fitted by a King model containing a central black hole of mass $M = 3 \times 10^9\ M_\odot$ and a point luminosity source. While such a model is not uniquely required by the data, it is perhaps the most plausible of several possible models considered. At present, M87 is probably the best case for a hypothetical massive black hole in a galaxy nucleus.

EVIDENCE I

PETER
Hal

AL, 221:

CT IN
D ARI

ROME K
Technol

AND

P. LA
on, Jet

0; accep

STRAC

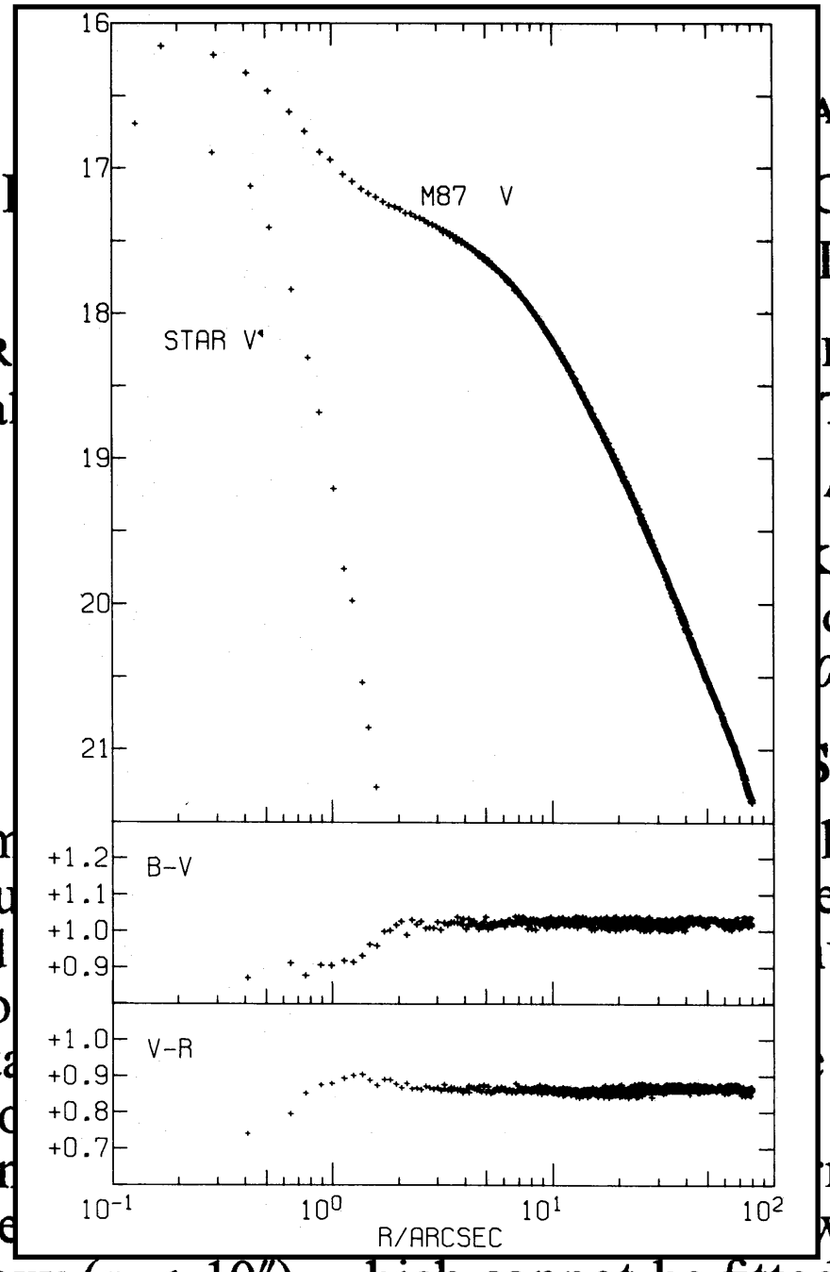

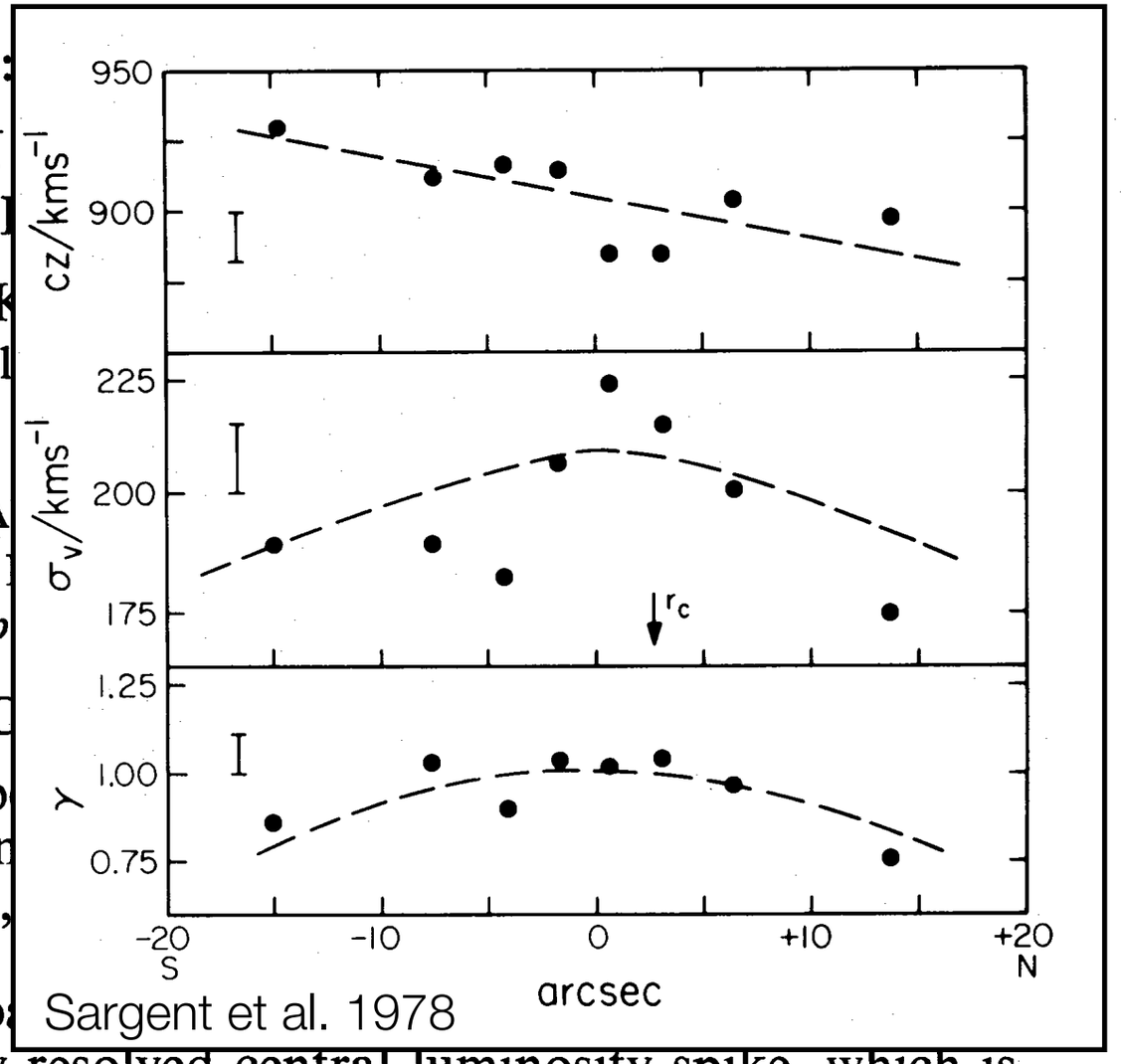

Sargent et al. 1978

have b
easuren
ucleus,

Two-dim
of the pecu
(*B*, *V*, and
accuracy o

The data
most obvic
not seen in
King mode

comp
barely resolved central luminosity spike, which is
mal ellipticals. Also, attempts to fit isothermal or
w additional excess luminosity in the central regions
of the galaxy ($r < 10''$), which cannot be fitted by such a model.

A model-independent dynamical analysis, using the photometric data combined with spectrographic results by Sargent *et al.*, shows that the nucleus of M87 contains a compact mass of low luminosity, with $M = 5 \times 10^9\ M_\odot$, $r < 100$ pc, and $M/\mathscr{L} > 60$. All of the existing data is well fitted by a King model containing a central black hole of mass $M = 3 \times 10^9\ M_\odot$ and a point luminosity source. While such a model is not uniquely required by the data, it is perhaps the most plausible of several possible models considered. At present, M87 is probably the best case for a hypothetical massive black hole in a galaxy nucleus.

Observed Kinematics
V, σ, h3, h4 -- this from SAURON

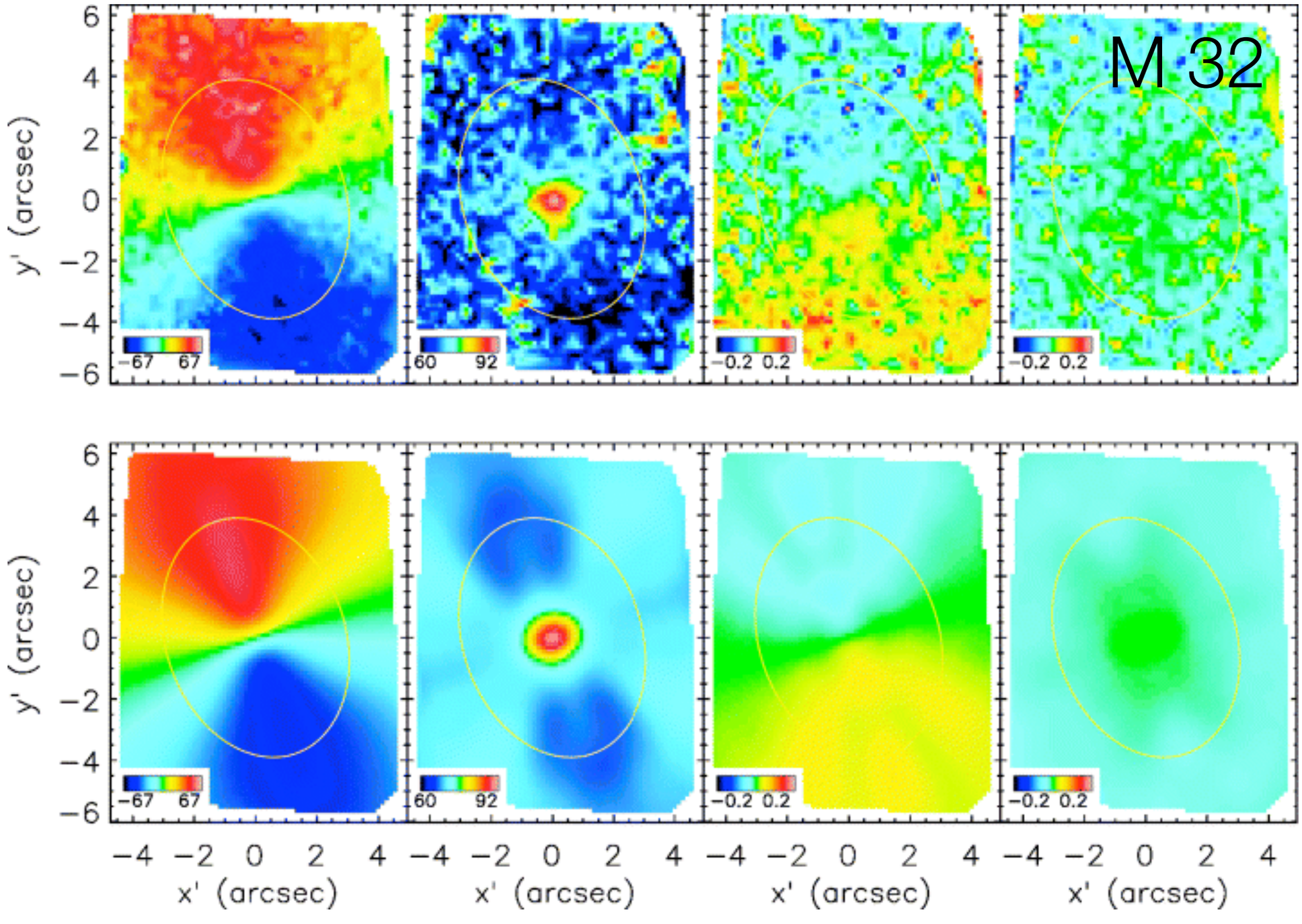

Stellar dynamical model
Based on a library of orbits

Verolme et al. 2002

Observed Kinematics
V, σ, h3, h4 -- this from SAURON

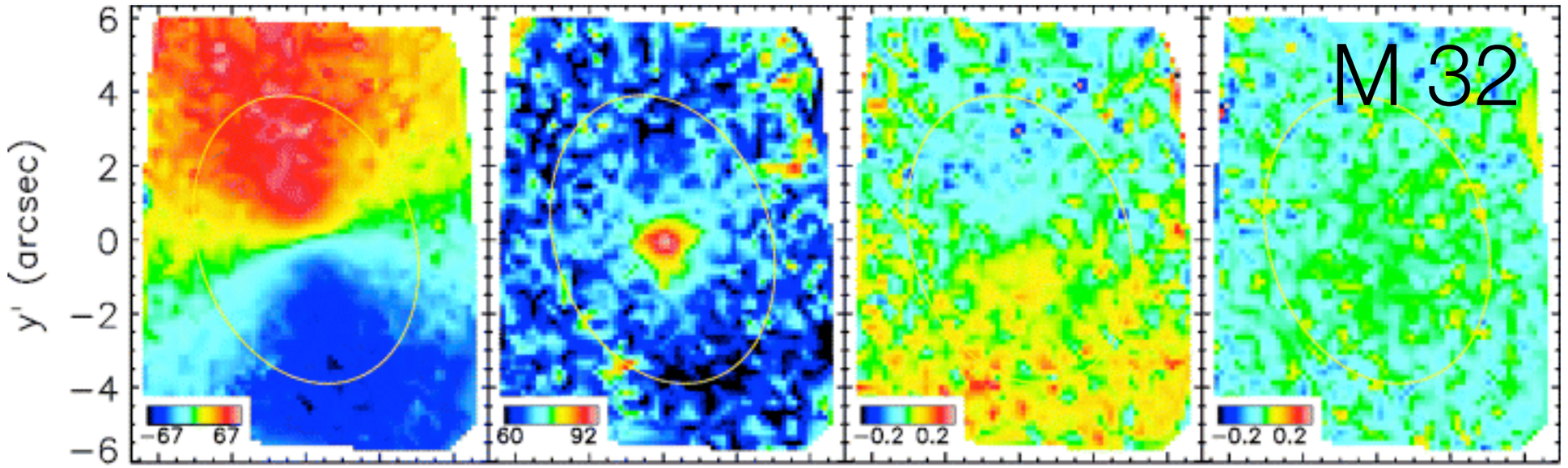

Stellar dynamical model
Based on a library of orbits

Verolme et al. 2002

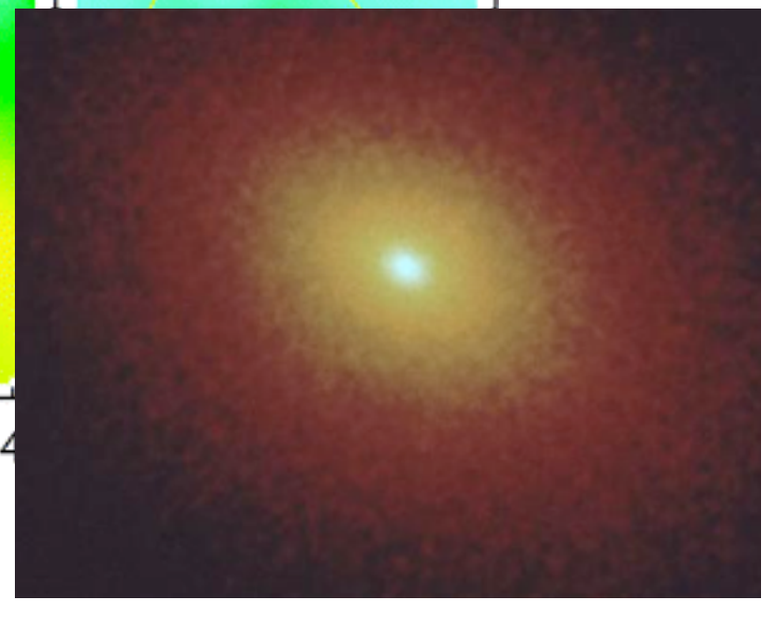

HST+ground-based
imaging (+deprojection)
gives mass distribution

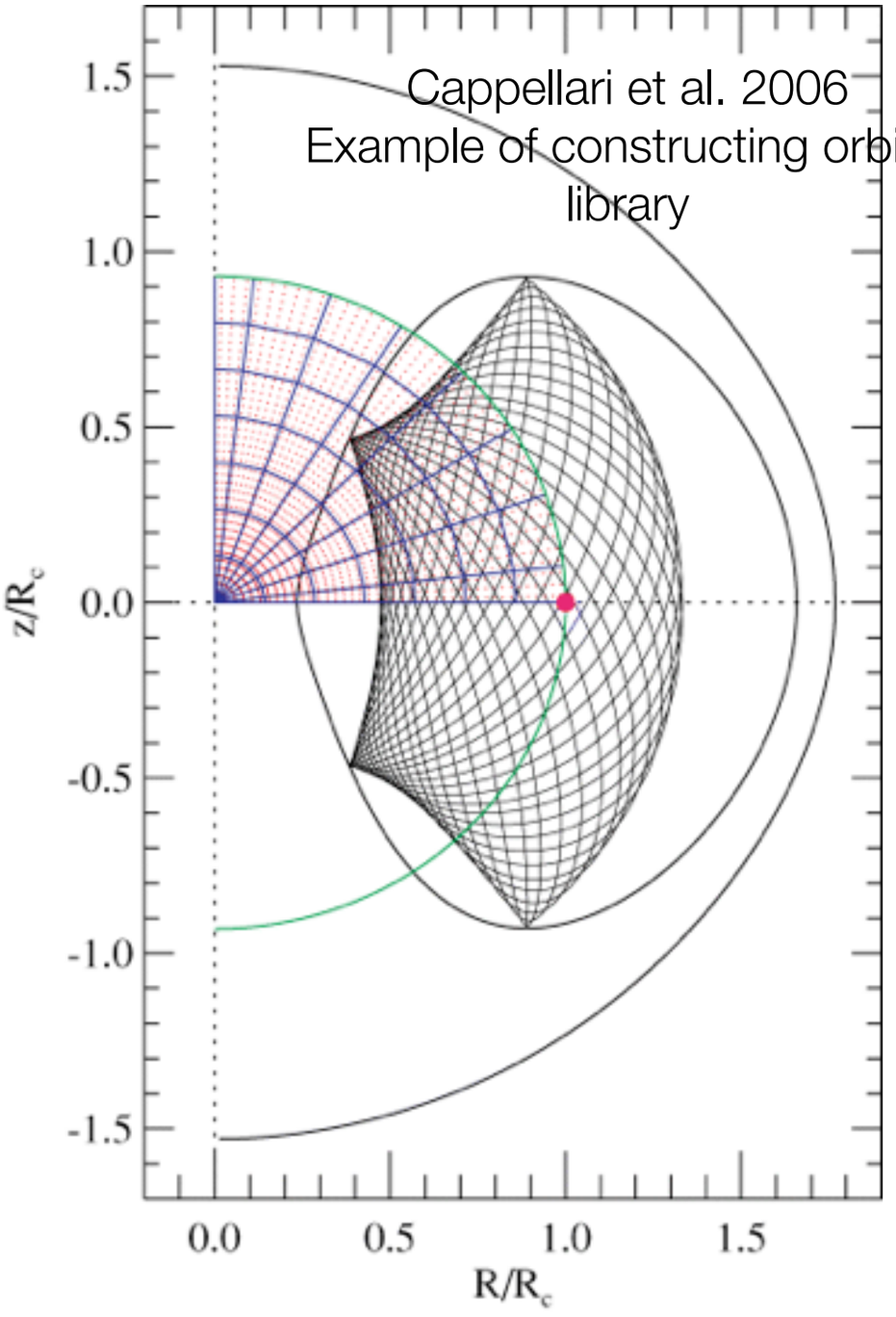

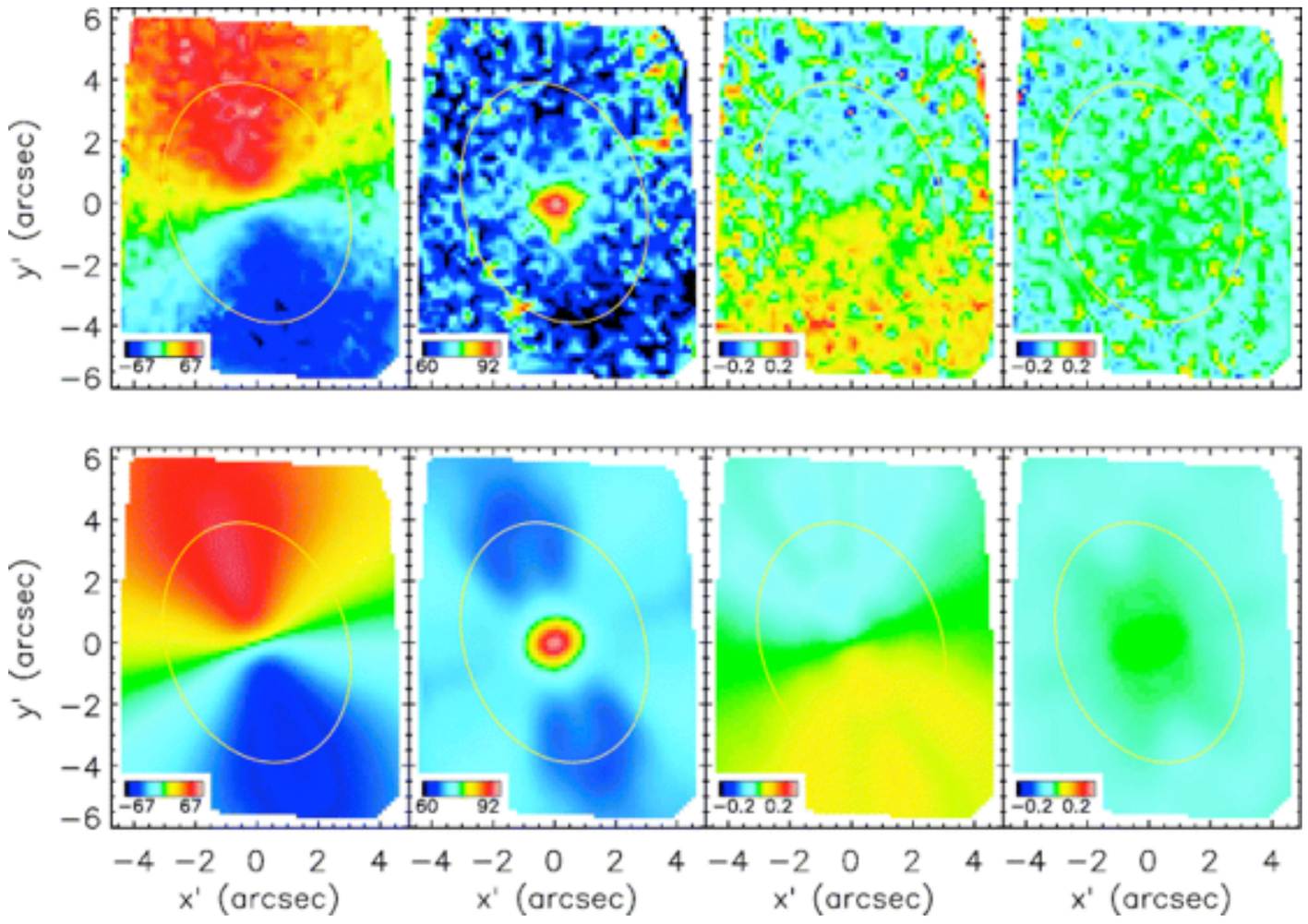

From the collisionless Boltzmann Equation we have:

$$M(r) = \frac{V^2 r}{G} + \frac{\sigma_r^2 r}{G}\left[-\frac{d\ln \nu}{d\ln r} - \frac{d\ln \sigma_r^2}{d\ln r} - \left(1 - \frac{\sigma_\theta^2}{\sigma_r^2}\right) - \left(1 - \frac{\sigma_\phi^2}{\sigma_r^2}\right)\right]$$

density of the tracer population

anisotropy

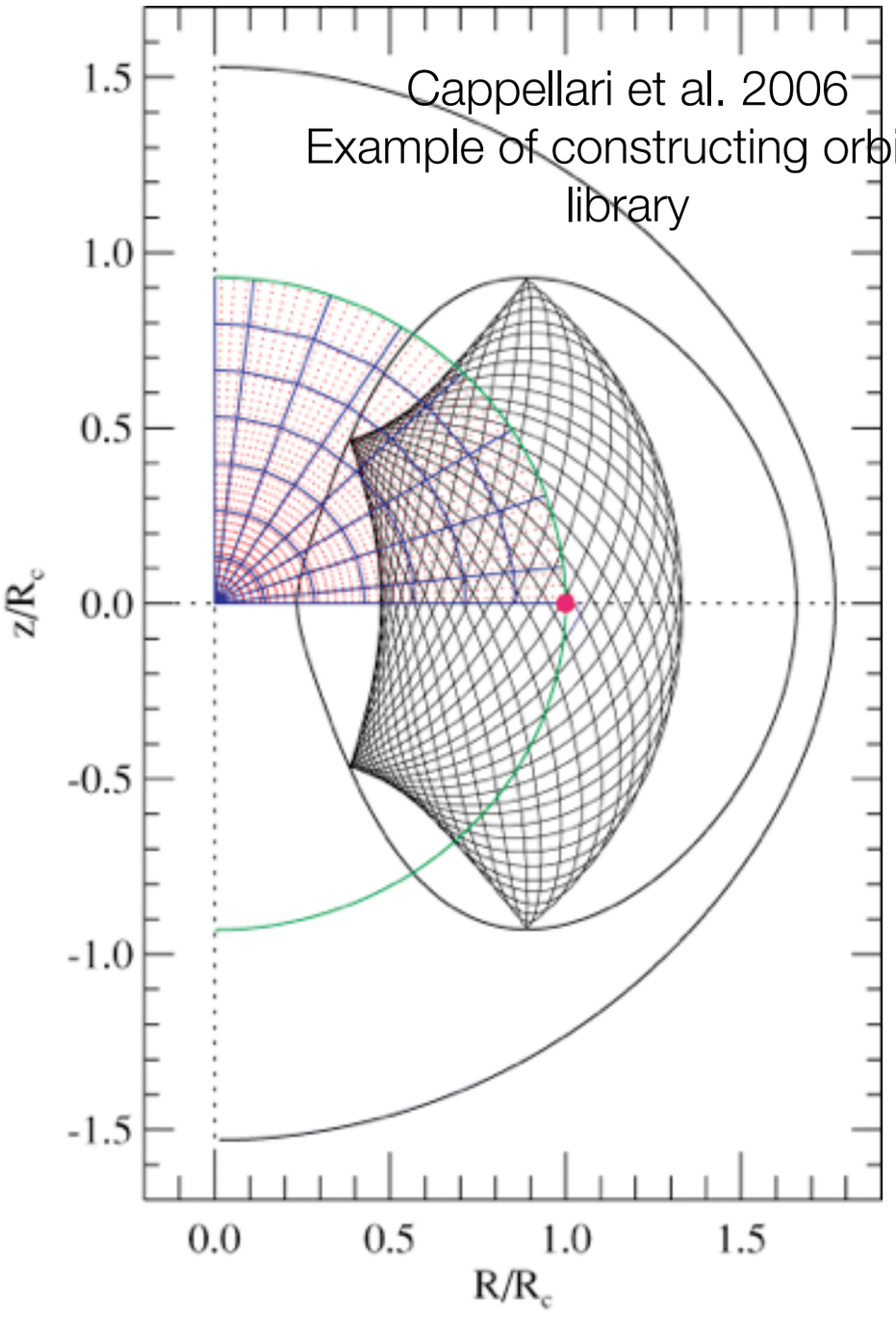

Outstanding uncertainties: triaxiality? DM halo?

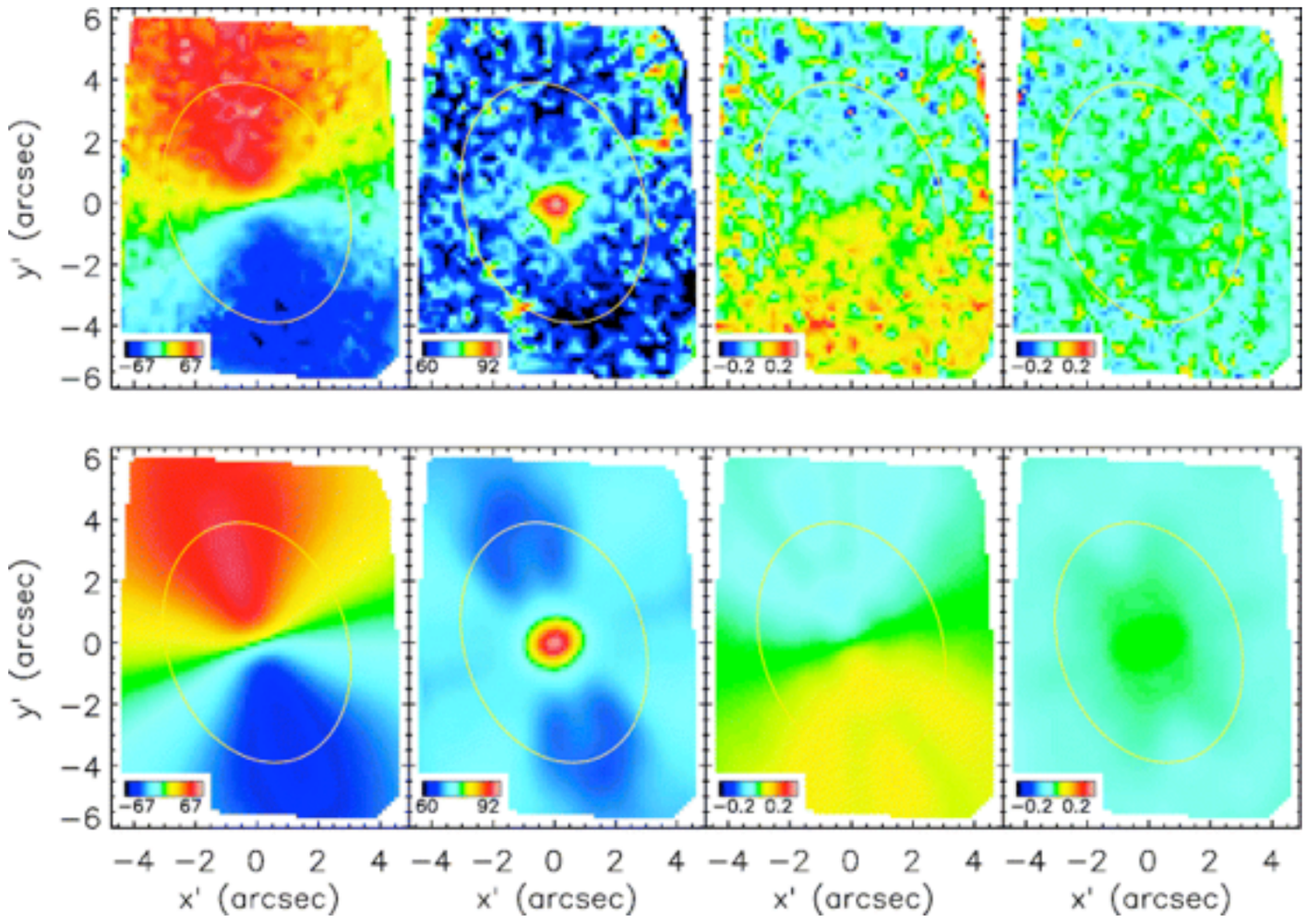

From the collisionless Boltzmann Equation we have:

$$M(r) = \frac{V^2 r}{G} + \frac{\sigma_r^2 r}{G}\left[-\frac{d\ln\nu}{d\ln r} - \frac{d\ln\sigma_r^2}{d\ln r} - \left(1 - \frac{\sigma_\theta^2}{\sigma_r^2}\right) - \left(1 - \frac{\sigma_\phi^2}{\sigma_r^2}\right)\right]$$

density of the tracer population

anisotropy

Gas-dynamical Measurements

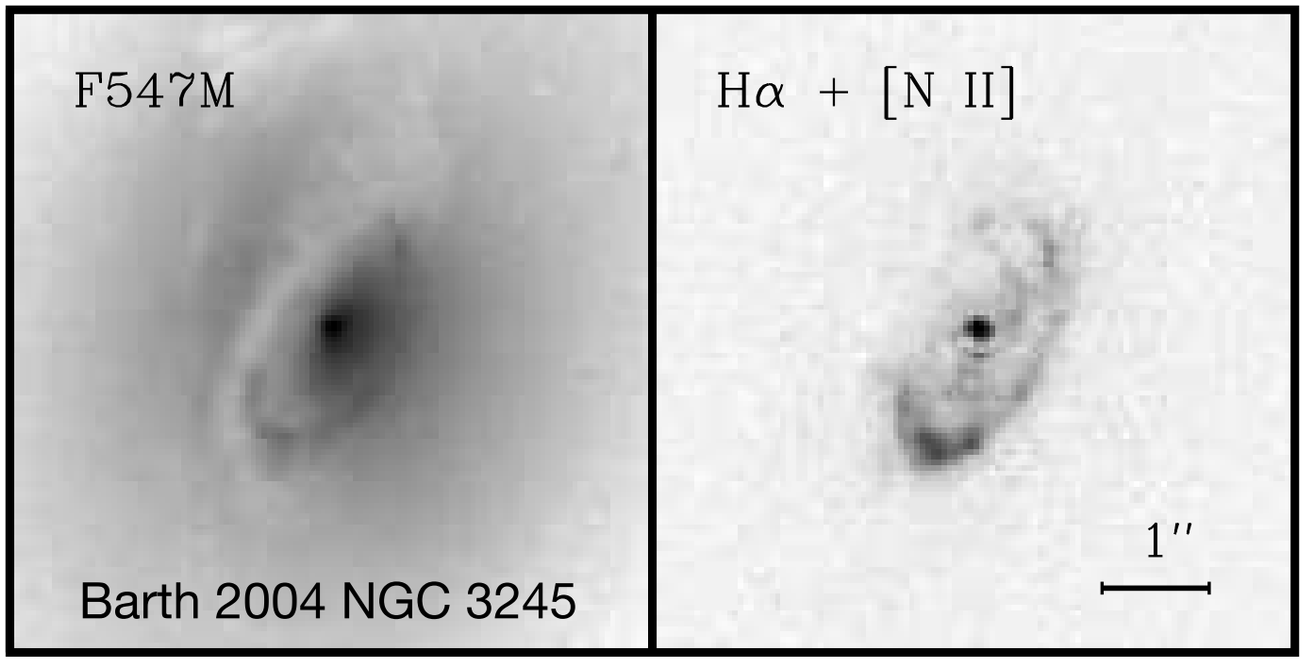

Example ionized gas disk. HST finds ~20% of ellipticals contain well-organized ionized gas disks at their center

Rotation curves for different enclosed masses. Like the stellar-dynamical case, a luminosity profile is needed to derive the potential

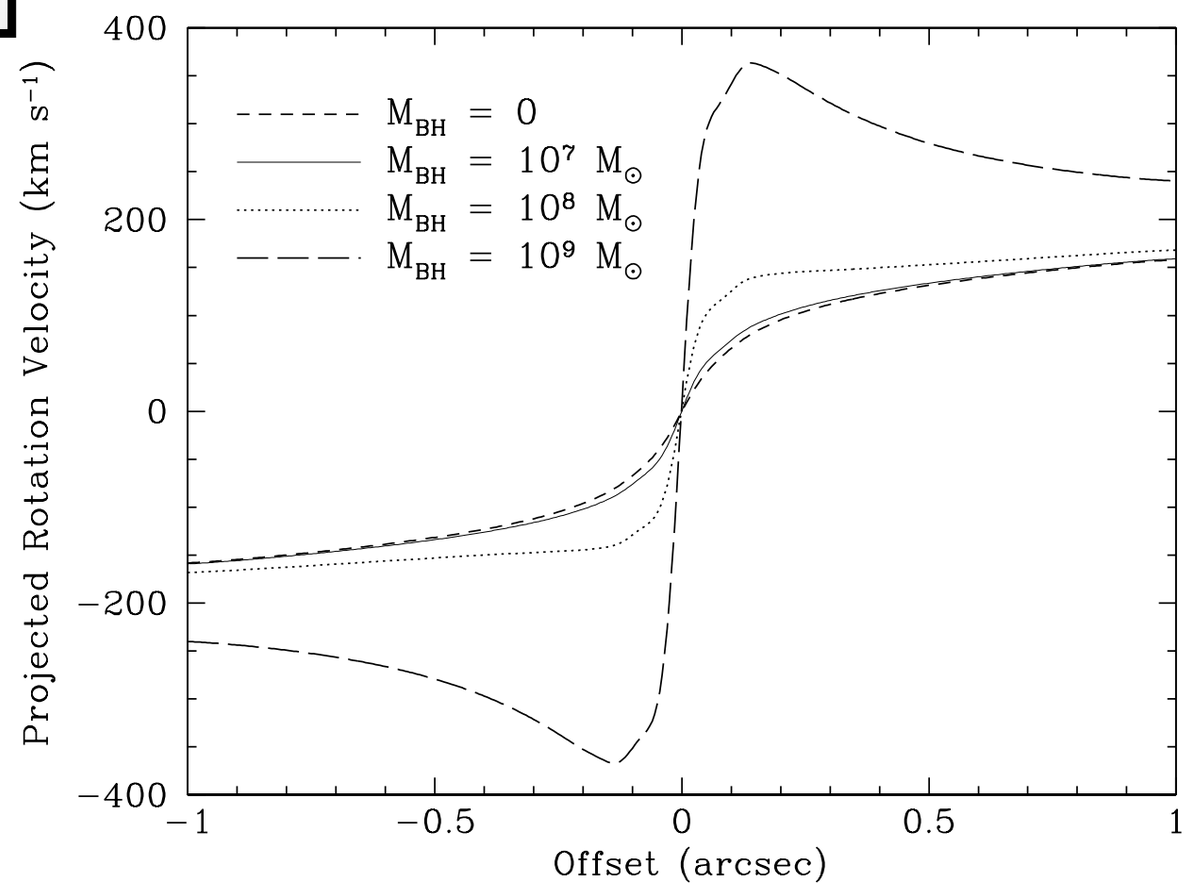

Gas-dynamical Measurements

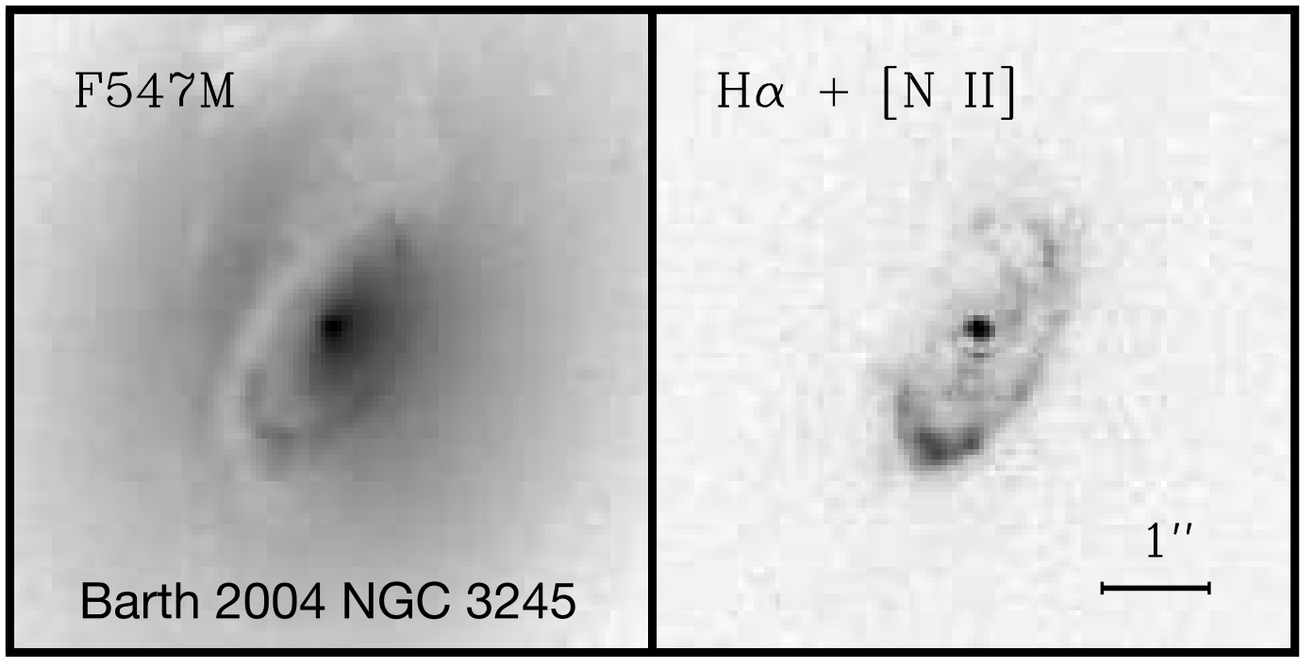

Example ionized gas disk. HST finds ~20% of ellipticals contain well-organized ionized gas disks at their center

Outstanding uncertainties: inclination? turbulence?

Rotation curves for different enclosed masses. Like the stellar-dynamical case, a luminosity profile is needed to derive the potential

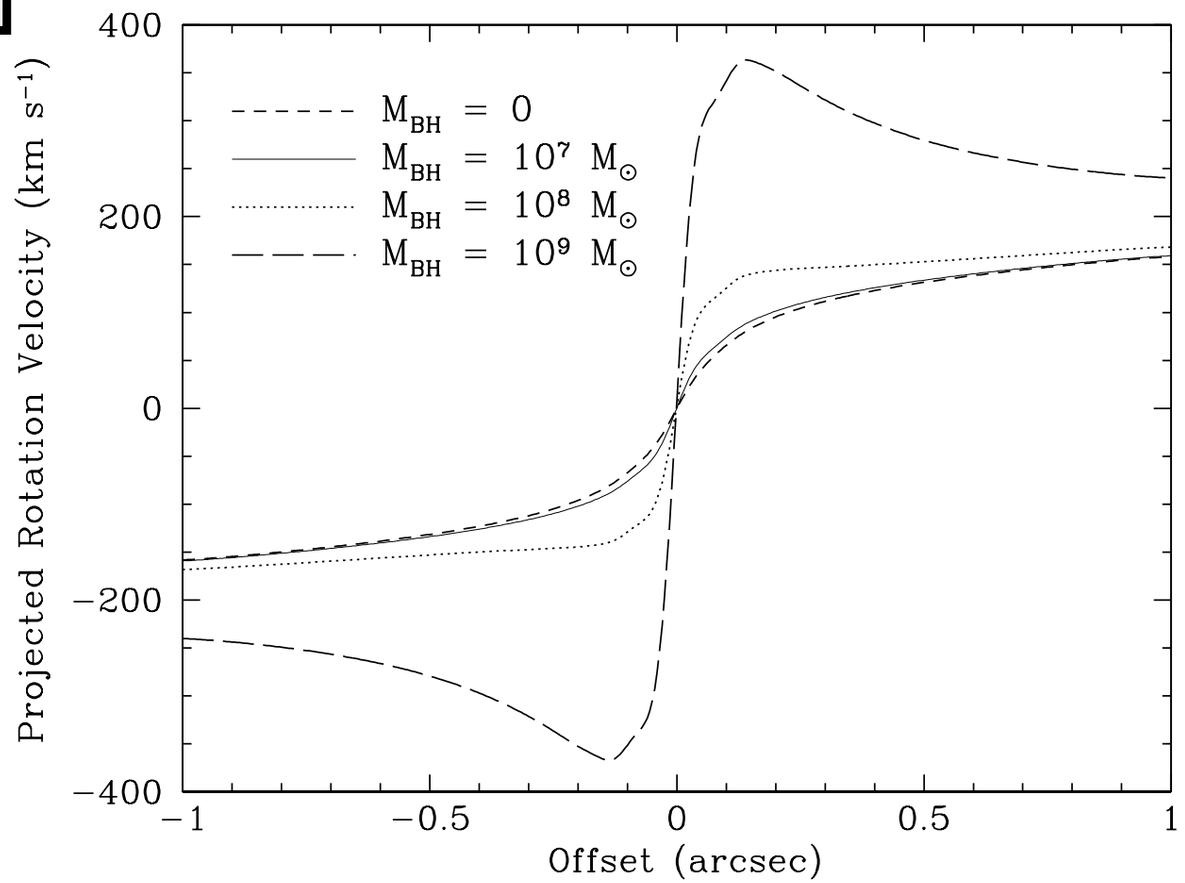

Galaxy M84 Nucleus

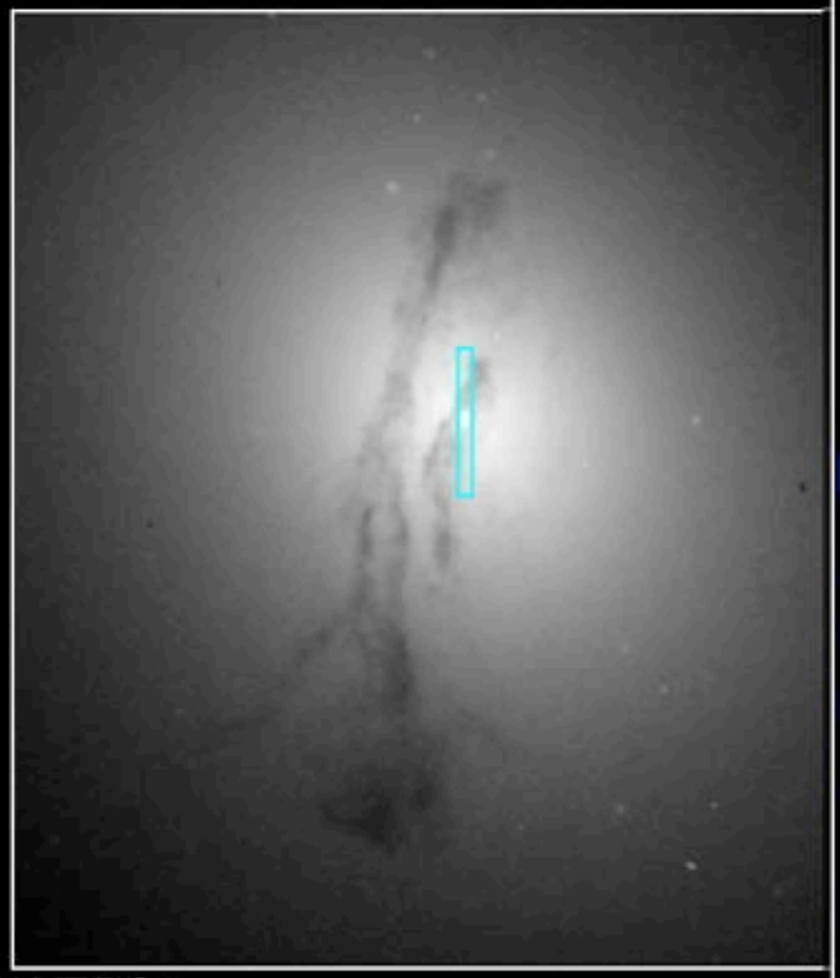

WFPC2

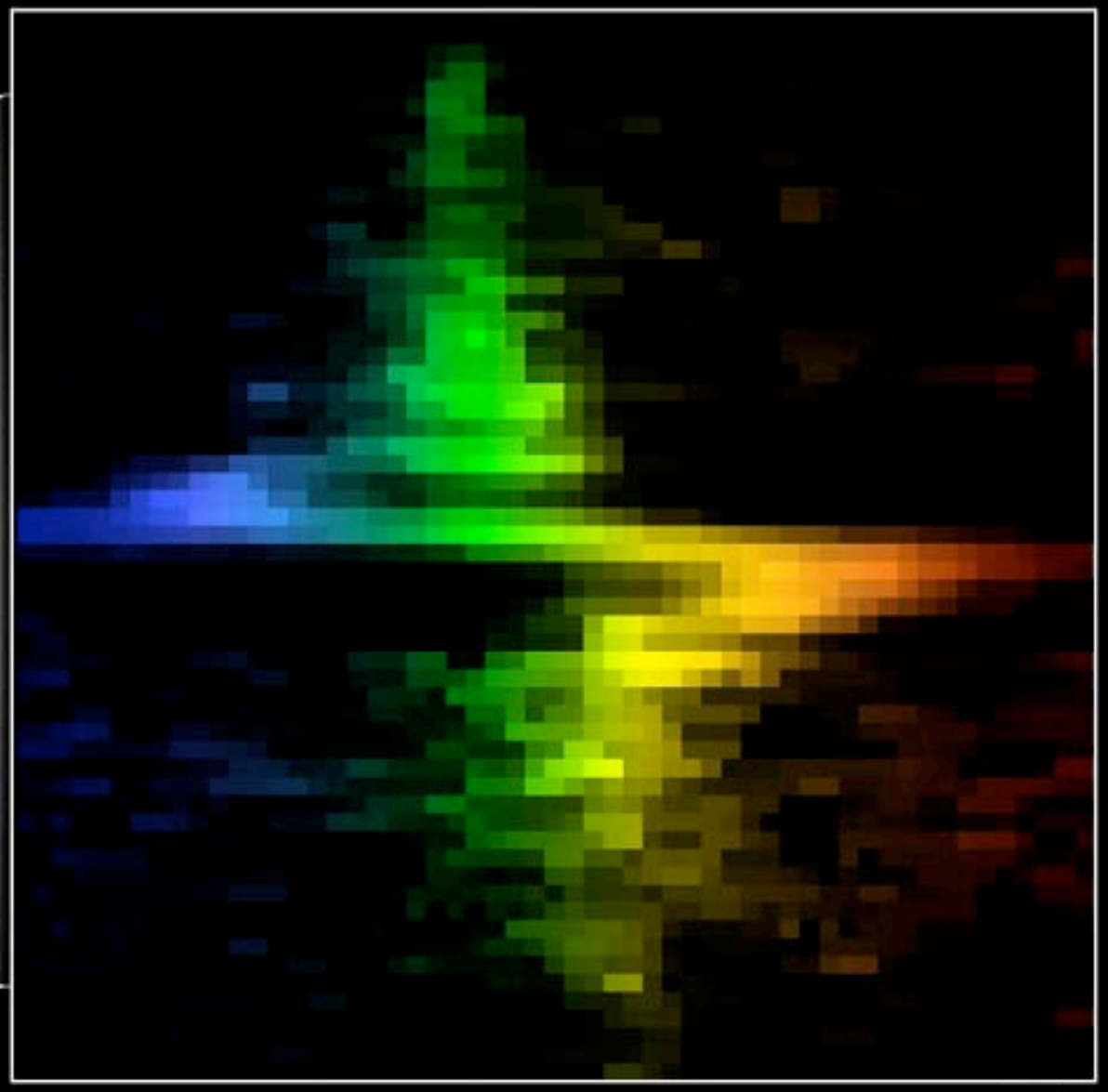

STIS

Hubble Space Telescope

PRC97-12 • ST ScI OPO • May 12, 1997 • B. Woodgate (GSFC), G. Bower (NOAO) and NASA

Megamasers: NGC 4258

- H_20 megamasers (microwave amplification by stimulated emission; 10^2-10^4 $L_\odot$) as dynamical tracers

- Very precise BH mass ($3.9\pm0.1 \times 10^7$ $M_\odot$), relatively free of systematic bias

- With accelerations, also measure an angular-diameter distance

- Along with MW, best case to rule out astrophysical alternatives to SMBH (e.g., Maoz et al. 1995, 1998)

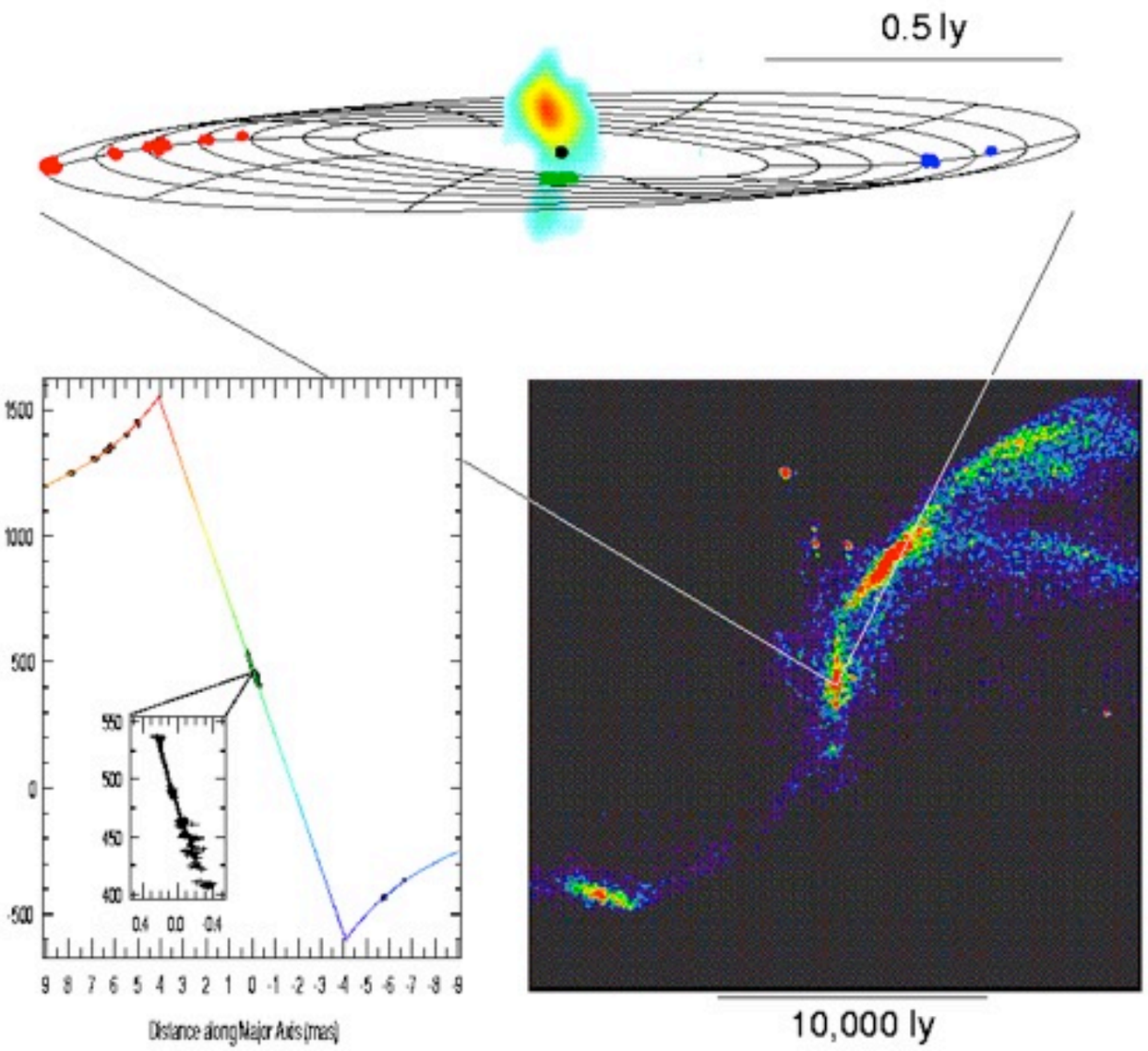

Miyoshi et al., Herrnstein et al., Greenhill, Humphreys, Moran

galaxy is ~7 Mpc away

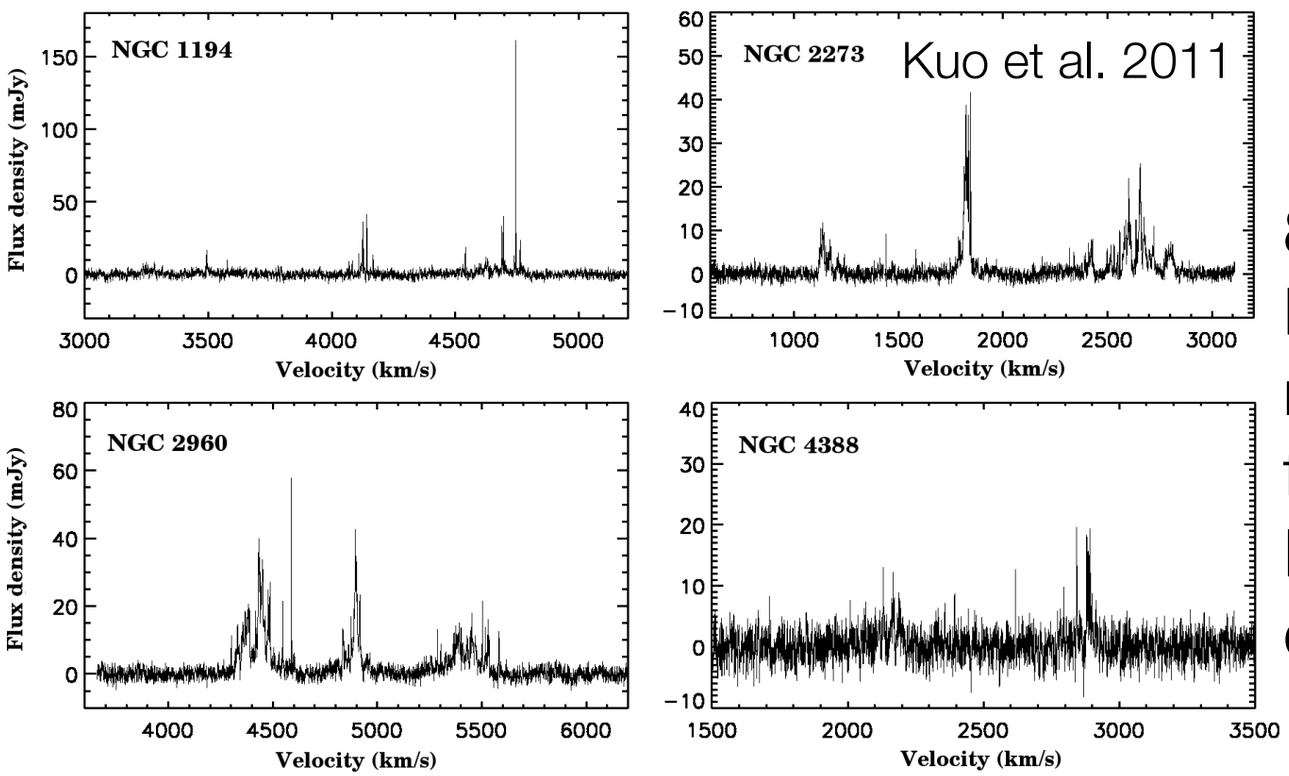

8 new megamaser disks with beautiful Keplerian rotation curves. Yield BH masses with <10% precision (!). Hoping for 10 more soon.

Important to cross-calibrate stellar-dynamical masses with maser masses.

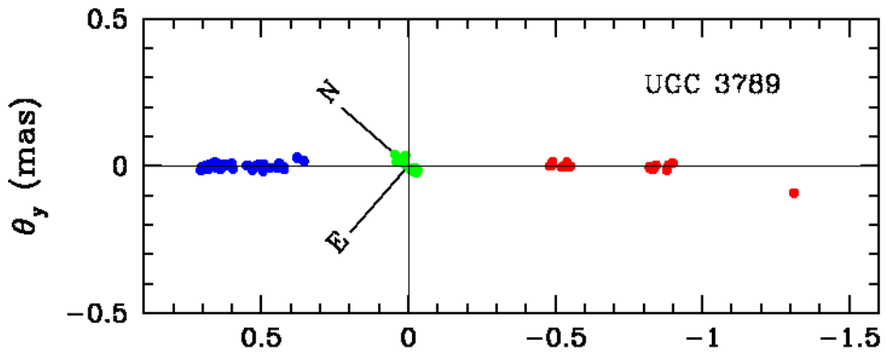

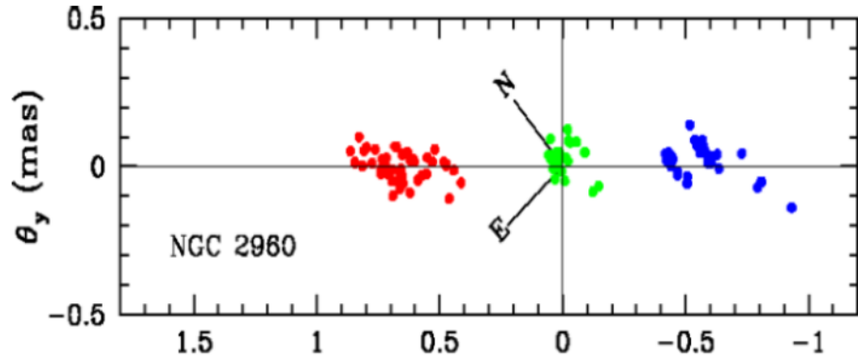

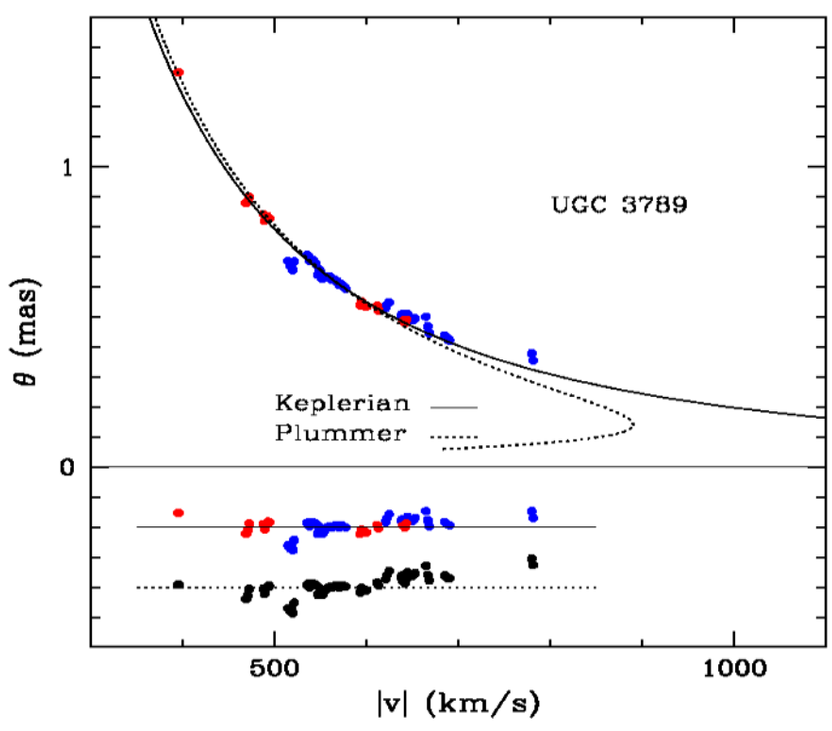

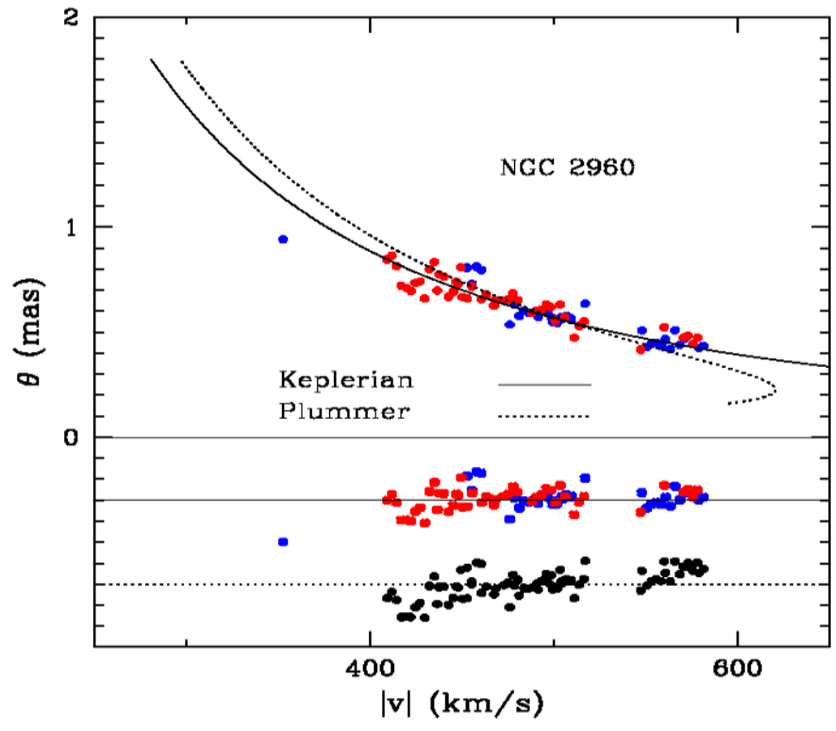

All Massive Galaxies Harbor Massive Black Holes

The first, and most basic, conclusion of the dynamical studies is that all bulge-dominated galaxies contain BHs. This is the same as the result from the active galaxies.

Maoz 1998

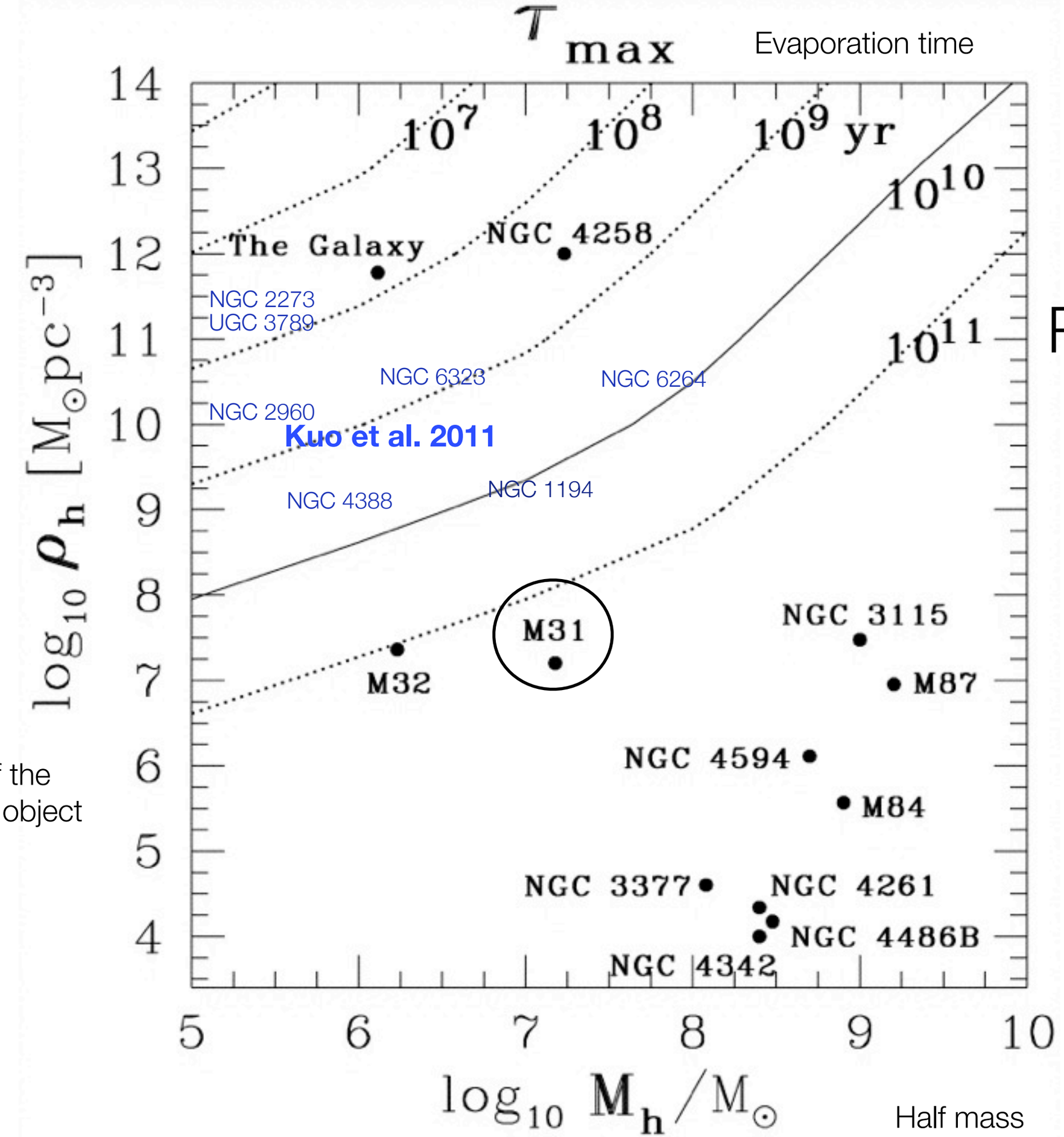

Density of the central dark object

Real BHs!

Scaling Relations -- First Luminosity

Kormendy & Richstone 1995

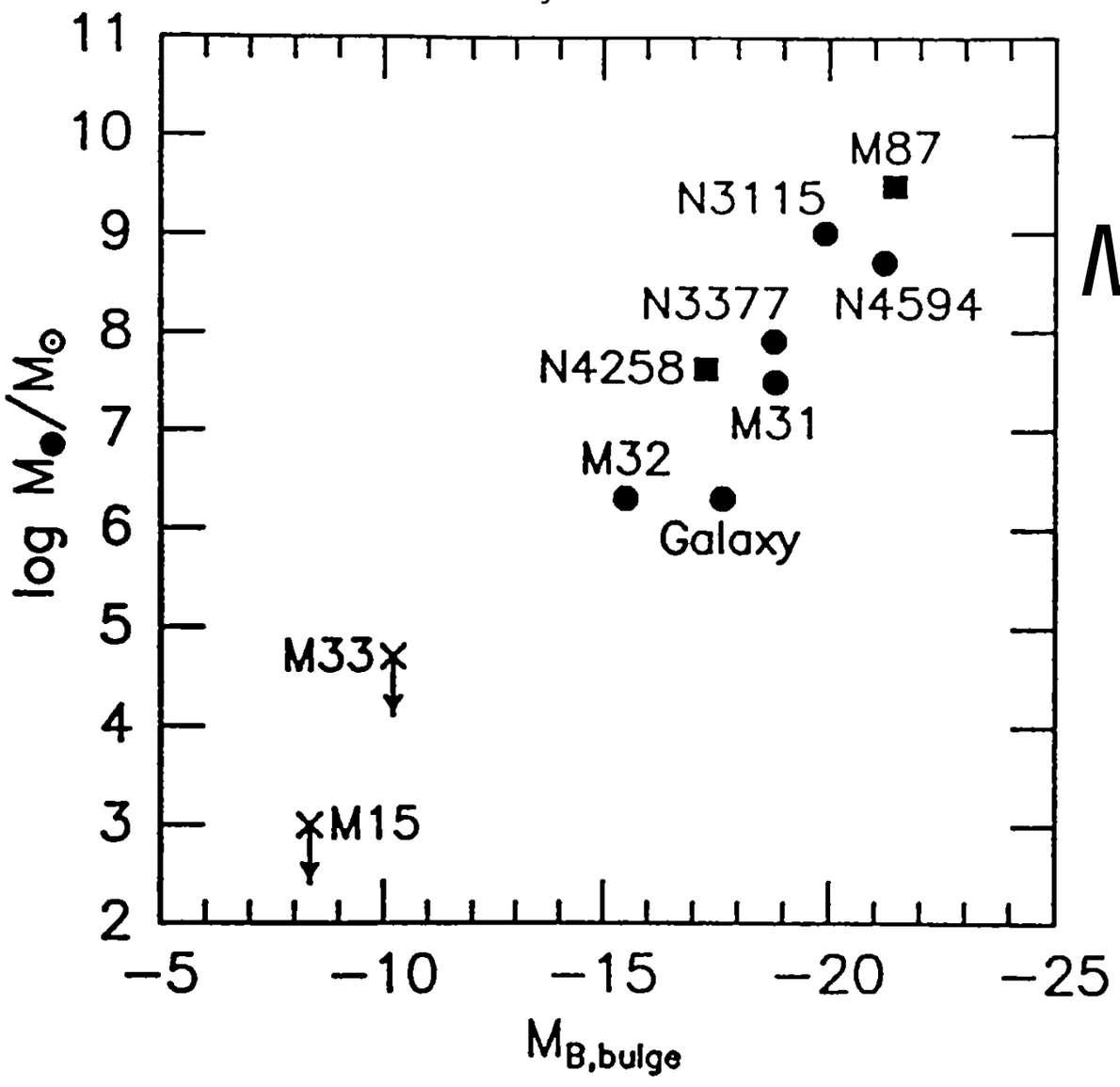

M_{BH}

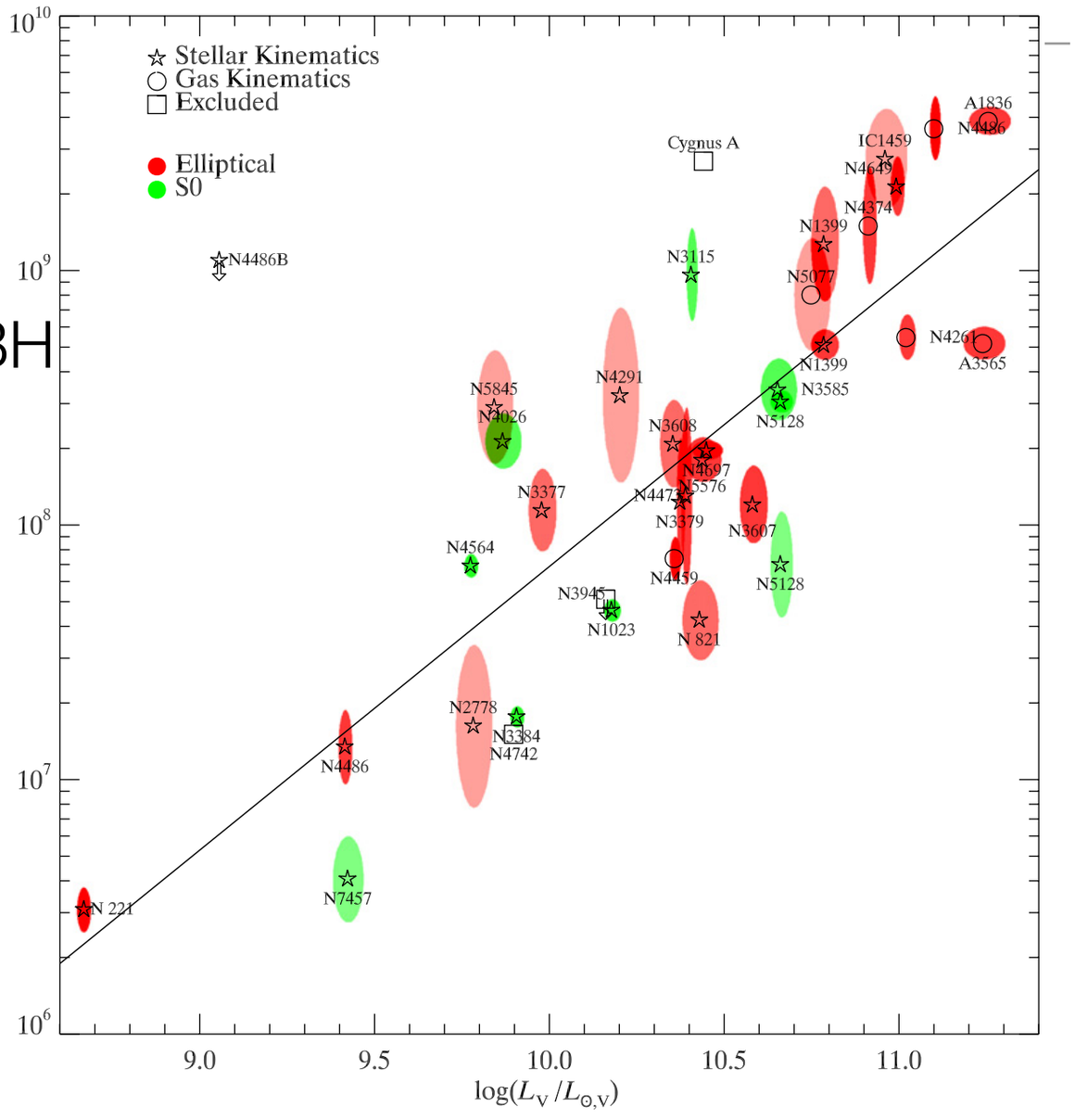

Gültekin et al. 2009 L_{BH}

Gültekin et al. 2009

Stellar dynamics
Gas dynamics
Masers
Excluded
Elliptical
S0
Spiral

gas
stars

Scatter is only a factor of 2-3

M_{BH}-σ★

$M\ (M_\odot)$

σ (km s^{-1})

10^{10}
10^{9}
10^{8}
10^{7}
10^{6}

60
80
100
200
300
400

A1836-BCG
N4486
IC1459
N4649
N1399
N3115
N5077
N1399
A3565-BCG
N5128
N3998
N 224
N3377
N4596
N1300
N1023
N2748
N4258
N2787
N 821
N2778
N4486A
N1068
N4435
N7457
N 221
MW
Circinus

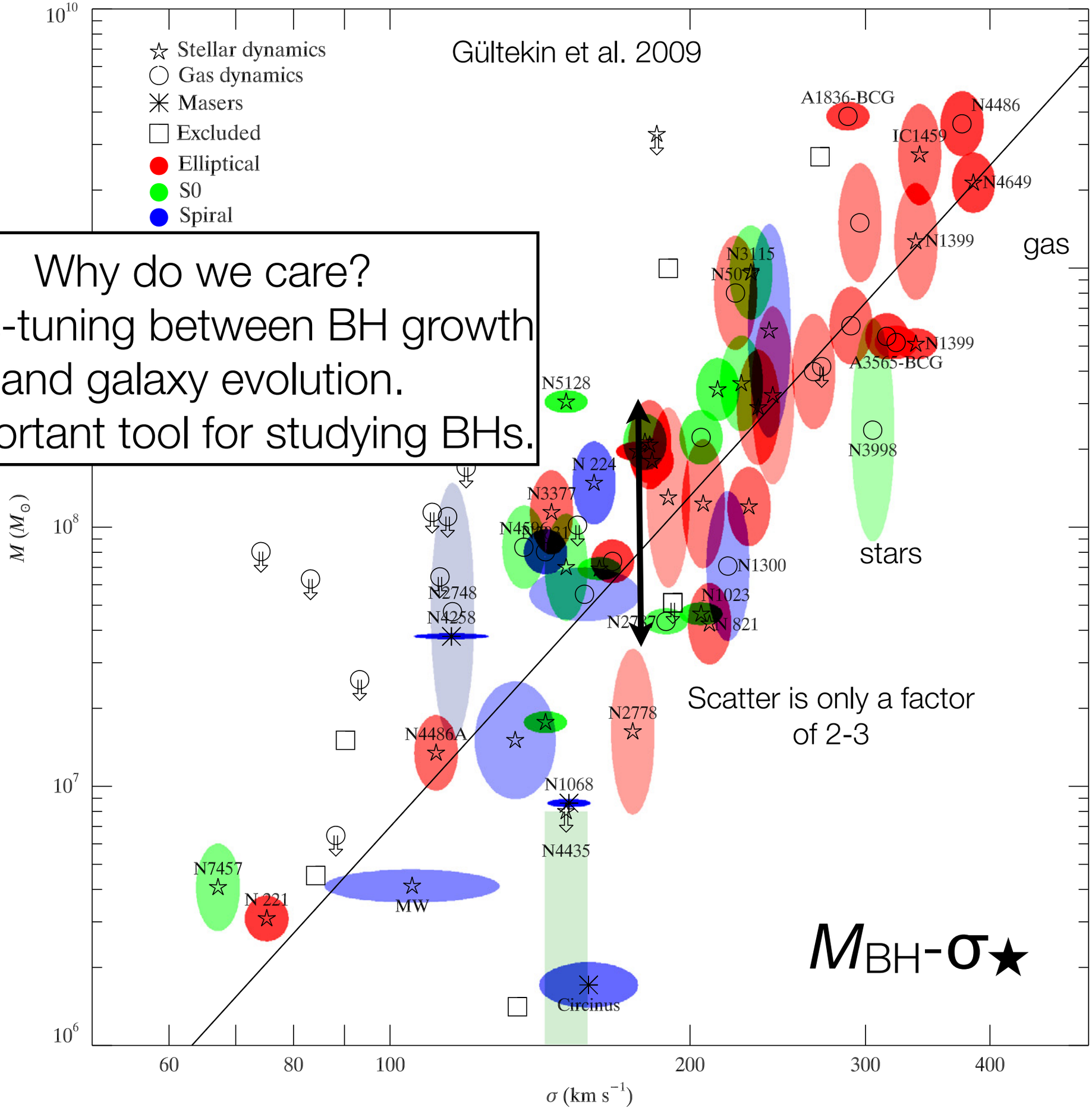
Gültekin et al. 2009
Stellar dynamics
Gas dynamics
Masers
Excluded
Elliptical
S0
Spiral
Why do we care?
1. Fine-tuning between BH growth and galaxy evolution.
2. Important tool for studying BHs.
gas
stars
Scatter is only a factor of 2-3
M_{BH}-σ★
$M\ (M_\odot)$
σ (km s^{-1})
10^{10}
10^8
10^7
10^6
60
80
100
200
300
400
A1836-BCG
N4486
IC1459
N4649
N1399
N3115
N5077
N1399
A3565-BCG
N5128
N3998
N 224
N3377
N1300
N2748
N4258
N1023
N 821
N2778
N4486A
N1068
N4435
N7457
N 221
MW
Circinus

Scaling Relations -- Also bulge mass

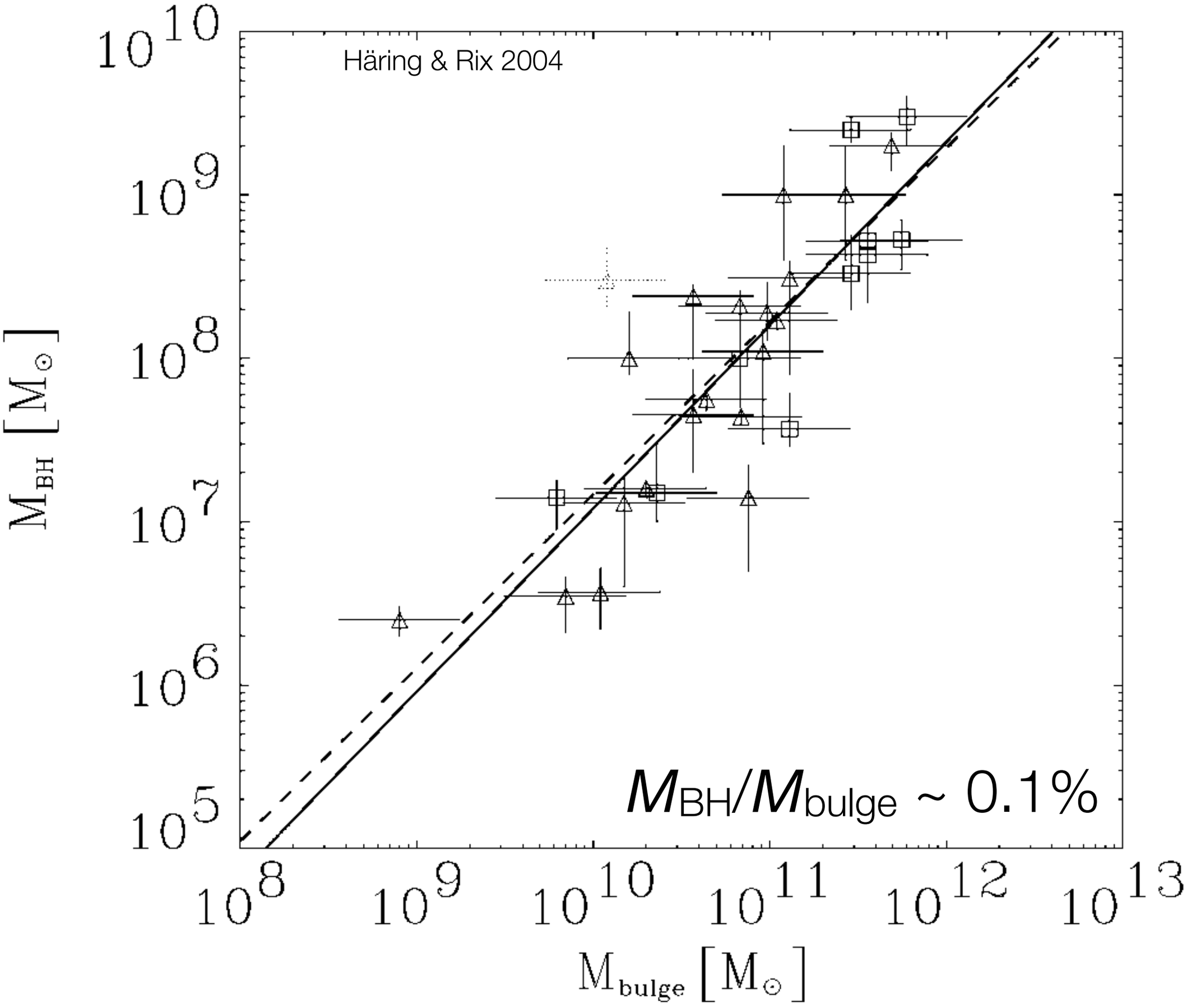

Dark Halo Mass?

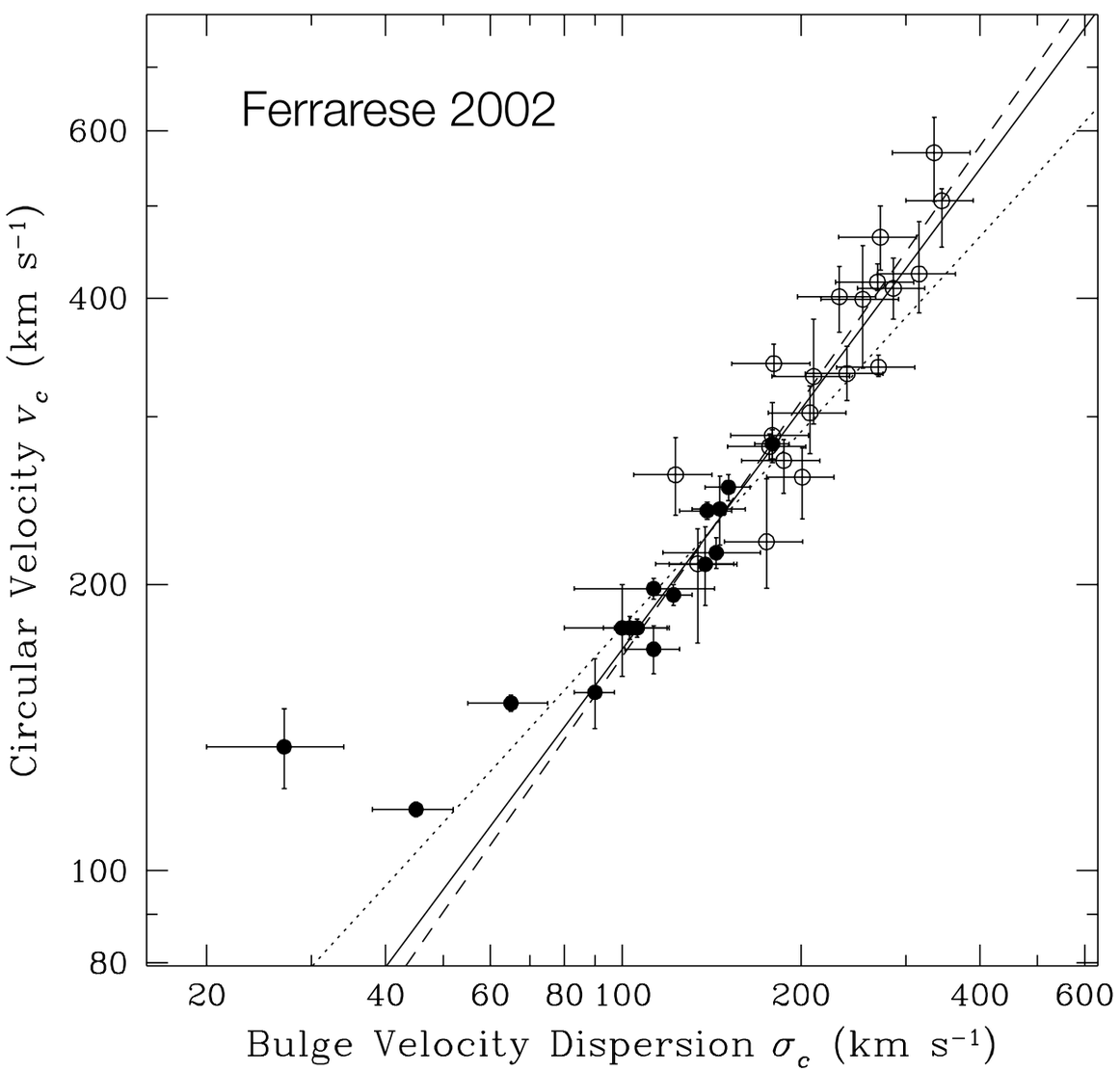

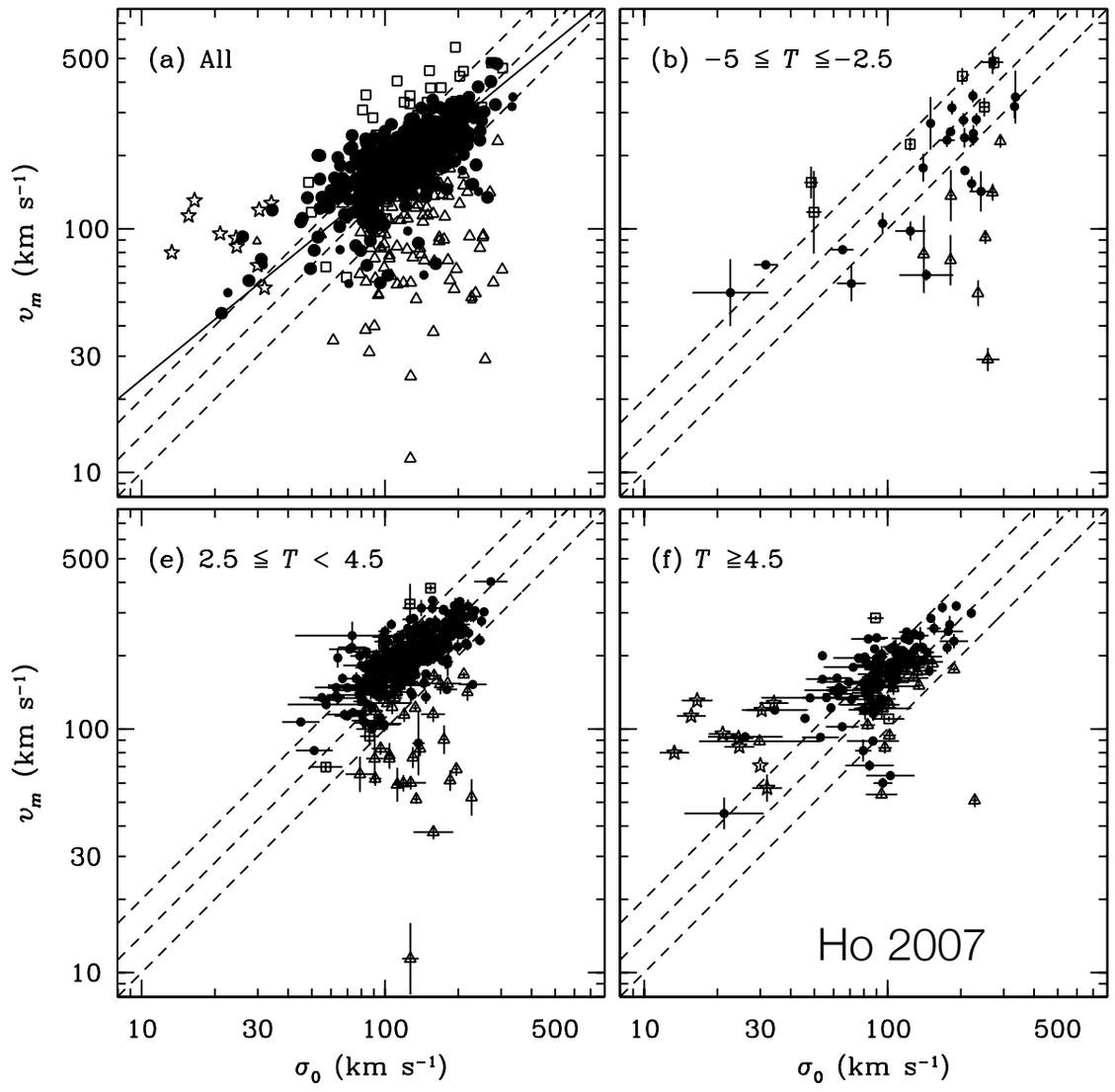

Dark Halo Mass?

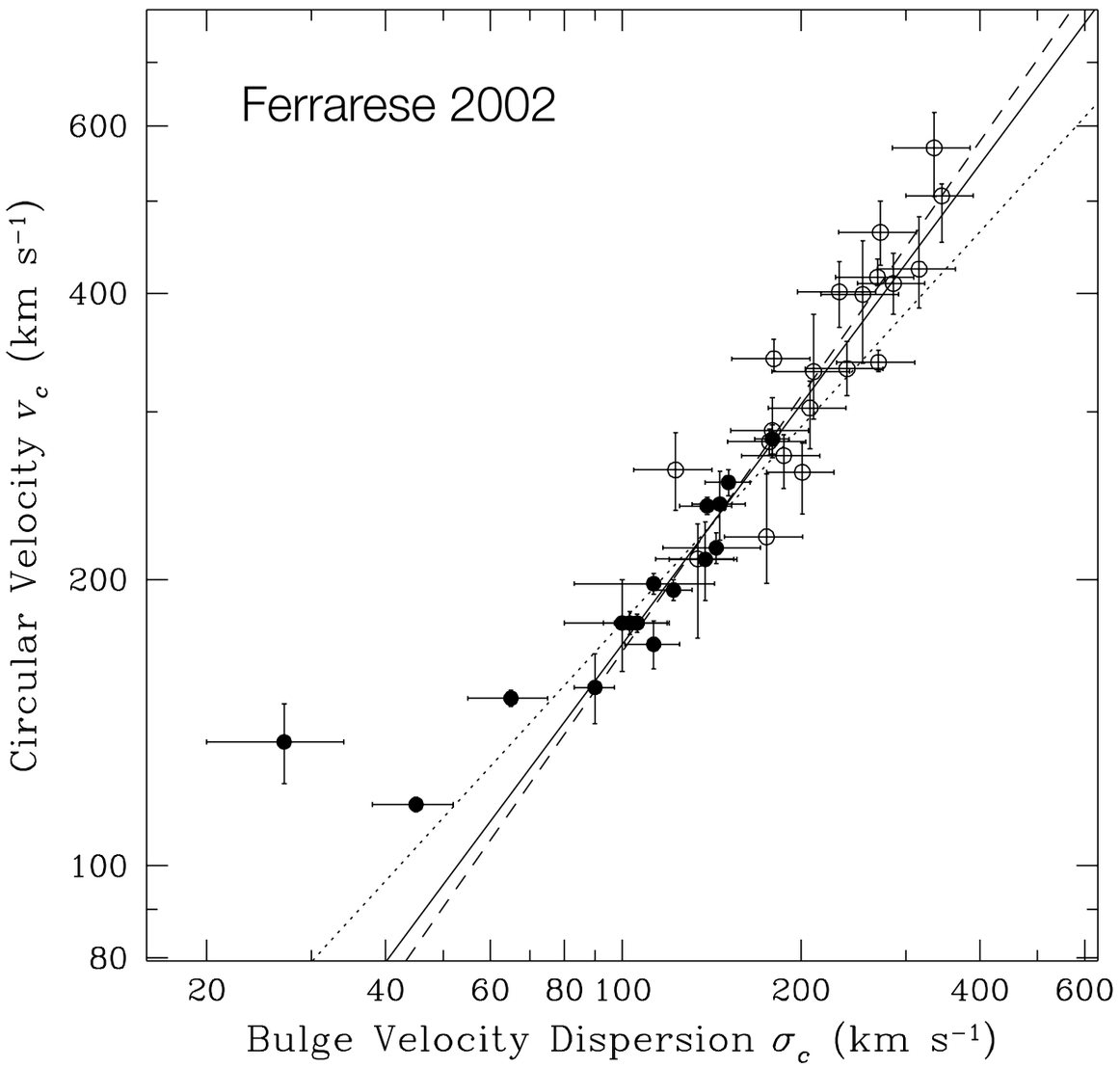

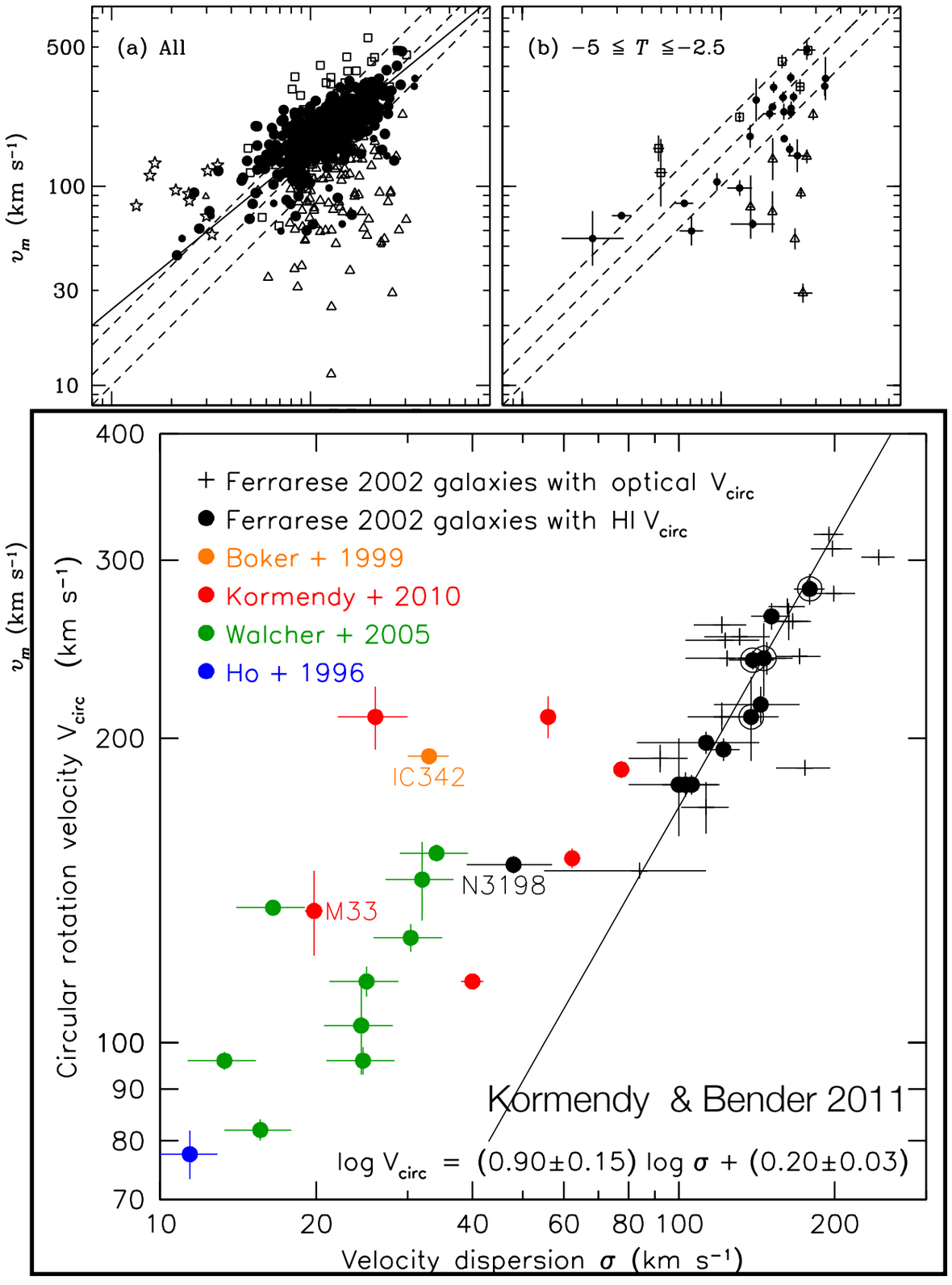

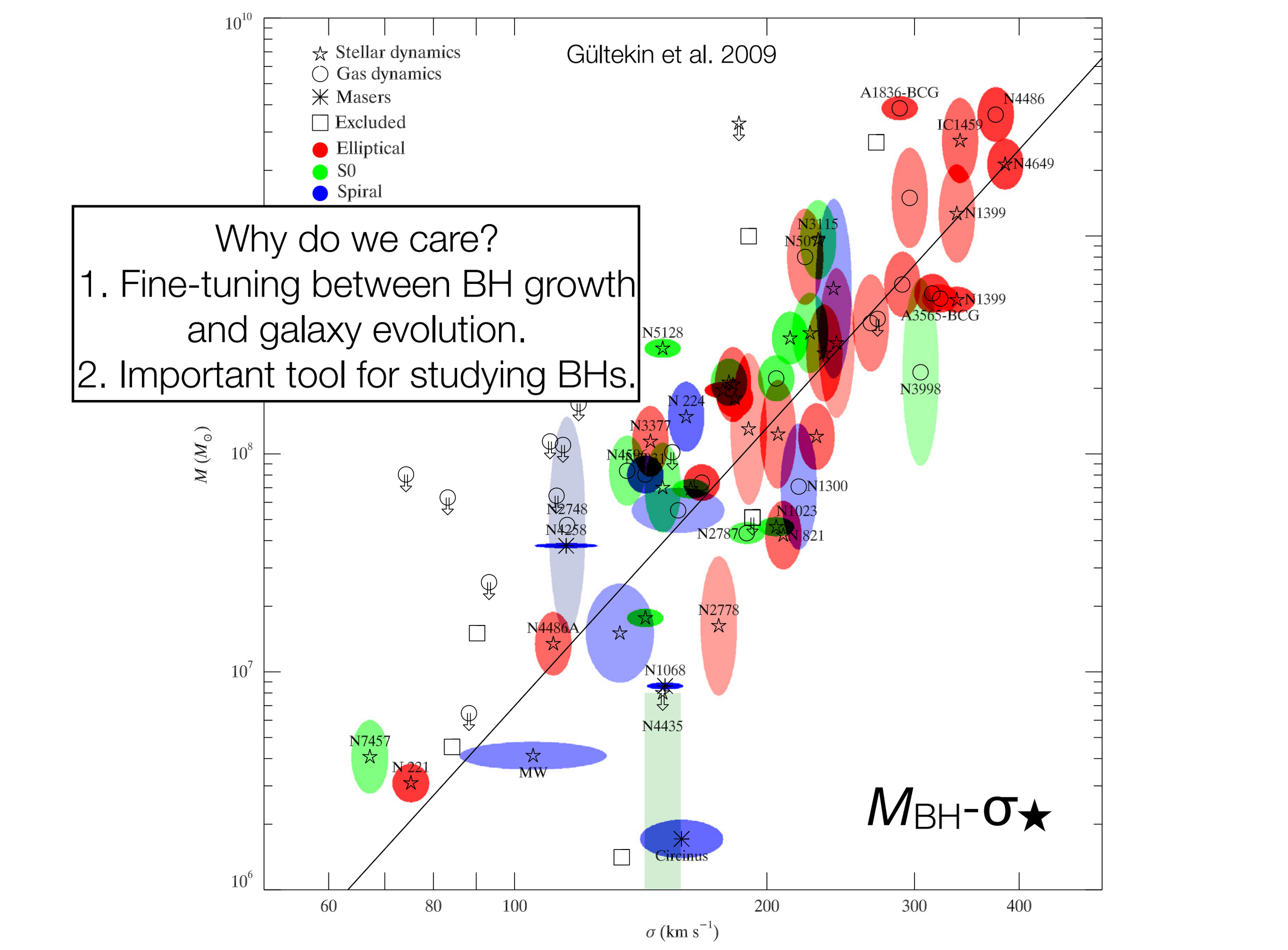
Gültekin et al. 2009
Stellar dynamics
Gas dynamics
Masers
Excluded
Elliptical
S0
Spiral
Why do we care?
1. Fine-tuning between BH growth and galaxy evolution.
2. Important tool for studying BHs.
M_{BH}-σ★
$M\ (M_\odot)$
σ (km s^{-1})
10^{10}
10^8
10^7
10^6
60
80
100
200
300
400
A1836-BCG
N4486
IC1459
N4649
N1399
N3115
N5077
N1399
A3565-BCG
N5128
N3998
N 224
N3377
N4596
N1300
N1023
N2748
N4258
N2787
N 821
N2778
N4486A
N1068
N4435
N7457
N 221
MW
Circinus

BH Mass Density

Use BH-bulge scaling relations + observed galaxy population to infer BH mass function and BH mass density today.

Then compare with integrated luminosity in quasars over cosmic time (the Sołtan argument; see Yu & Tremaine 2002) -- BHs mostly grew in Eddington-limited, optically bright phases

Need to know *intrinsic* scatter

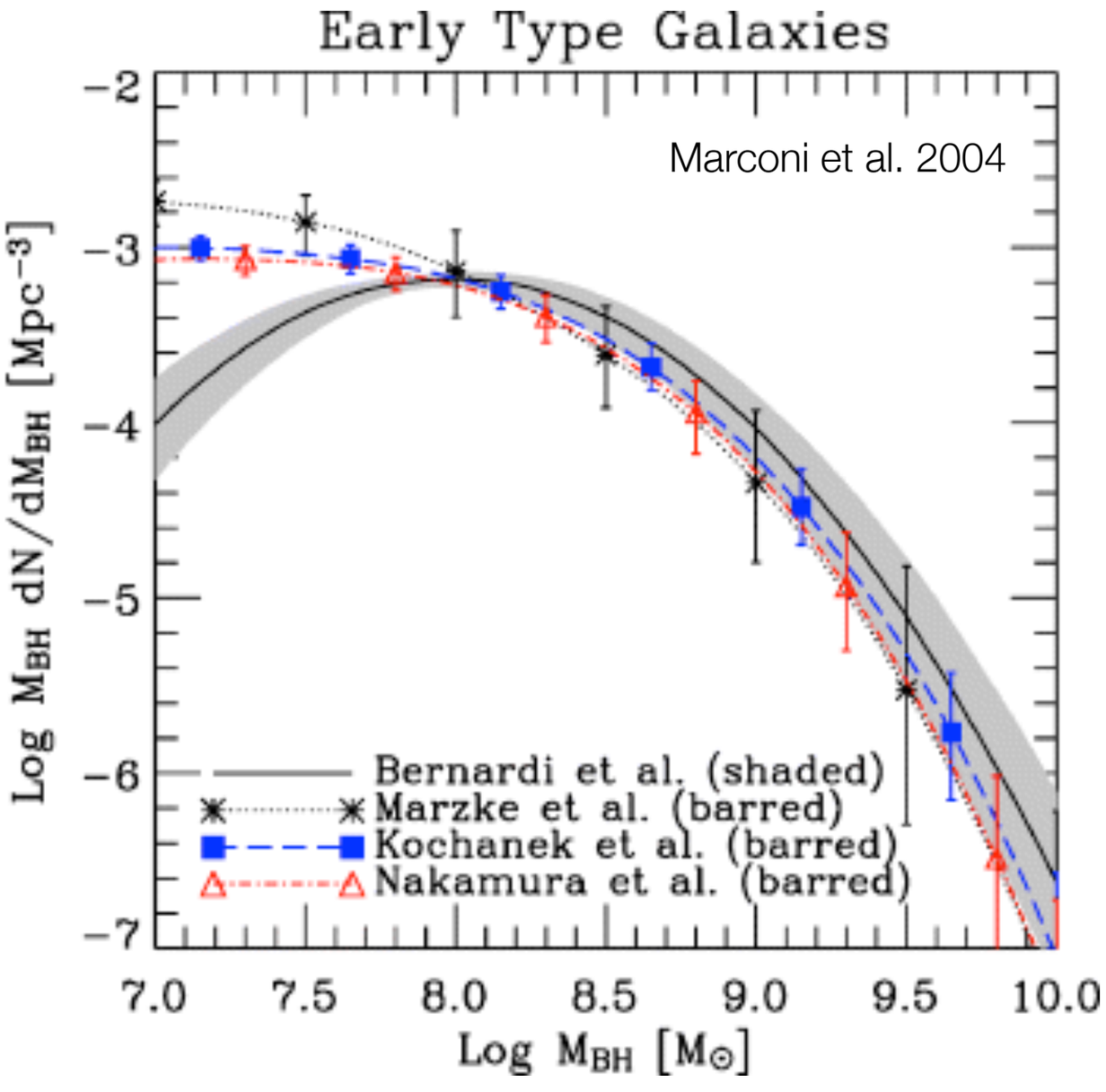

Space density of most massive BHs...

What is the shape of the mass function at the most massive end?
M_{BH}-$\sigma_\star$ relation and M_{BH}-L_{bulge}

relations don't predict the same mass function.

We want to know what the primary correlation is.

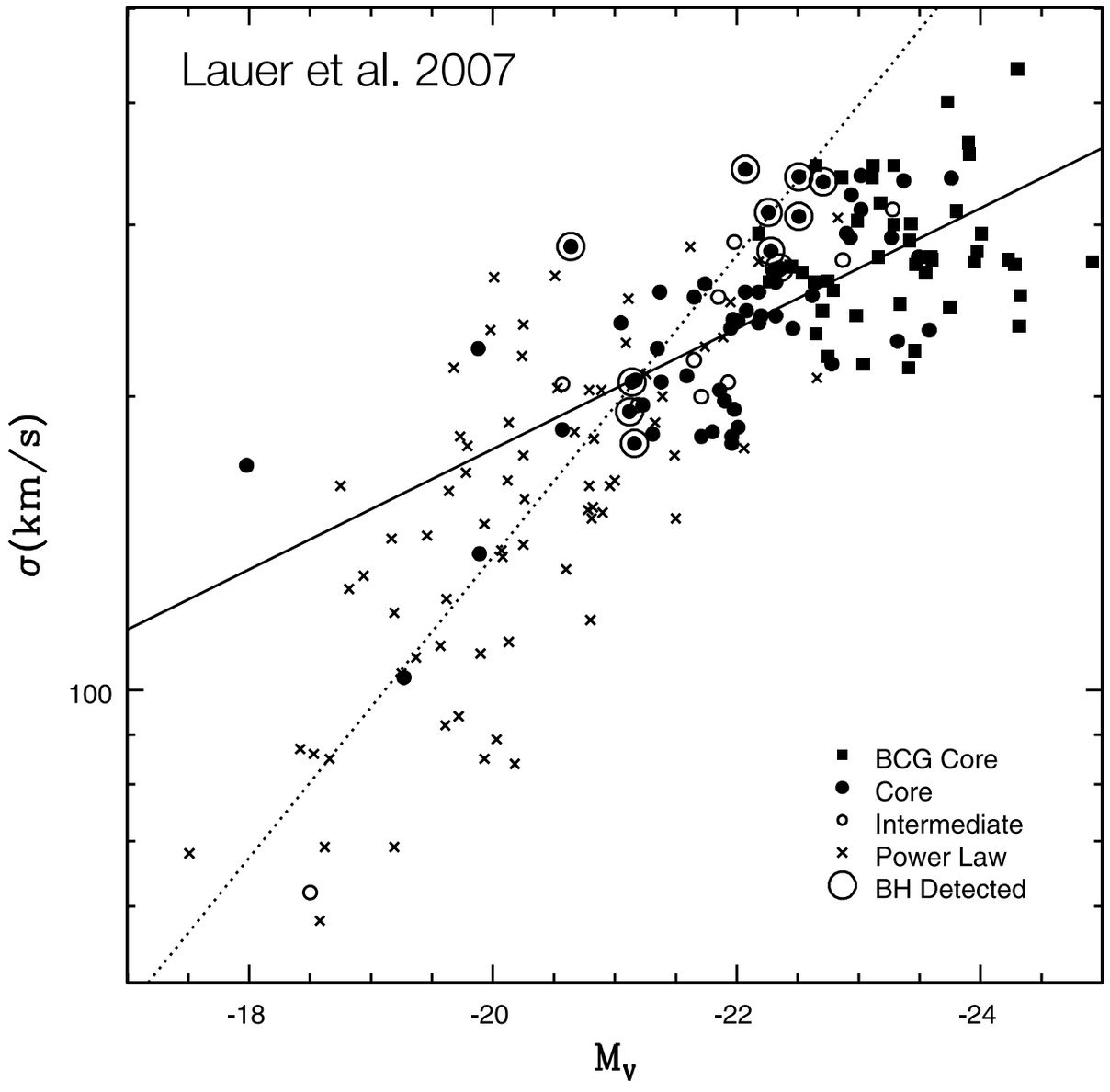

Origin of Scaling Relations?

Feedback (ala Hopkins/Springel/ Hernquist)?

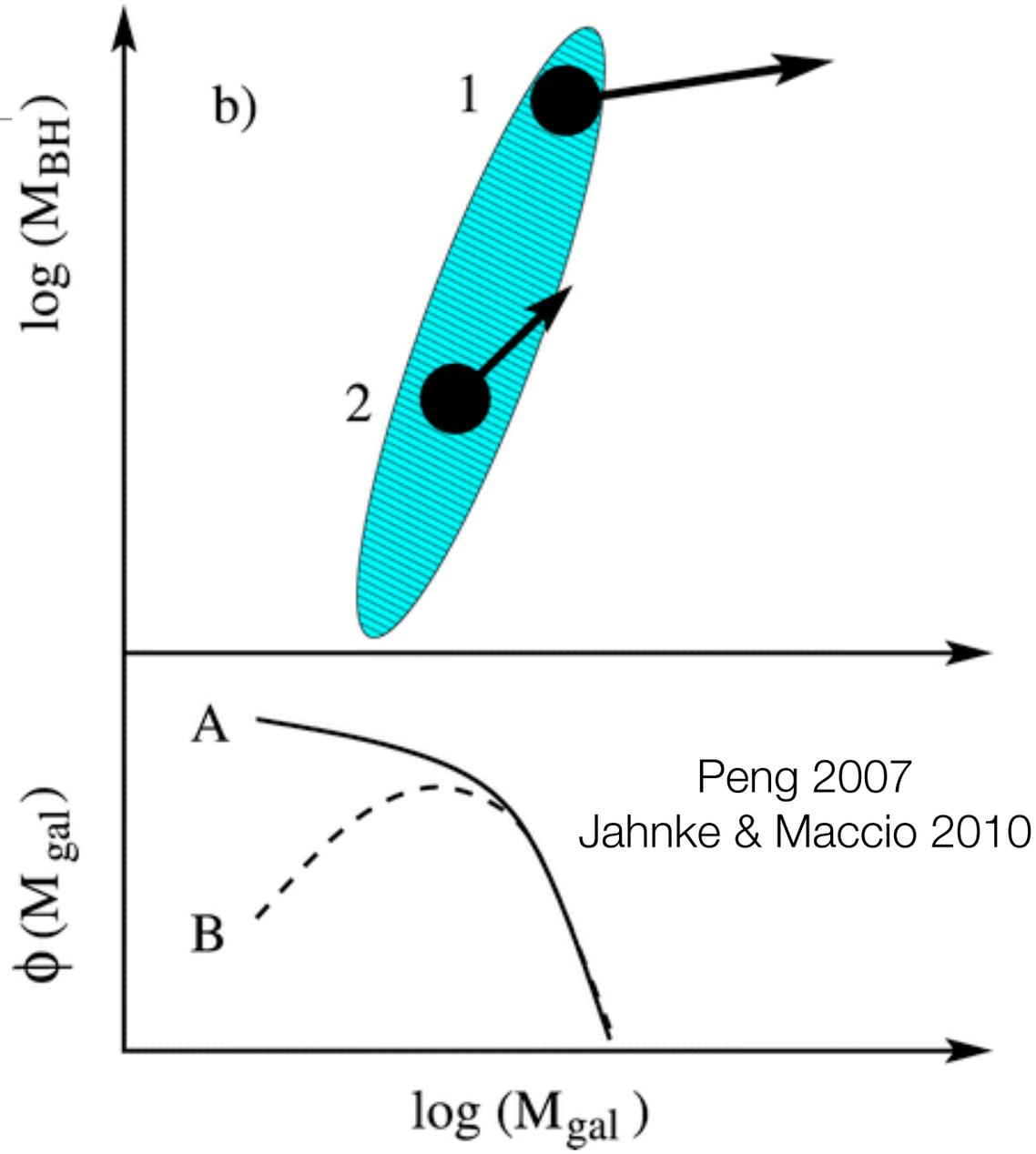

Or just hierarchical merging?

Need to know how BH-bulge scaling relations and scatter depend on galaxy morphology and mass.

Gültekin et al. 2009

M_{BH}-$\sigma_\star$

☆ Stellar dynamics
◯ Gas dynamics
✳ Masers
□ Excluded
● Elliptical
● S0
● Spiral

$M\ (M_\odot)$

10^{10}
10^{9}
10^{8}
10^{7}
10^{6}

A1836-BCG
N4486
IC1459
N4649
N1399
N3115
N5077
N1399
A3565-BCG
N5128
N3998
N 224
N3377
N4596
N1300
N1023
N2748
N4258
N2787
N 821
N2778
N4486A
N1068
N4435
N7457
N 221
MW
Circinus

60
80
100
200
300
400

σ (km s^{-1})

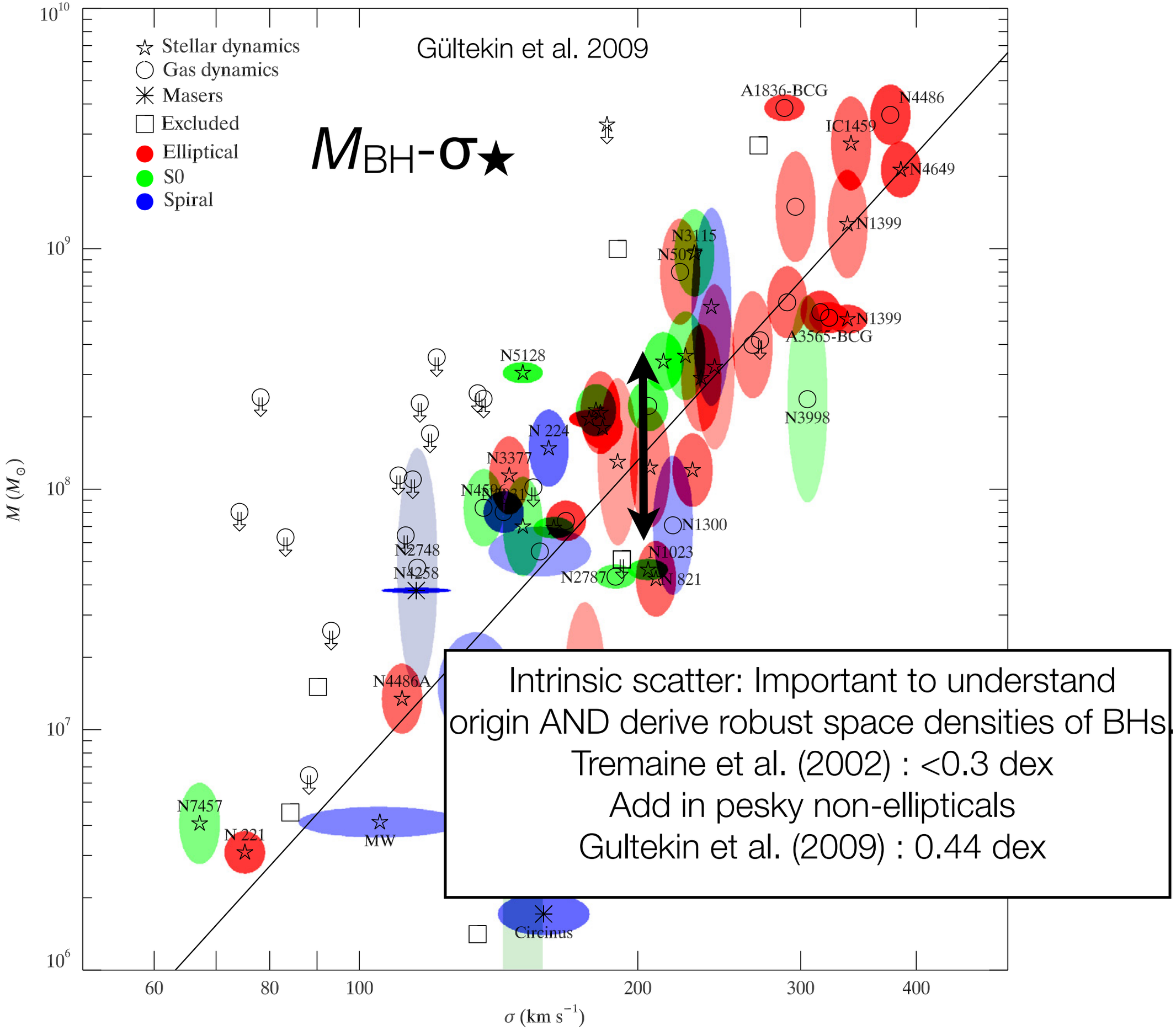
Gültekin et al. 2009
Stellar dynamics
Gas dynamics
Masers
Excluded
Elliptical
S0
Spiral
M_{BH}-σ★
$M\ (M_\odot)$
σ (km s^{-1})
10^{10}
10^9
10^8
10^7
10^6
60
80
100
200
300
400
A1836-BCG
N4486
IC1459
N4649
N1399
N3115
N5077
N1399
A3565-BCG
N5128
N3998
N 224
N3377
N4596
N1300
N1023
N2748
N4258
N2787
N 821
N4486A
N7457
N 221
MW
Circinus
Intrinsic scatter: Important to understand origin AND derive robust space densities of BHs.
Tremaine et al. (2002) : <0.3 dex
Add in pesky non-ellipticals
Gultekin et al. (2009) : 0.44 dex

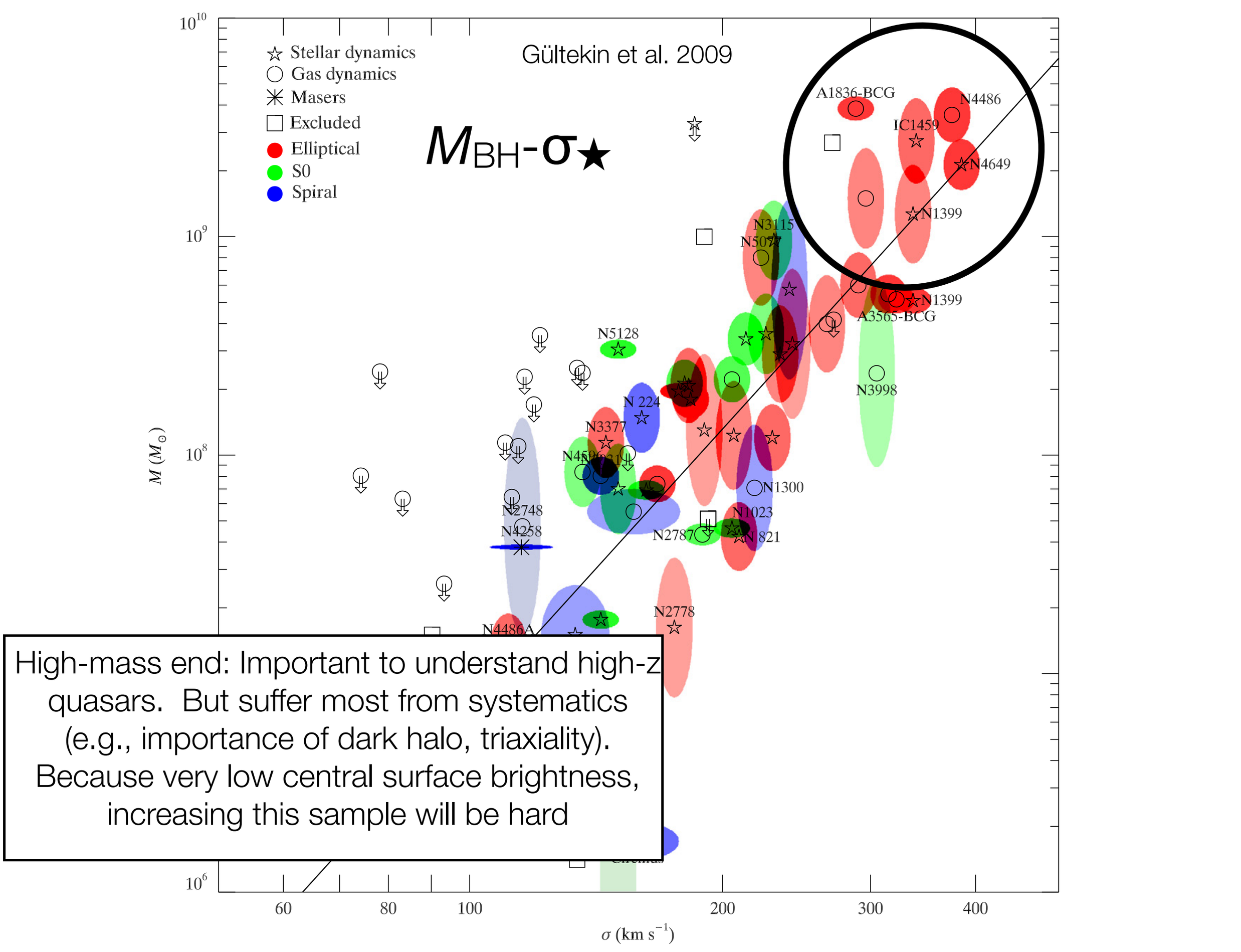
Gültekin et al. 2009
M_{BH}-σ★
Stellar dynamics
Gas dynamics
Masers
Excluded
Elliptical
S0
Spiral
$M\ (M_\odot)$
σ (km s^{-1})
10^{10}
10^9
10^8
10^6
60
80
100
200
300
400
A1836-BCG
N4486
IC1459
N4649
N1399
N3115
N5077
N1399
A3565-BCG
N5128
N3998
N 224
N3377
N1300
N1023
N2748
N4258
N2787
N 821
N2778
N4486A
High-mass end: Important to understand high-z quasars. But suffer most from systematics (e.g., importance of dark halo, triaxiality). Because very low central surface brightness, increasing this sample will be hard

Most Massive Black Holes Ever Weighed

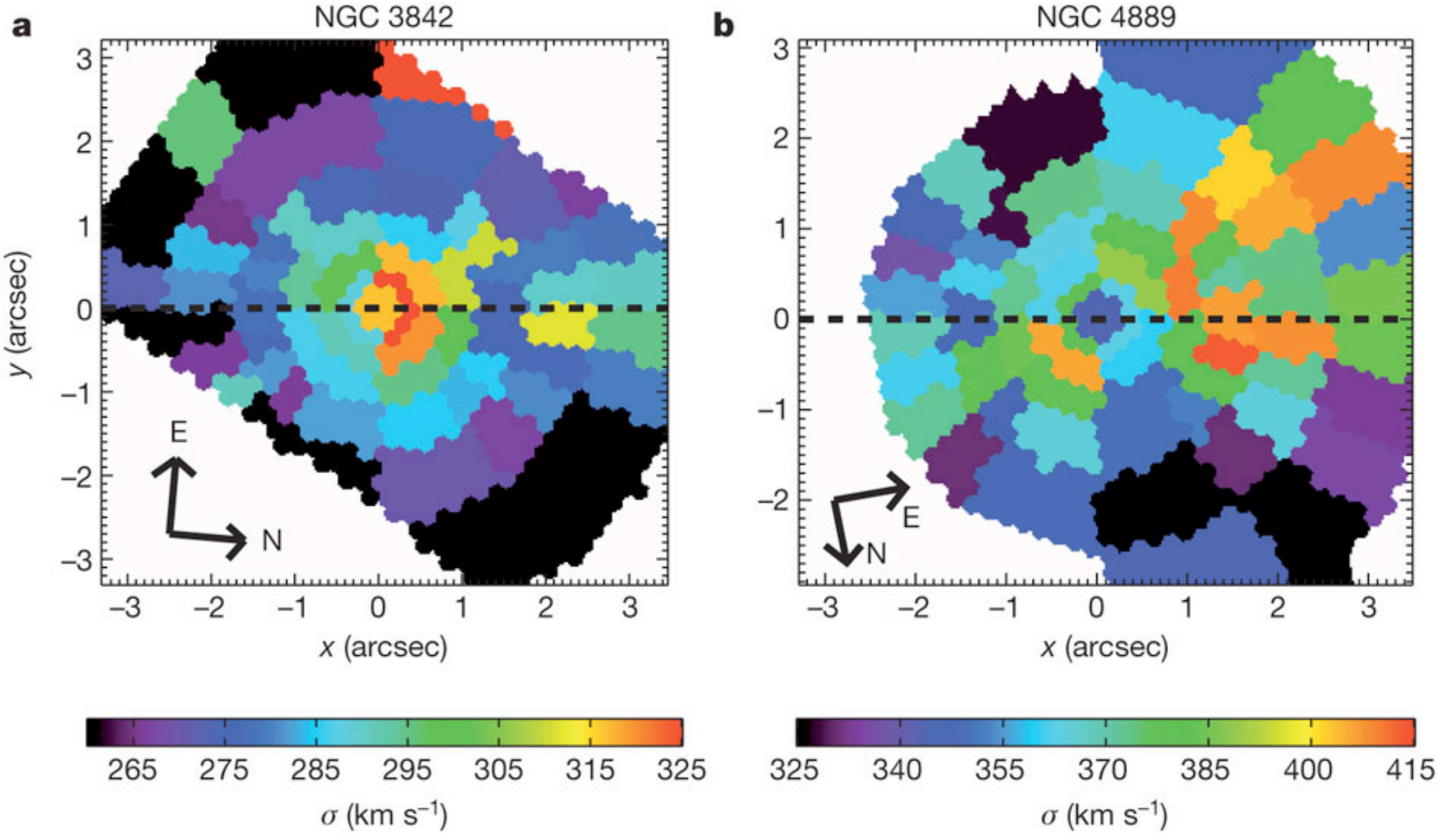

McConnell et al 2011

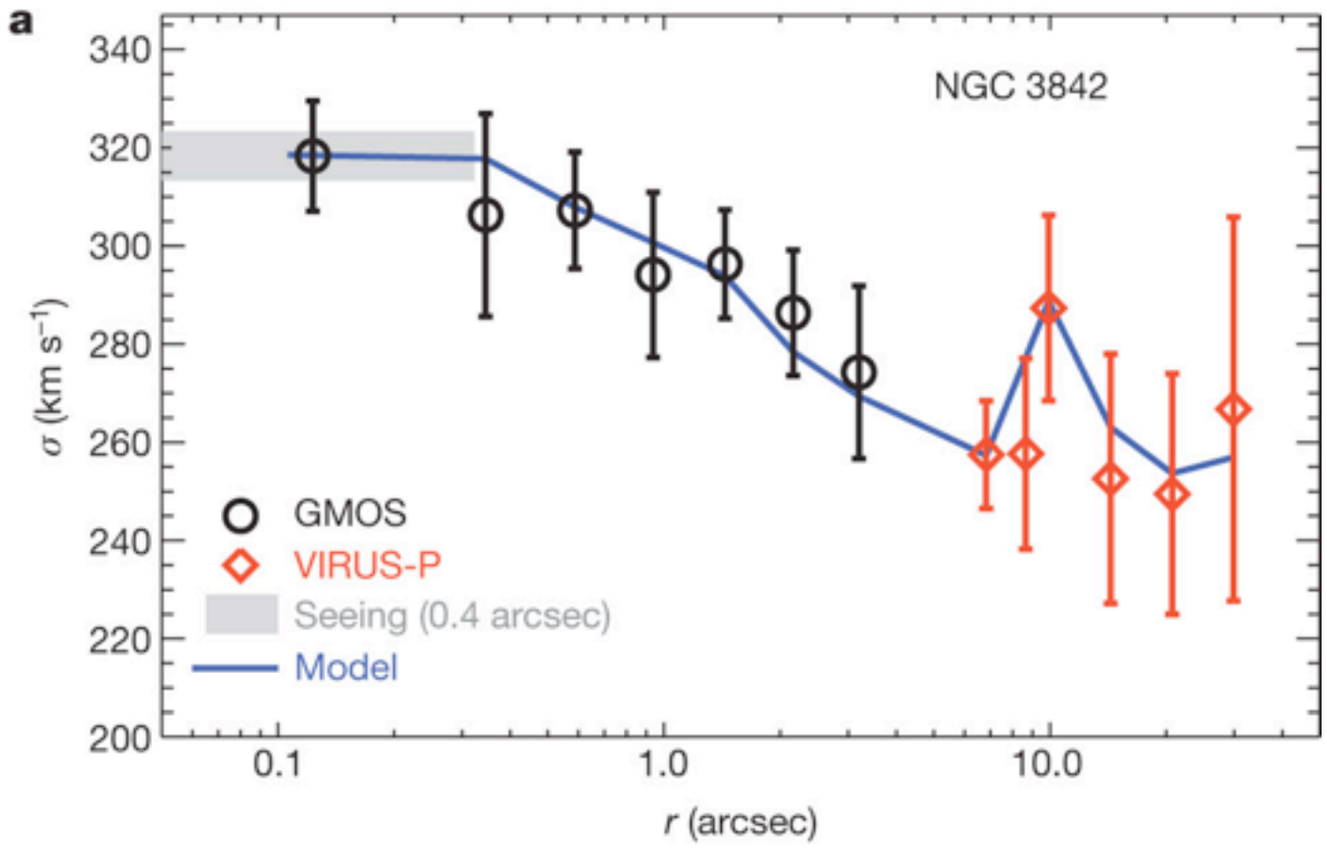

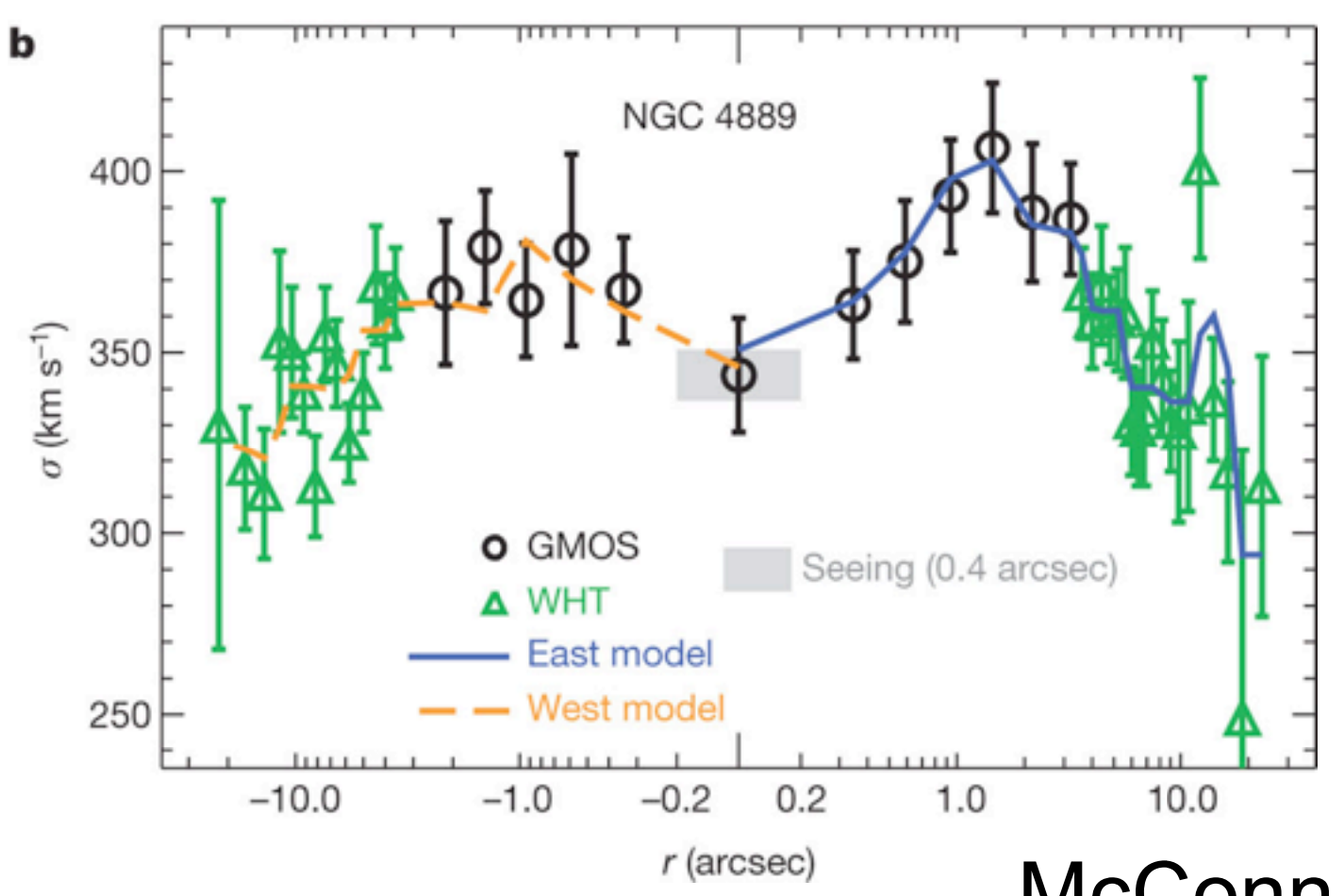

Signature of the most massive known BH is a *dip* in the central stellar velocity dispersion.

McConnell et al 2011

Gültekin et al. 2009

Low-mass end: 1. Large range in host morphologies/merger histories -- strong constraints on BH-galaxy coevolution.
2. At the lowest masses, shape of BH-bulge correlations will constrain seed formation models

Stellar dynamics
Gas dynamics
Masers
Excluded
Elliptical
S0
Spiral

M_{BH}-$\sigma_\star$

M ($M_\odot$)

σ (km s^{-1})

10^{10}
10^{9}
10^{8}
10^{7}
10^{6}

60
80
100
200
300
400

A3565-BCG
N5128
N3998
N 224
N3377
N1300
N2748
N1023
N4258
N2787
N 821
N2778
N4486A
N1068
N4435
N7457
N 221
MW
Circinus

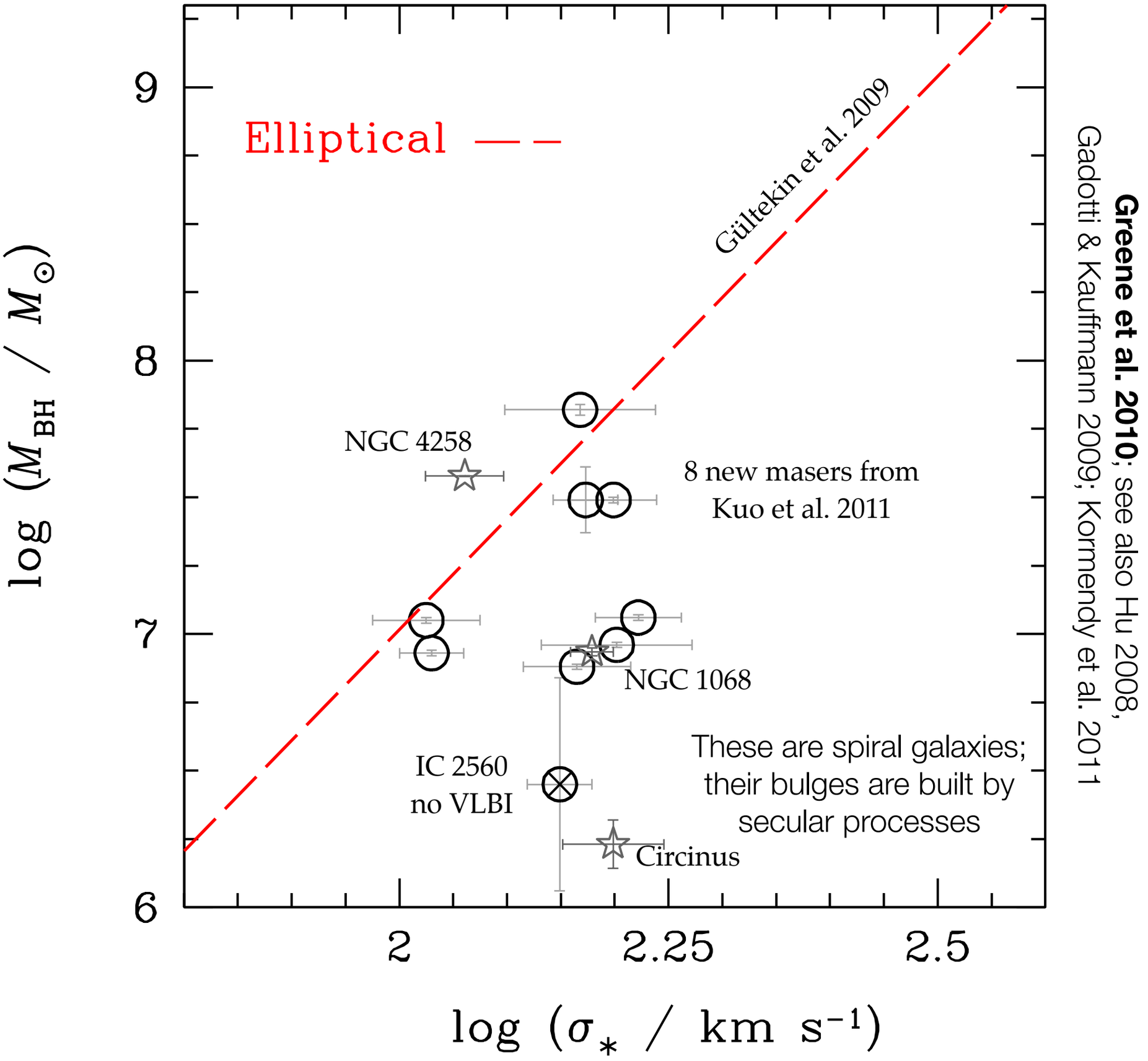

The M_{BH}-$\sigma_\star$ relation is ***not*** universal

Greene et al. 2010; see also Hu 2008,
Gadotti & Kauffmann 2009; Kormendy et al. 2011

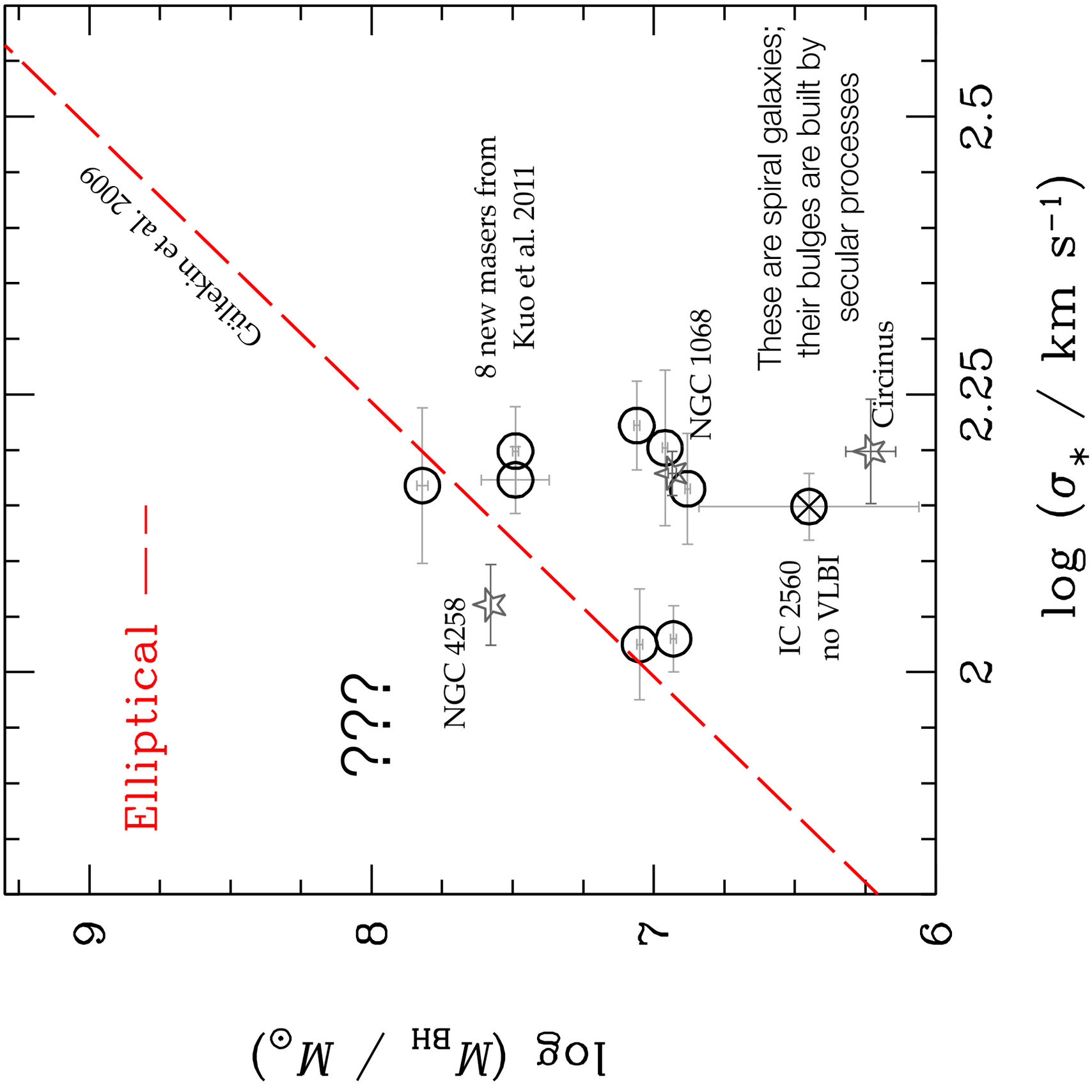

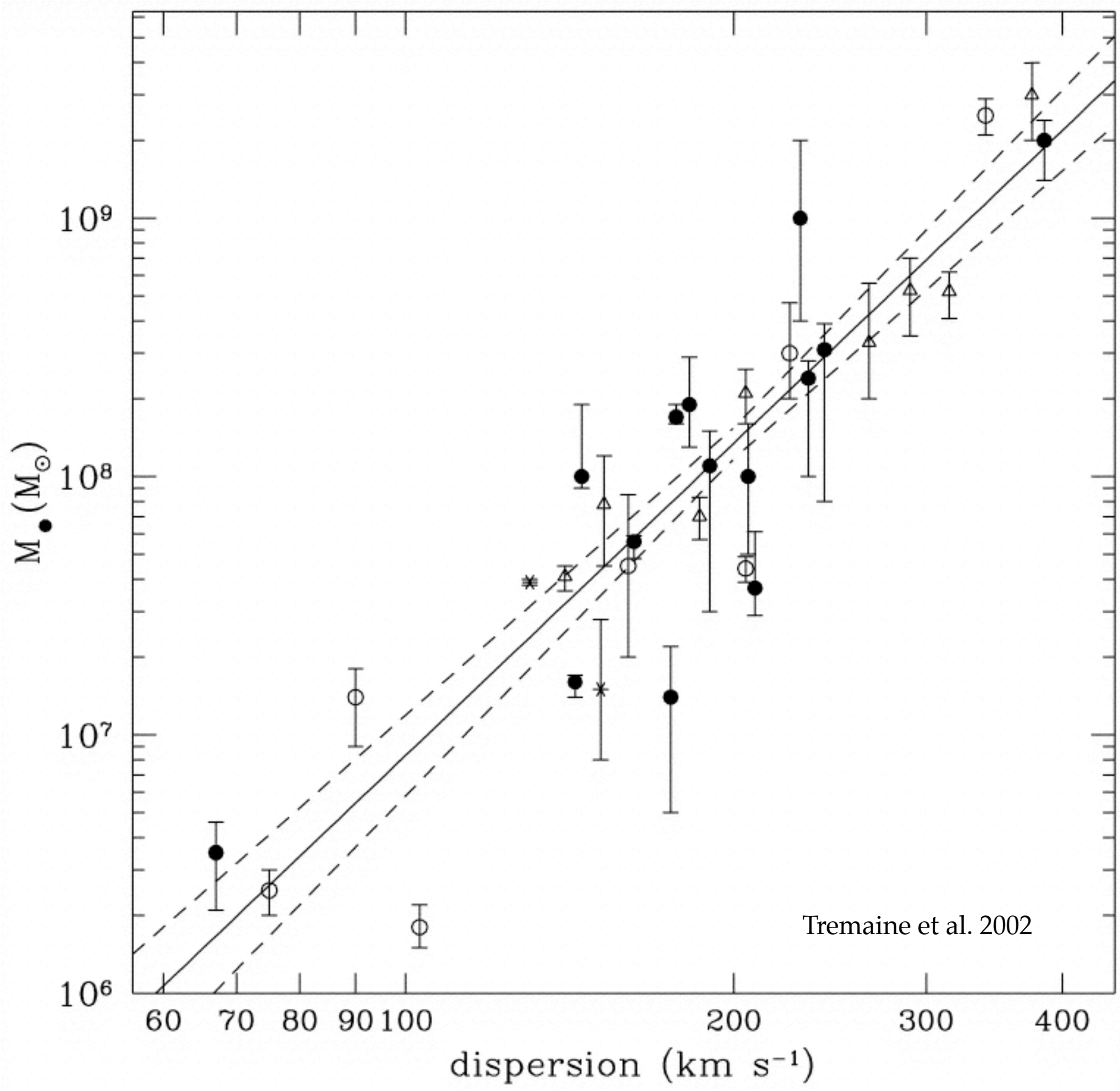
10^9
10^8
10^7
10^6
$M_\bullet (M_\odot)$
60
70
80
90
100
200
300
400
dispersion (km s^{-1})
Tremaine et al. 2002

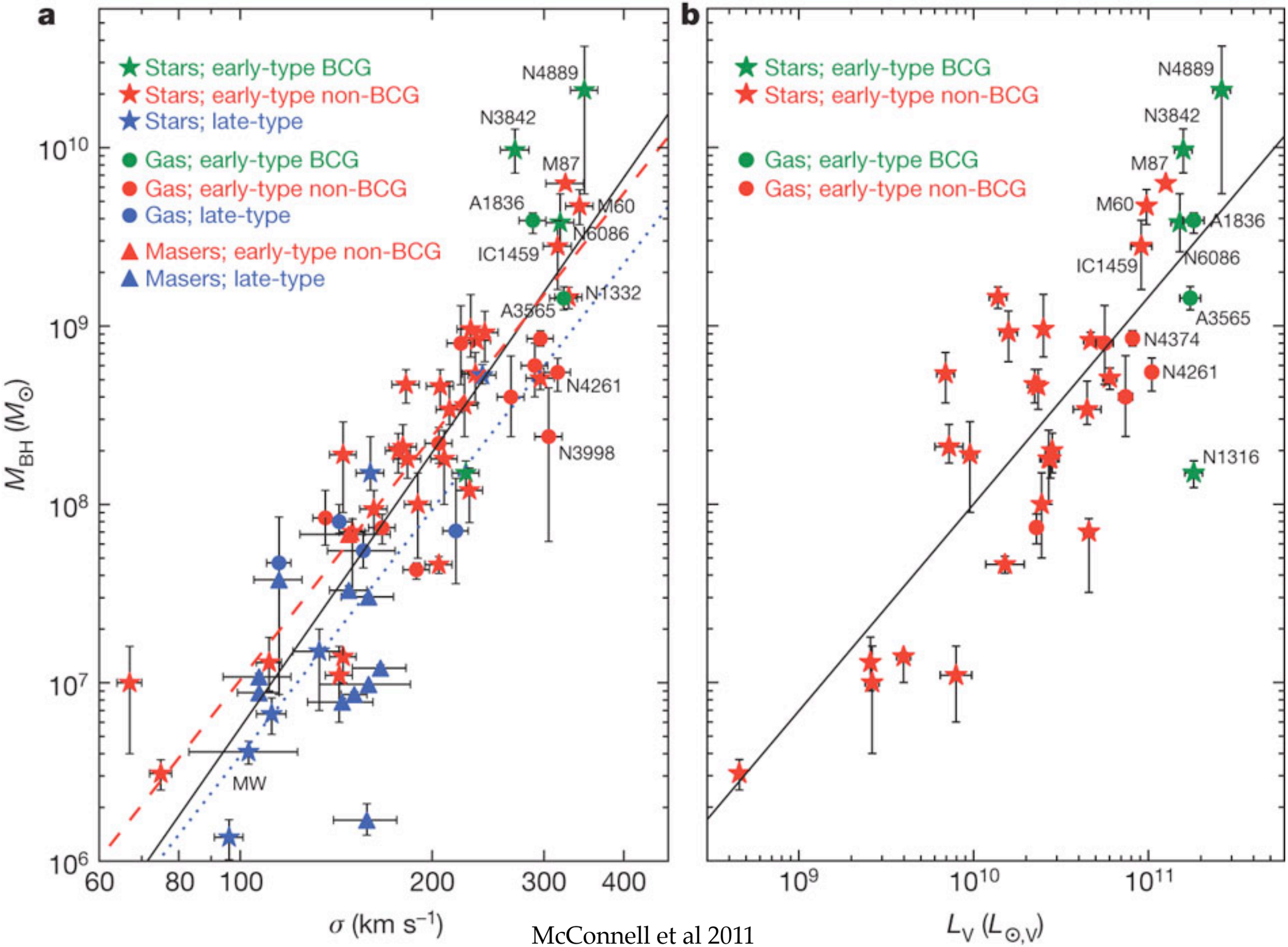

McConnell et al 2011

Black Hole Demographics

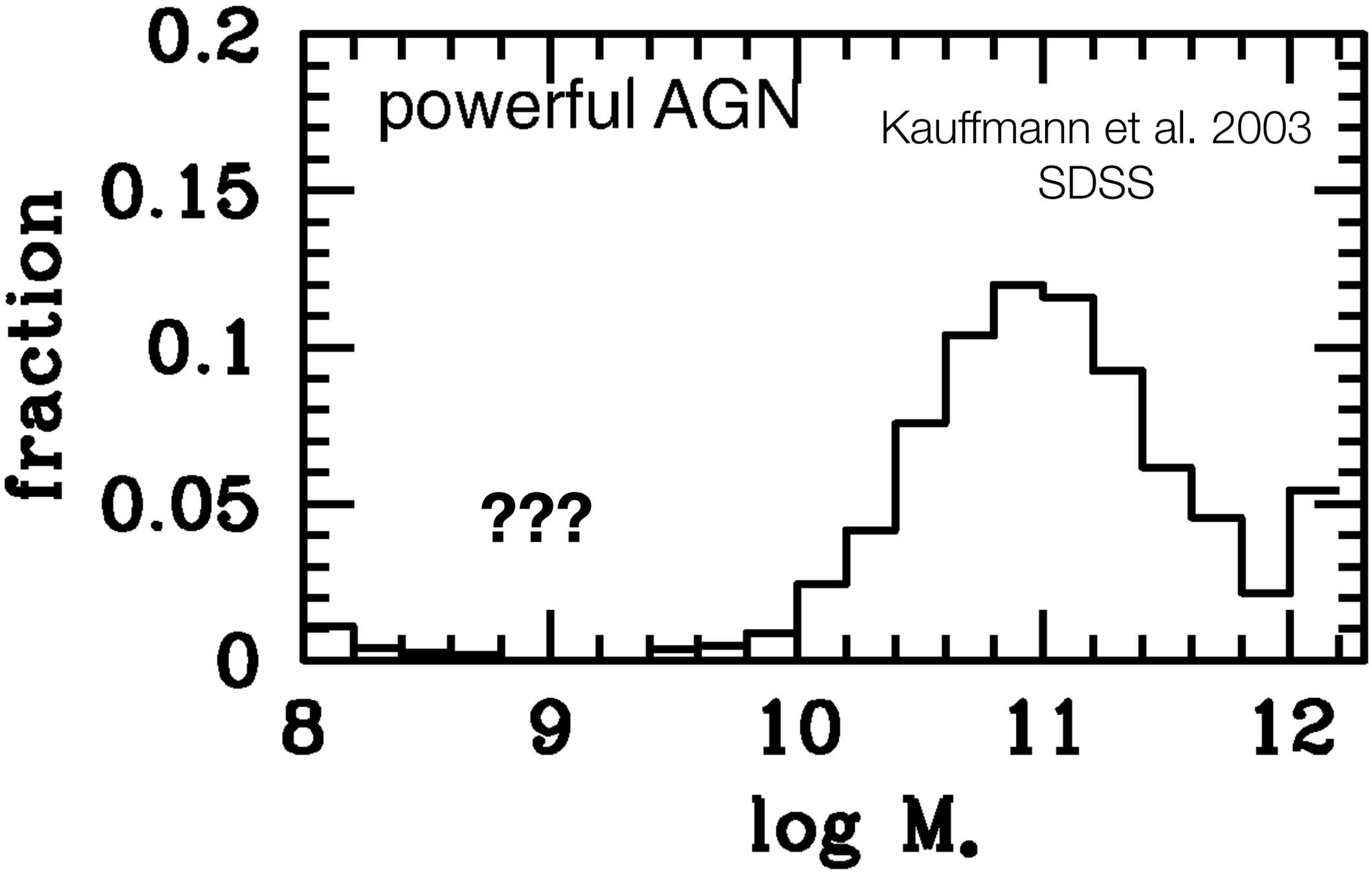

Are there no BHs in low-mass galaxies? Or are we just confused because of star formation, dust, and wimpy active galaxies?

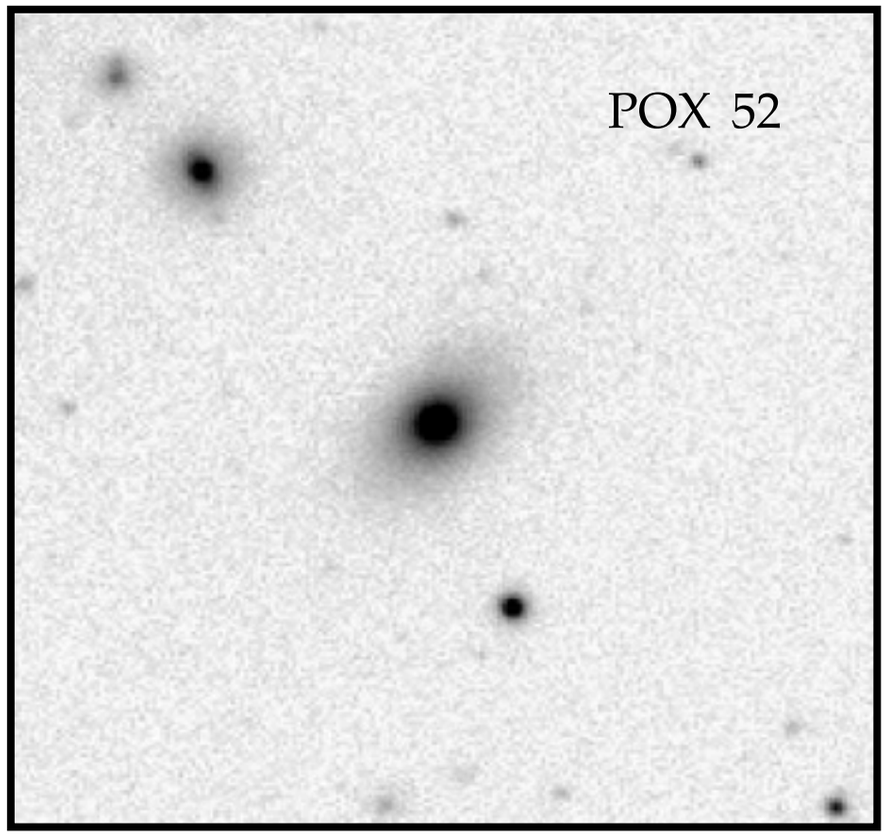

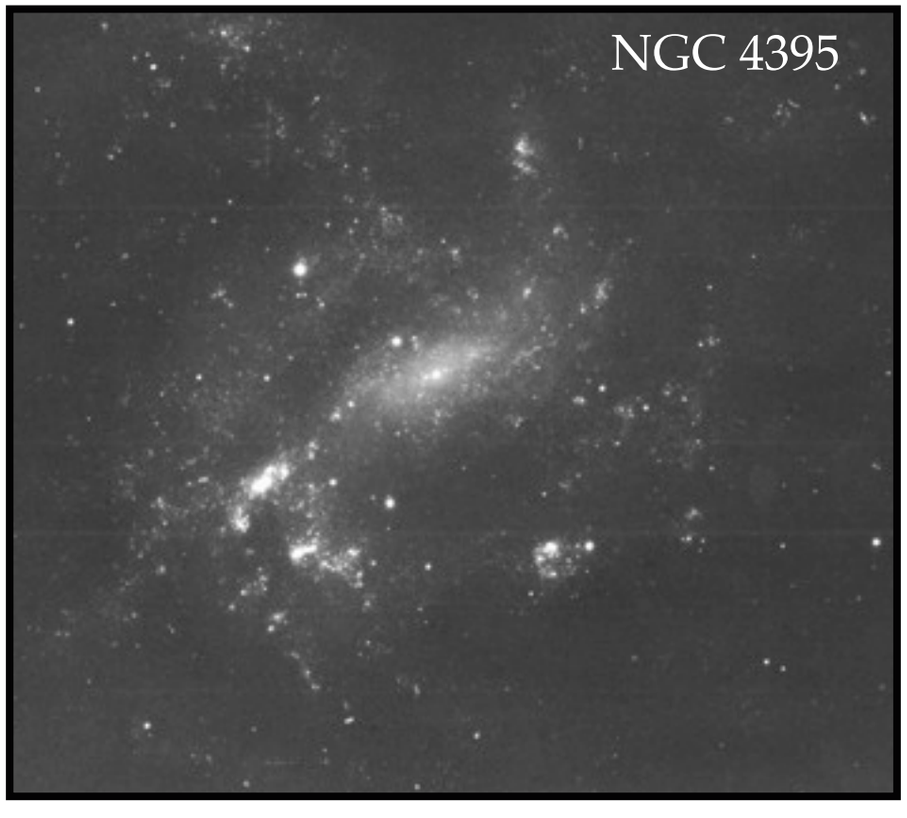

Barth et al. 2004

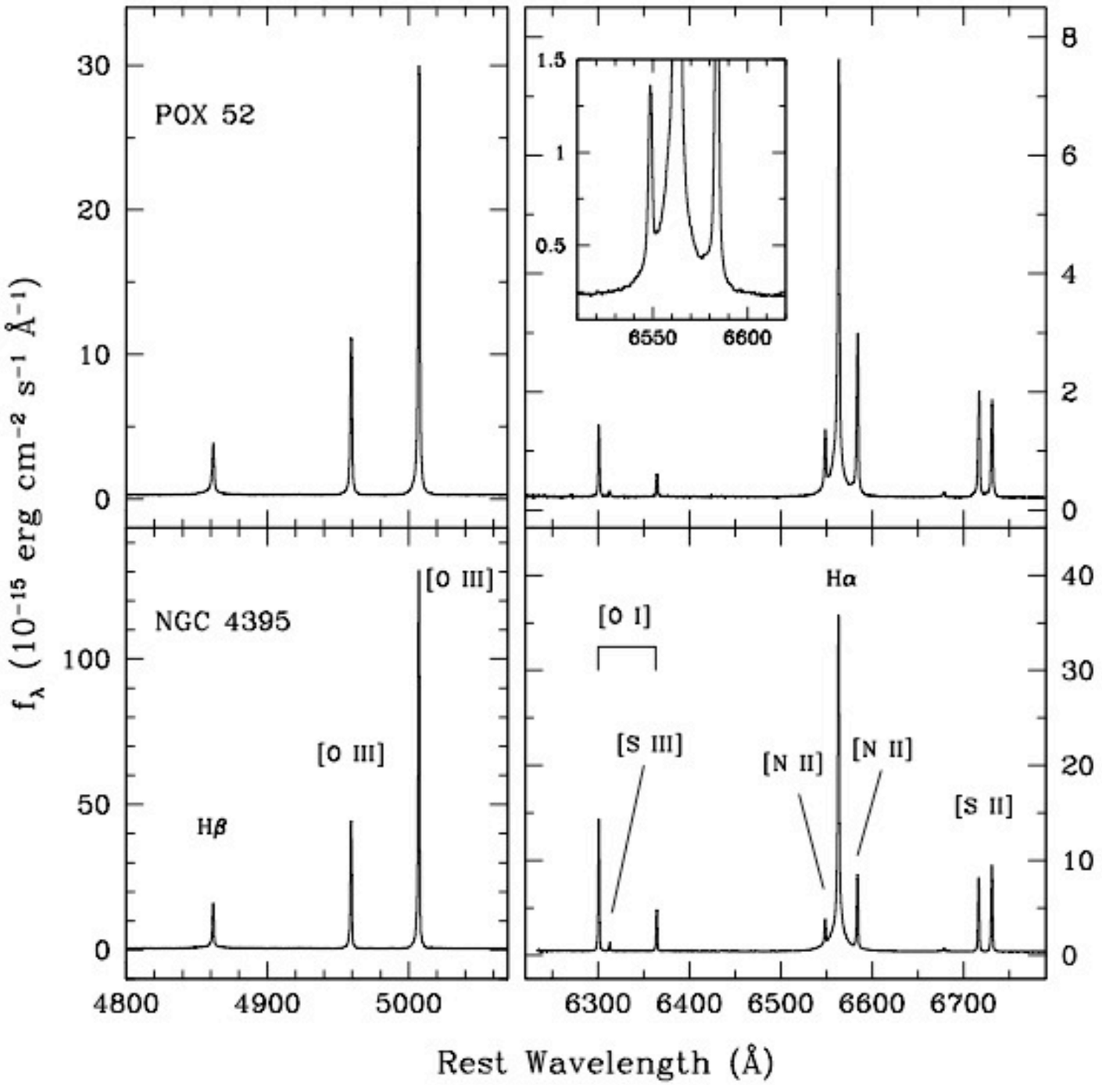

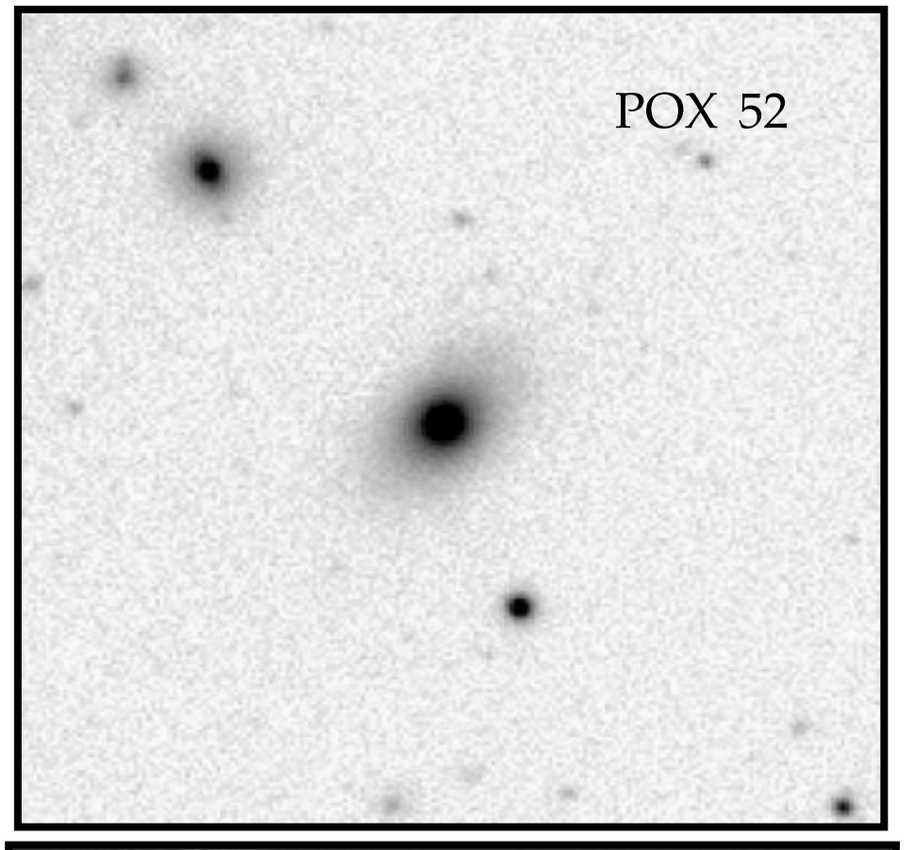

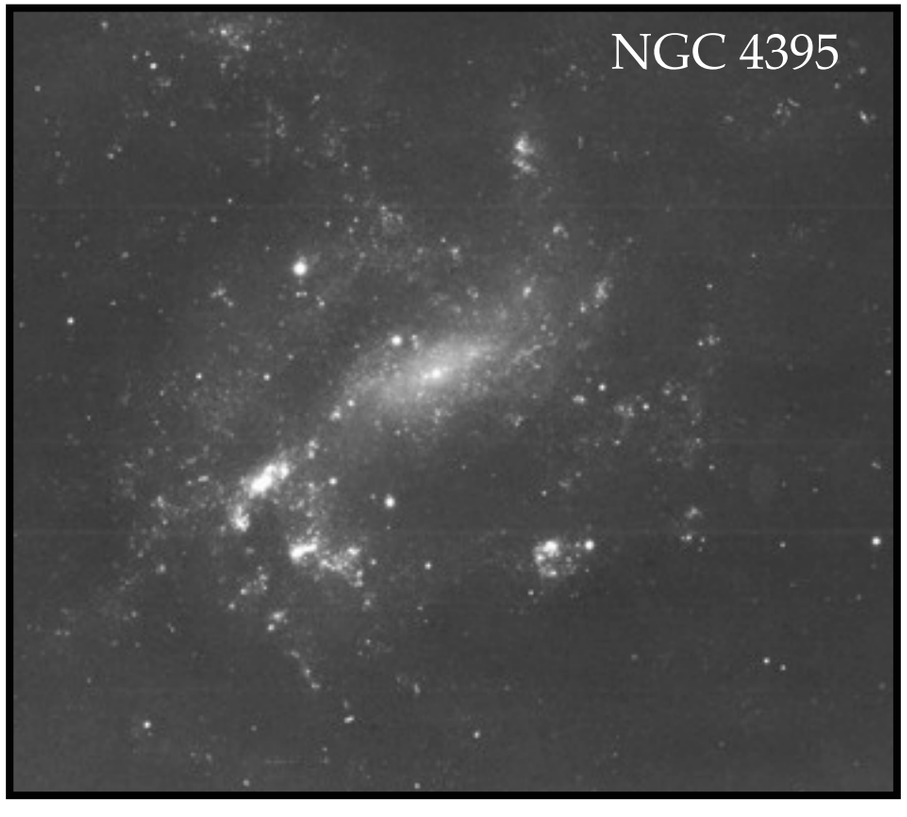

Barth et al. 2004

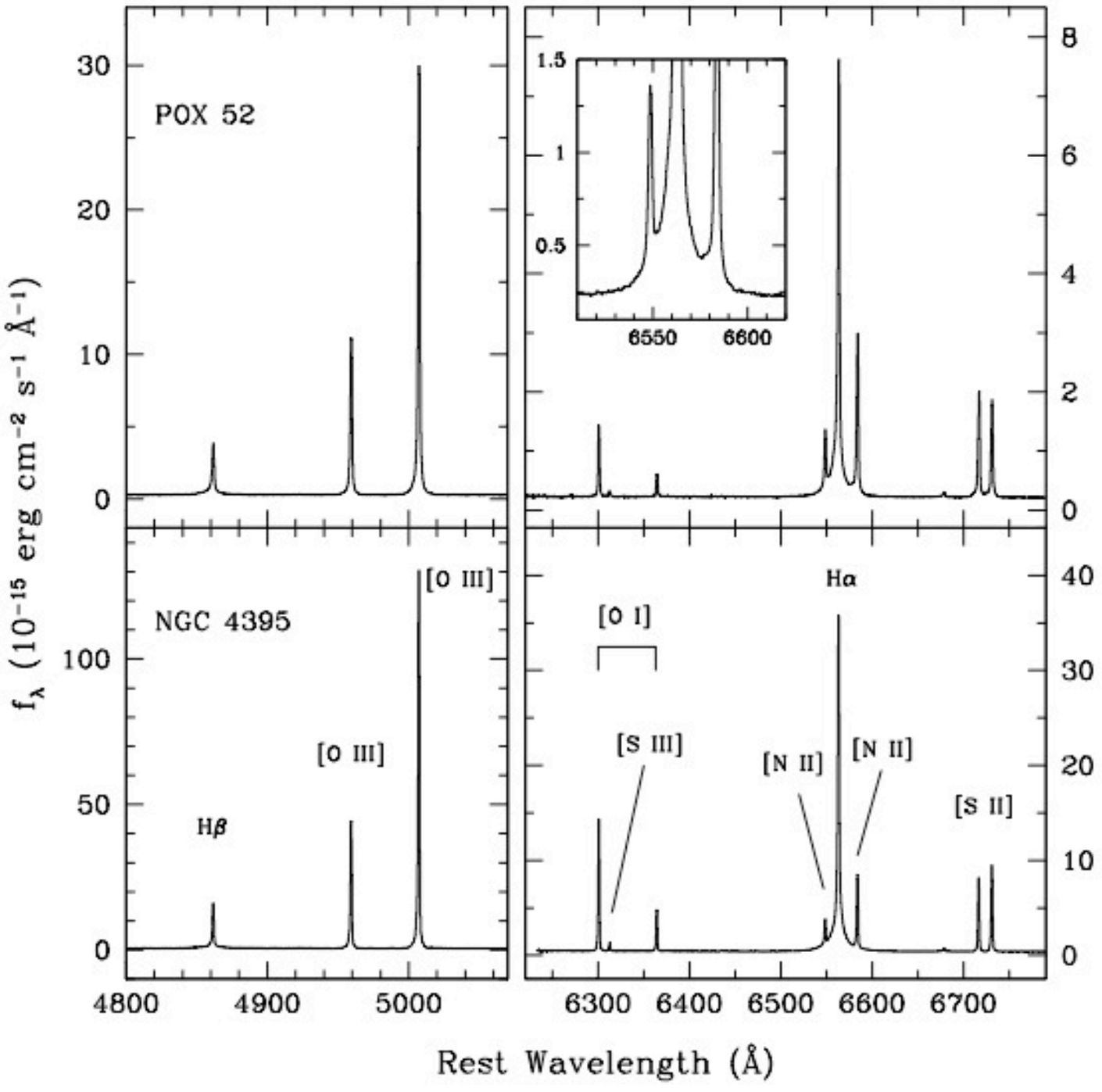

Both objects have $M_{BH} \sim 10^5\ M_\odot$

Neither have classical bulges.

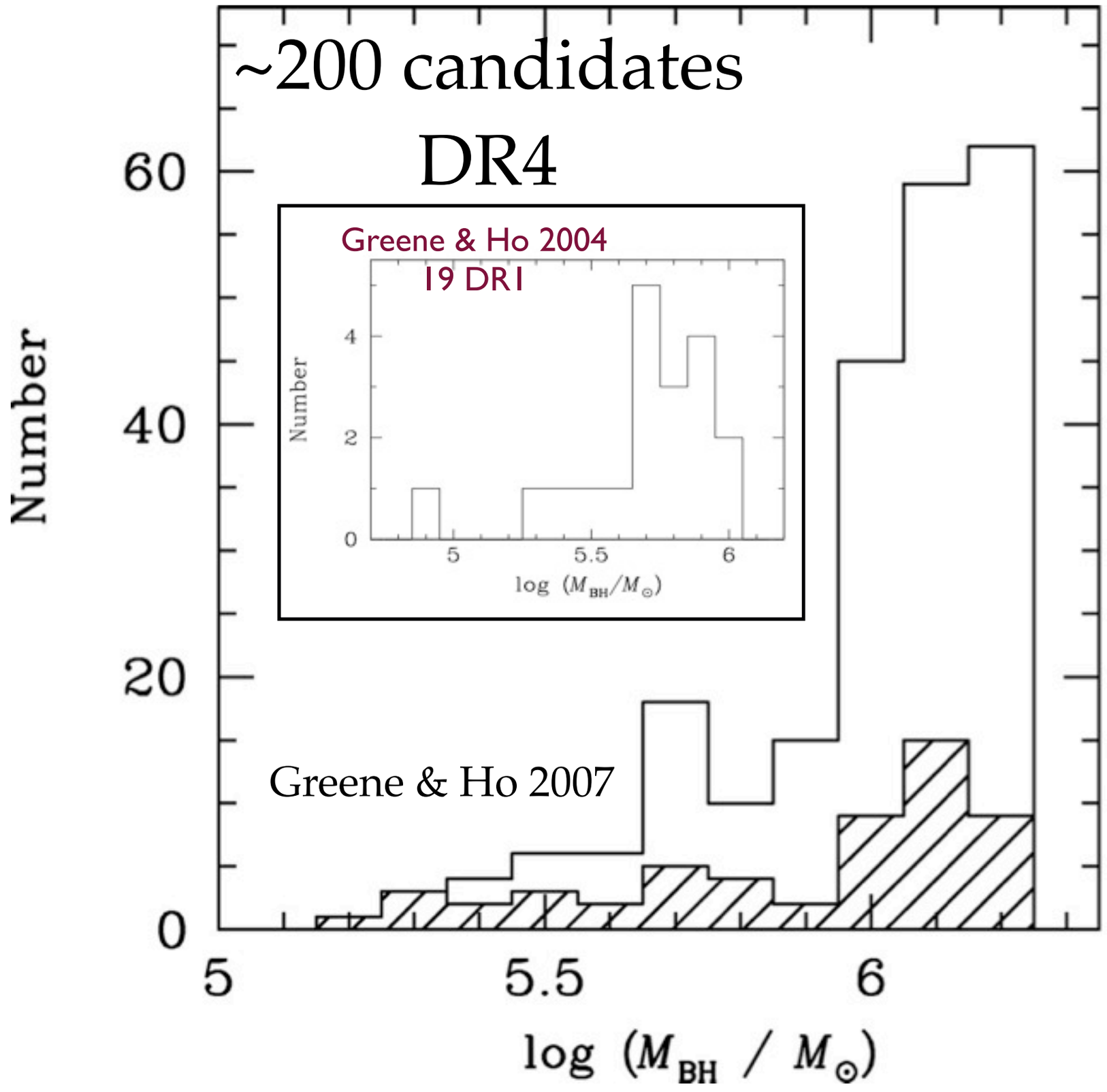

See also Dong et al. for an alternate search technique

BH mass selected but biased to relatively luminous host galaxies and high Eddington ratios

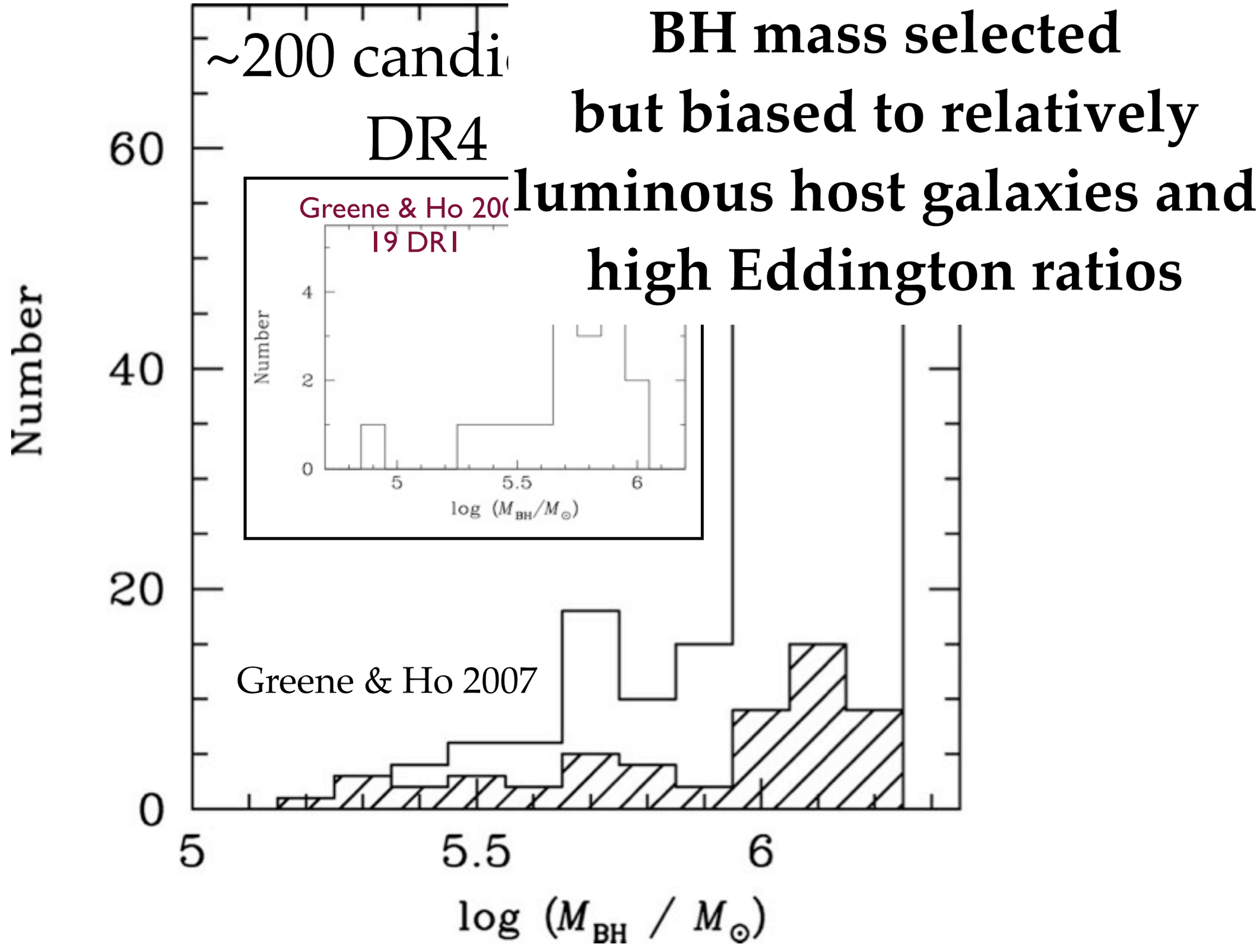

See also Dong et al. for an alternate search technique

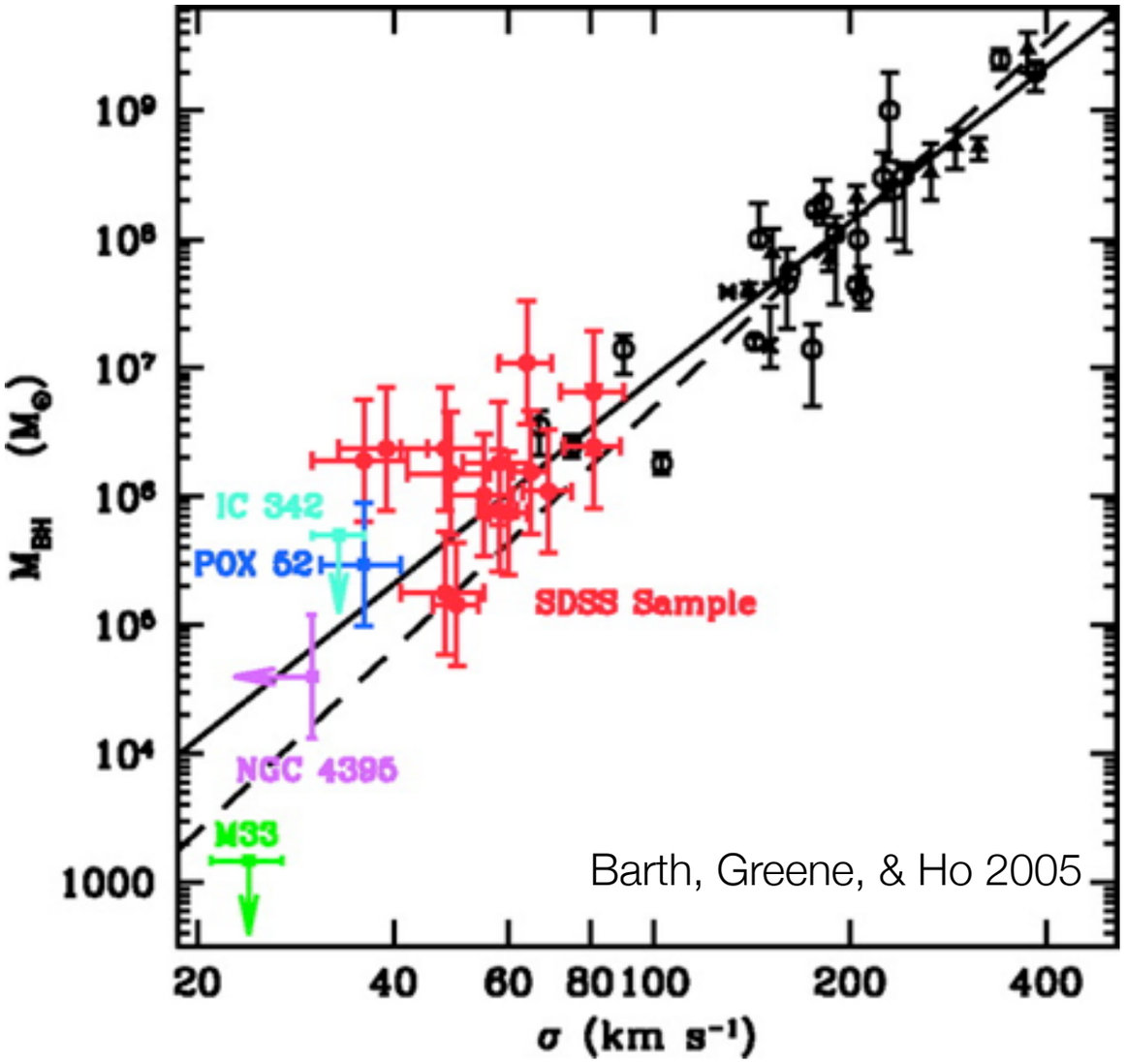
10^9
10^8
10^7
10^6
10^5
10^4
1000
M_{BH} ($M_\odot$)
IC 342
POX 52
NGC 4395
M33
SDSS Sample
Barth, Greene, & Ho 2005
20
40
60
80
100
200
400
σ (km s^{-1})

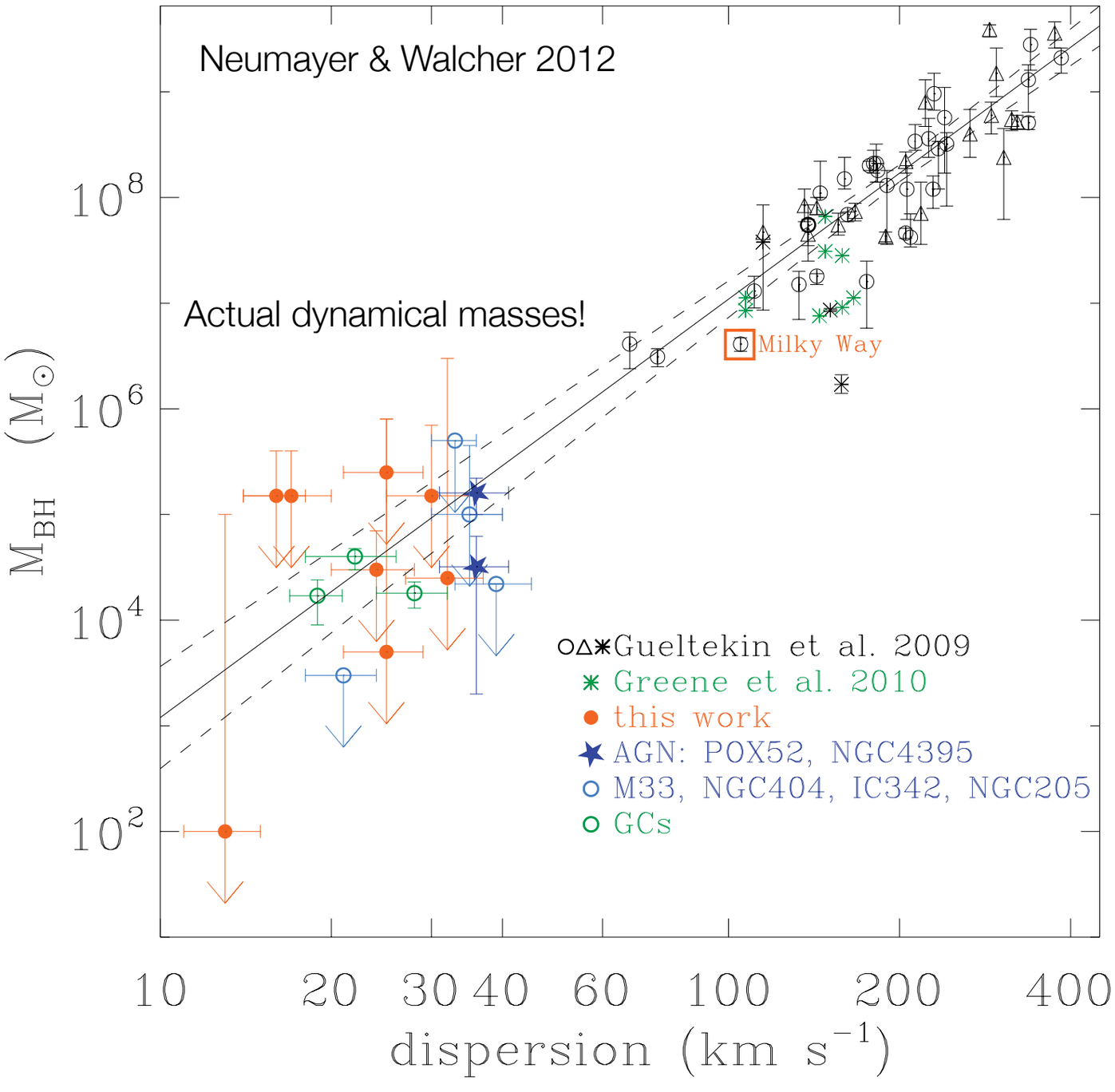
Neumayer & Walcher 2012
Actual dynamical masses!
Milky Way
10^8
10^6
10^4
10^2
M_{BH} ($M_\odot$)
○△✳Gueltekin et al. 2009
✳ Greene et al. 2010
● this work
★ AGN: POX52, NGC4395
○ M33, NGC404, IC342, NGC205
○ GCs
10
20
30
40
60
100
200
400
dispersion (km s^{-1})

Volume-limited Search

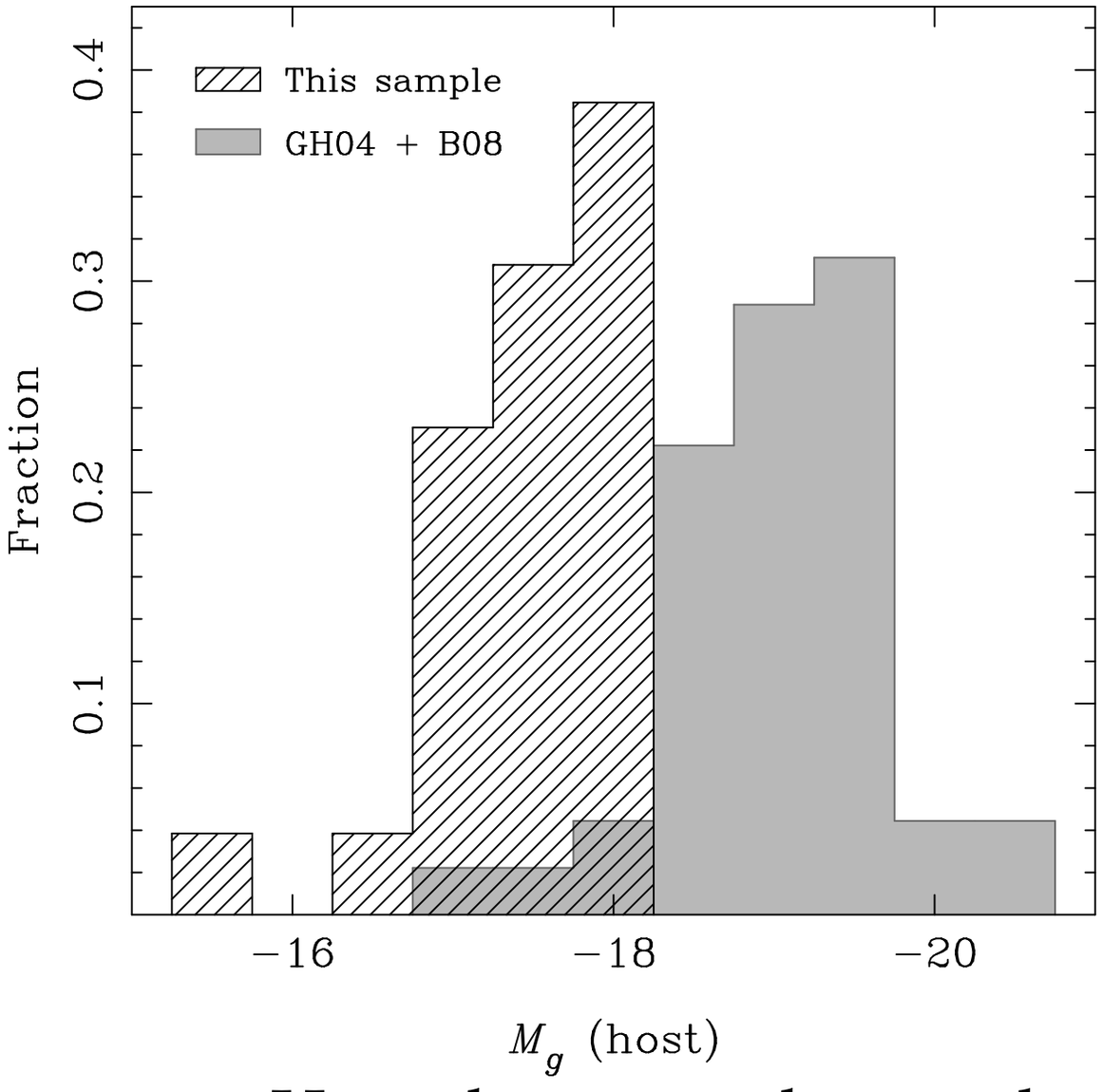

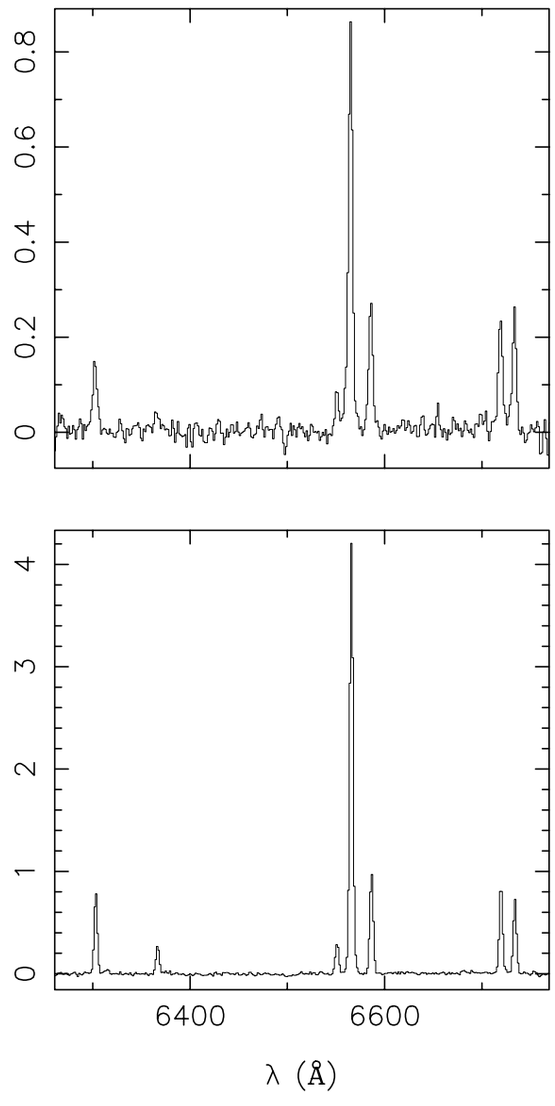

How about actual space densities of BHs with $M_{BH} < 10^6\ M_\odot$?

Moran et al. in prep

Black Hole Mass at Higher Redshift

Reverberation Mapping

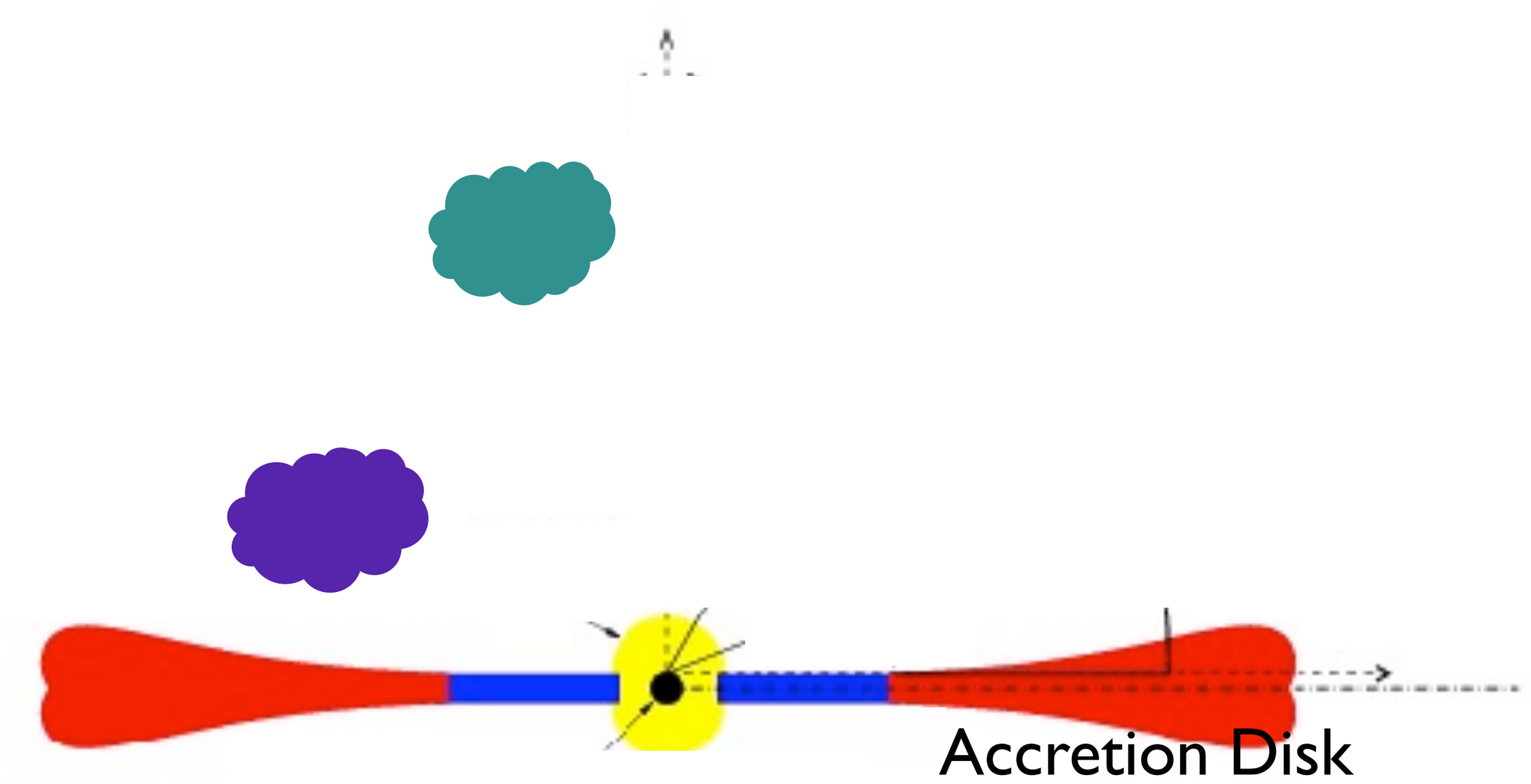

Reverberation Mapping

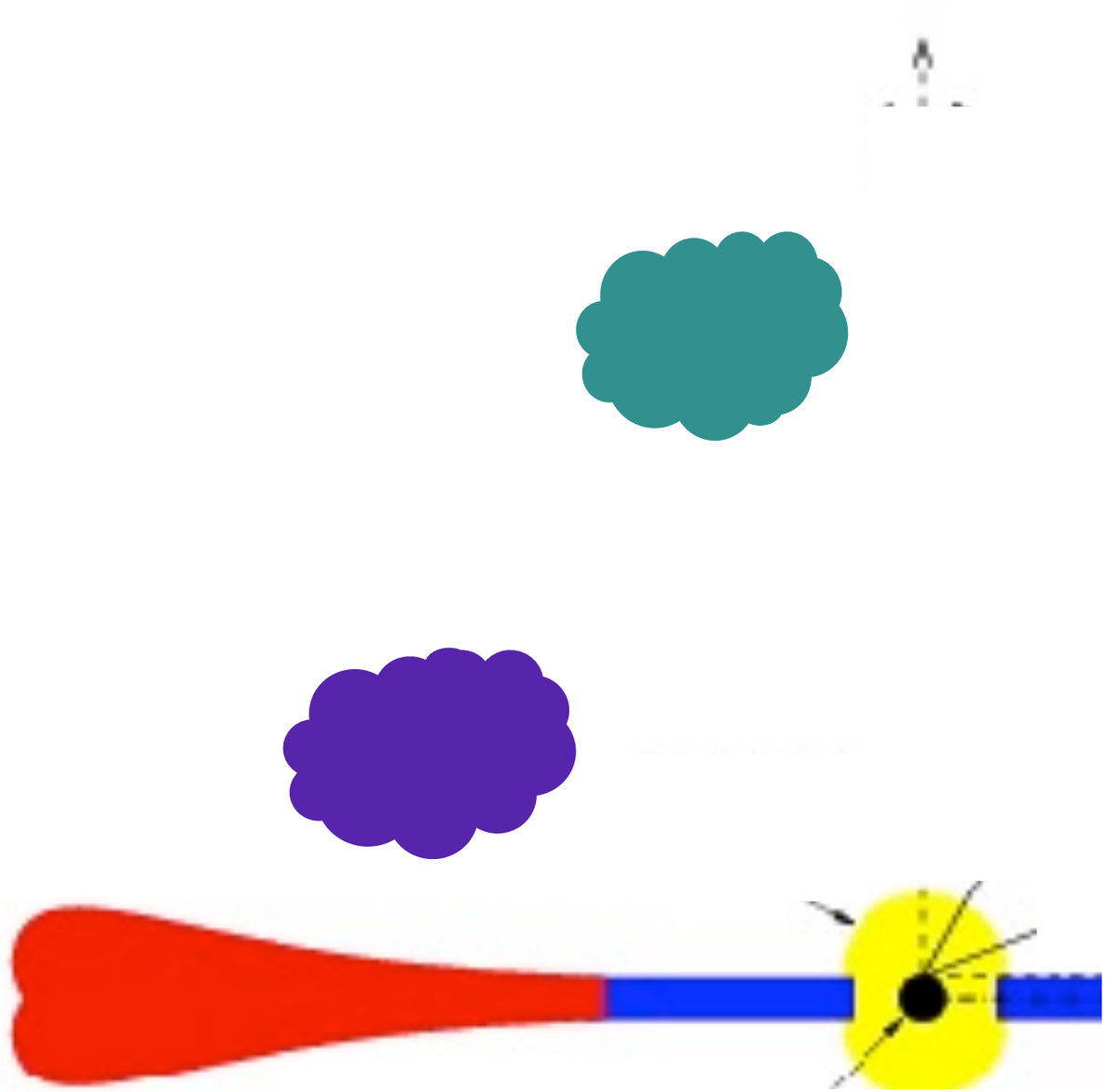

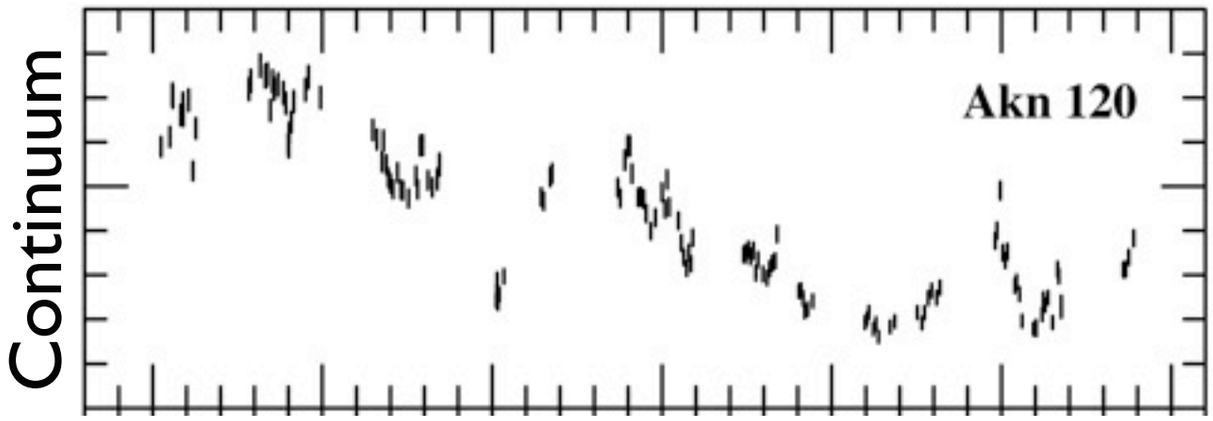

Reverberation Mapping

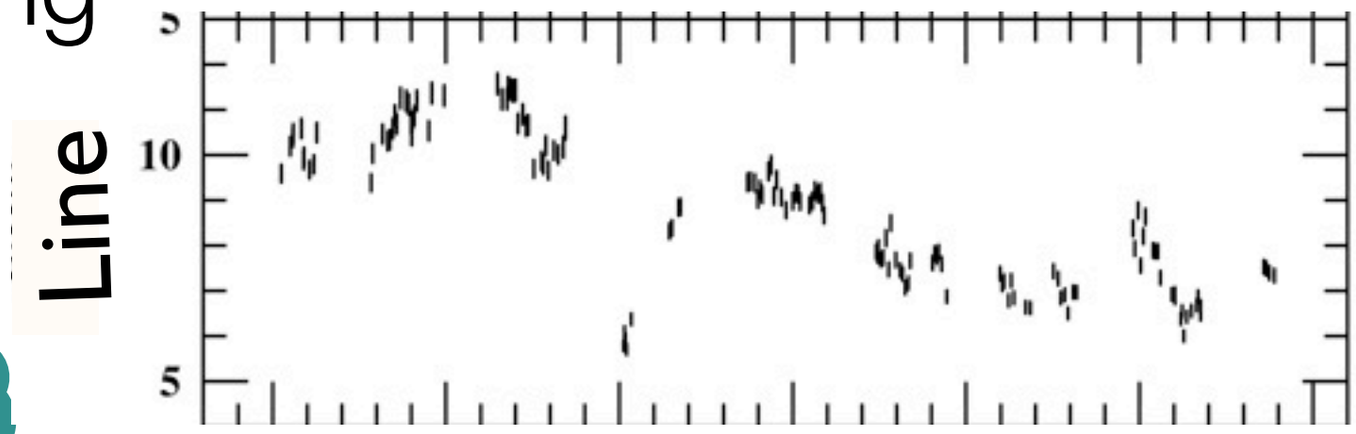

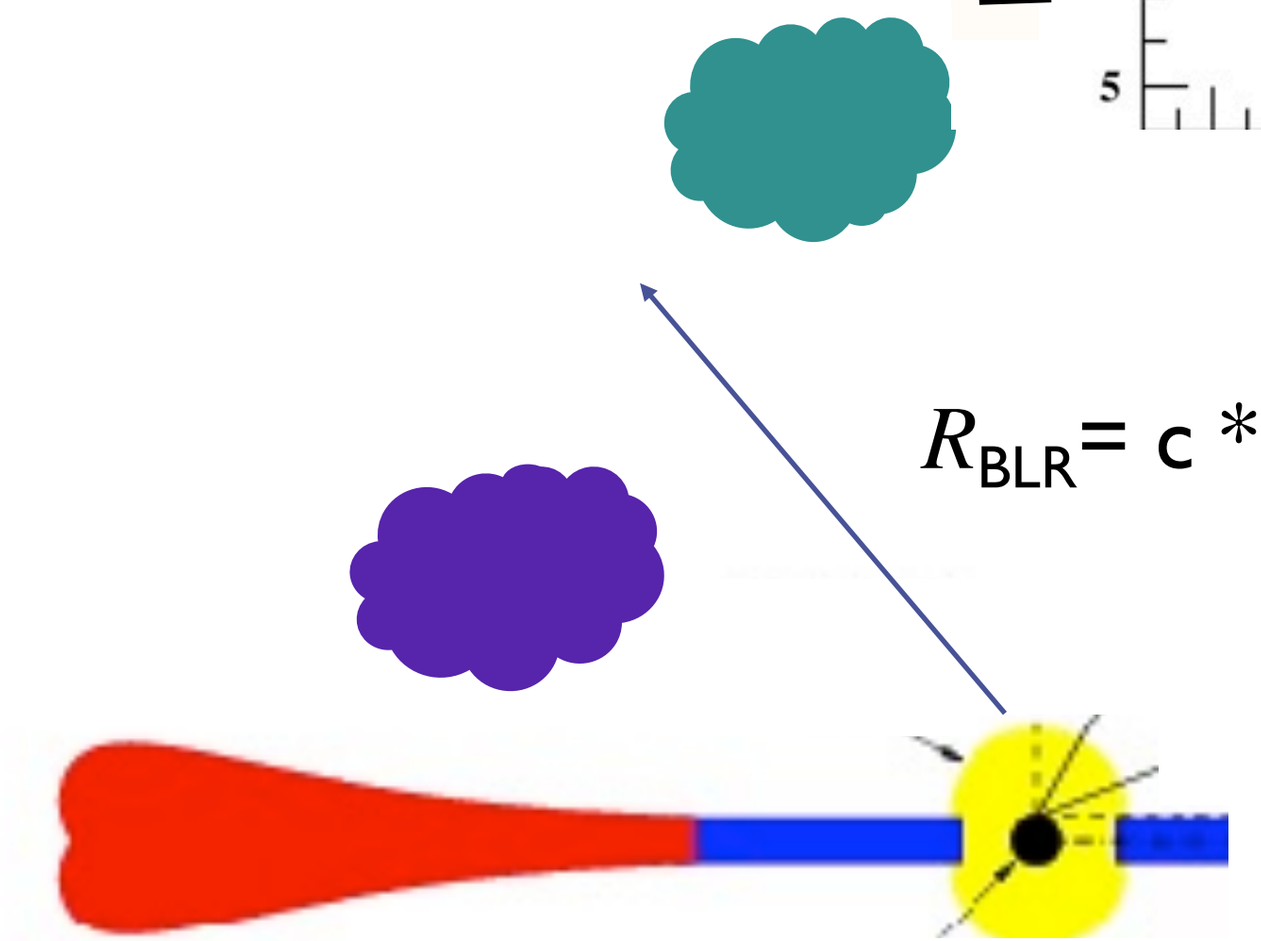

R_{BLR}= c * time-lag

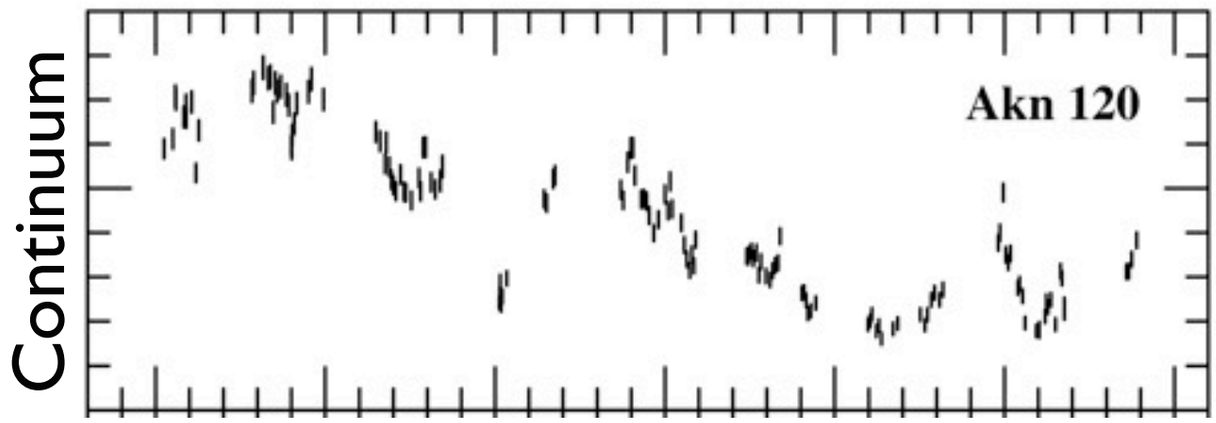

Time (days)

Lag (τ) between line and continuum variations

$R_{BLR} \sim c\,\tau$

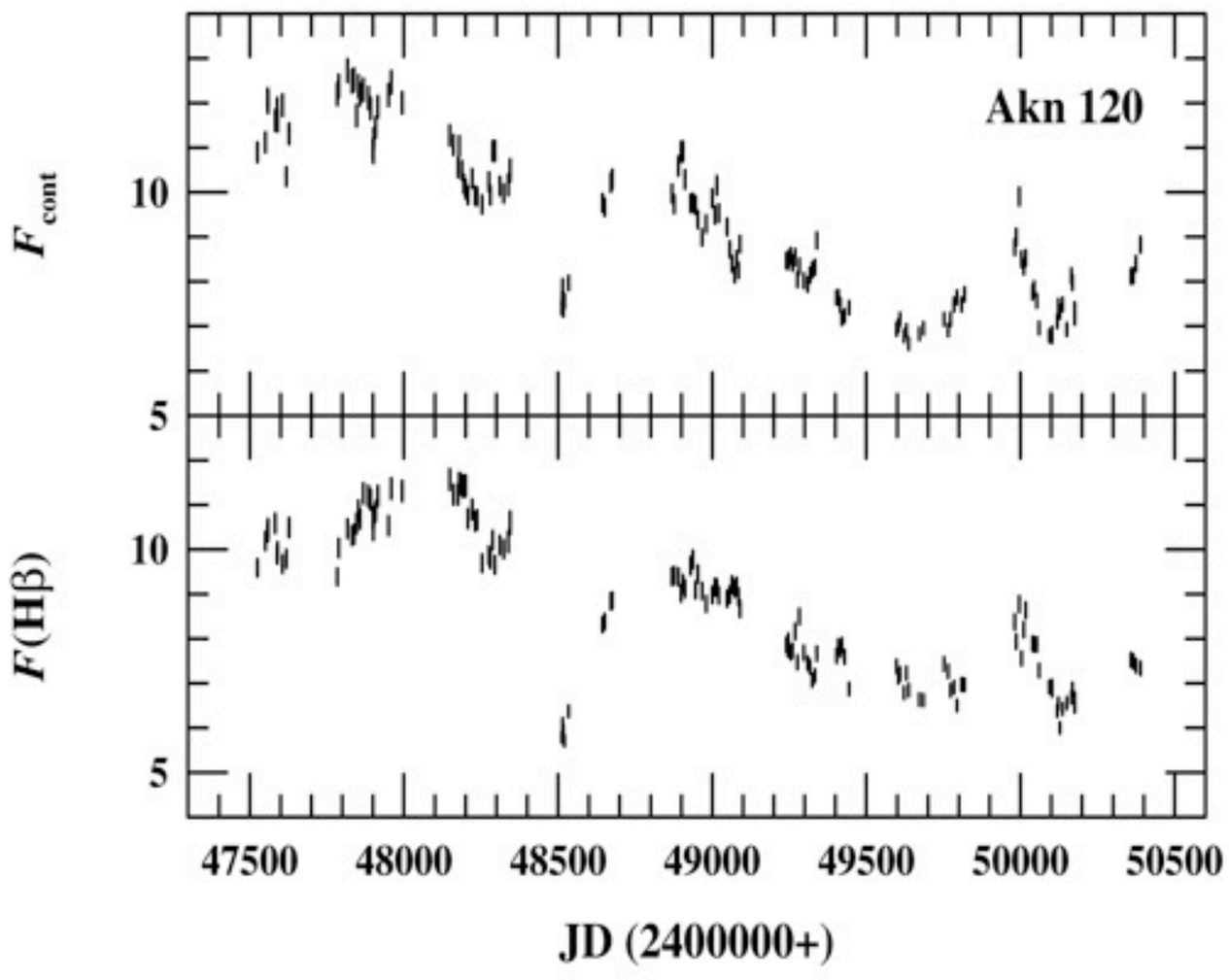

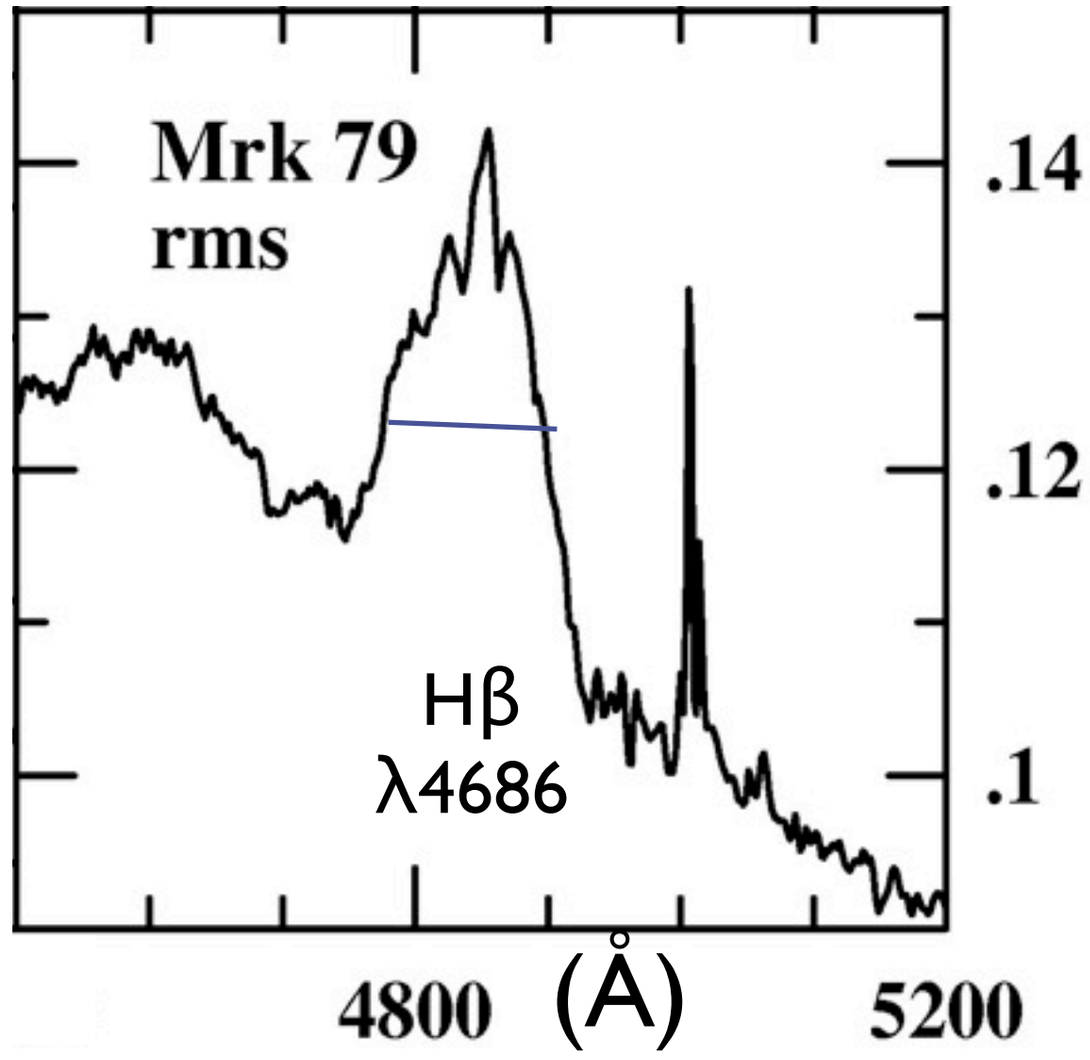

$$M_{BH} = f\, R_{BLR}\, \upsilon^2 / G$$

Can we believe them?

Gebhardt et al. 2000

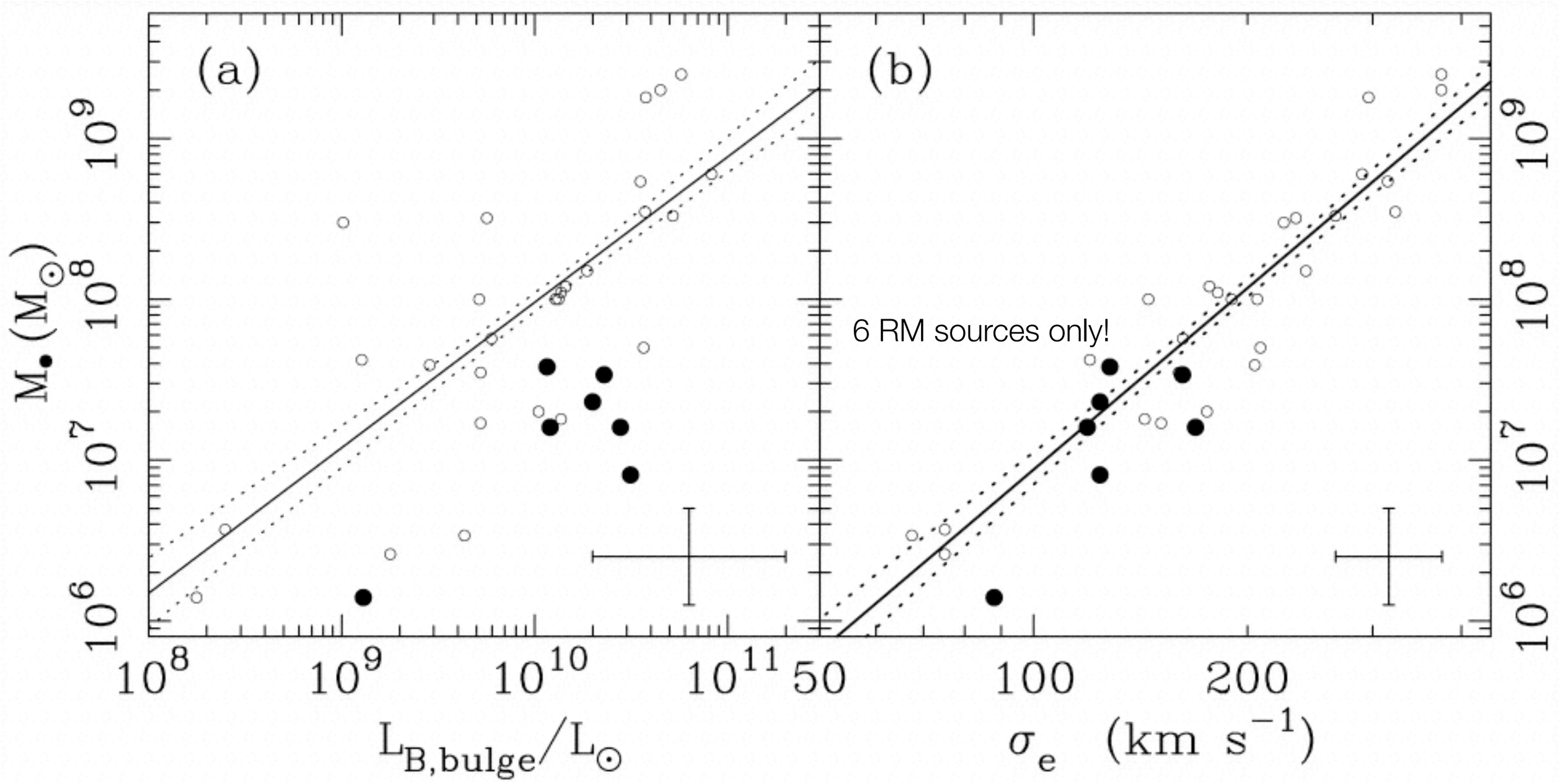

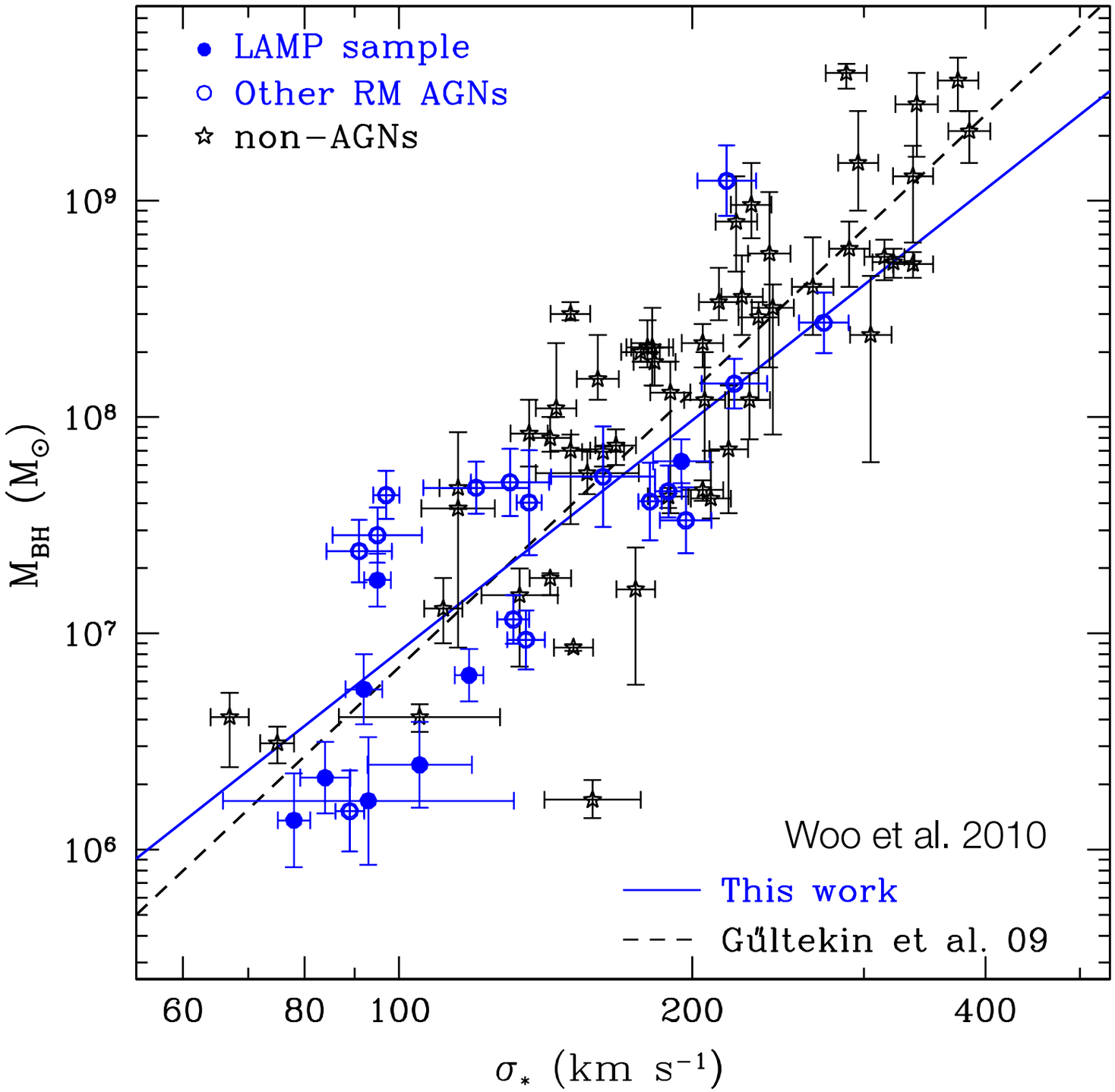

Lick AGN Monitoring Project (PI Barth). We reproduce the M_{BH}-$\sigma_\star$ relation with the RM sources...Dynamical masses are hard (Hicks et al., Davies et al., Onken et al.)

Radius-Luminosity Relation

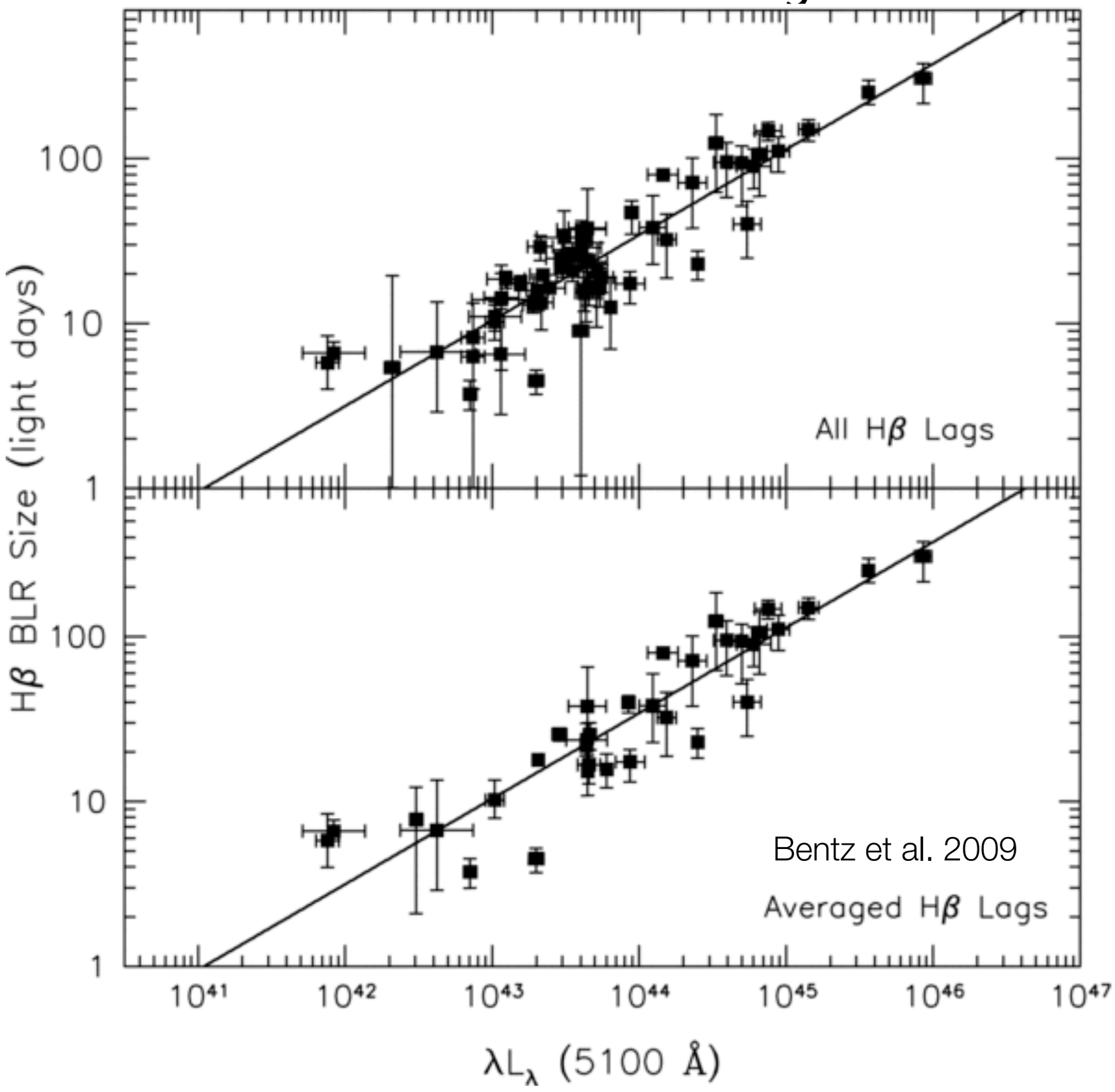

Lag (τ) between line and continuum variations

$R_{BLR} \sim c\,\tau$

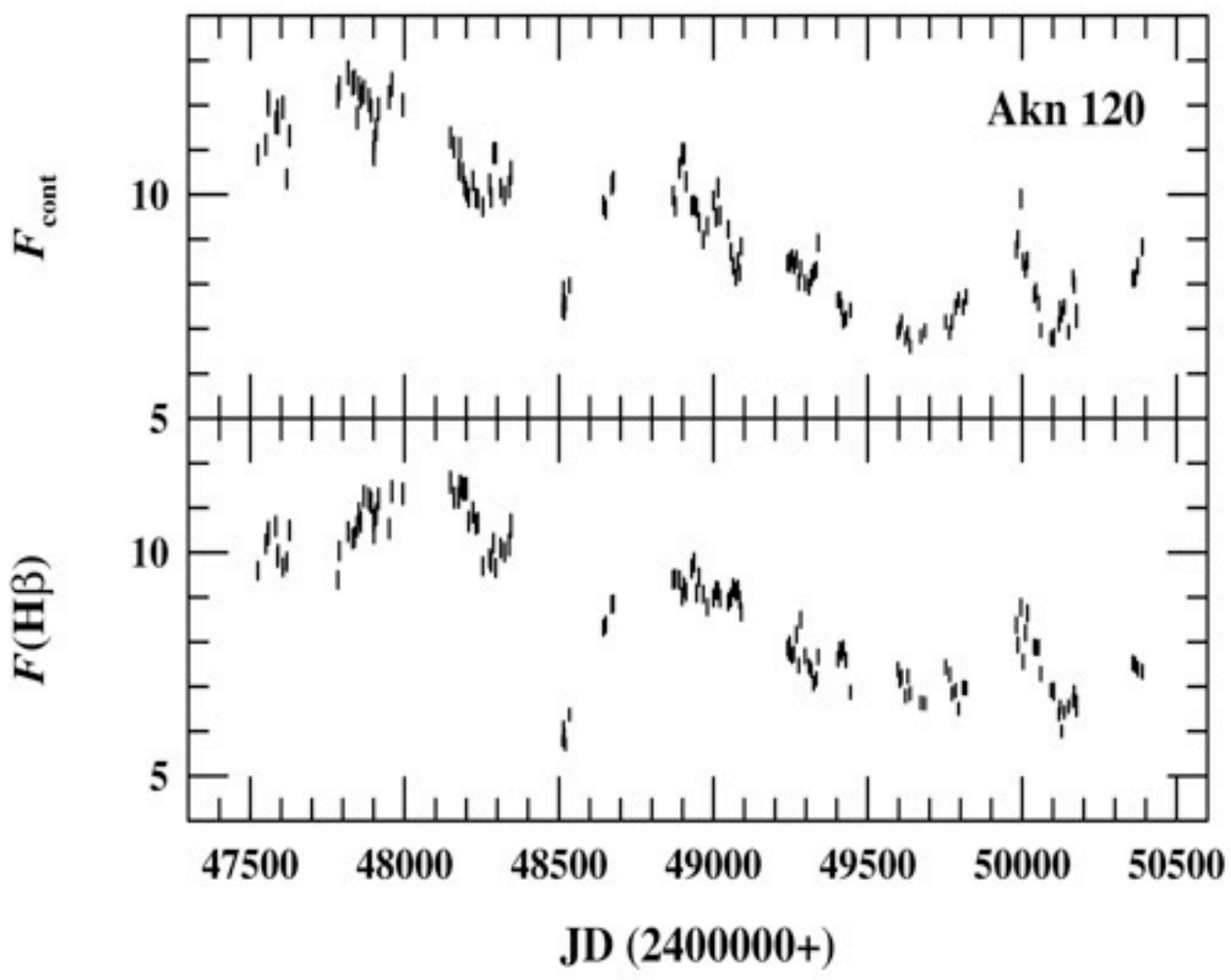

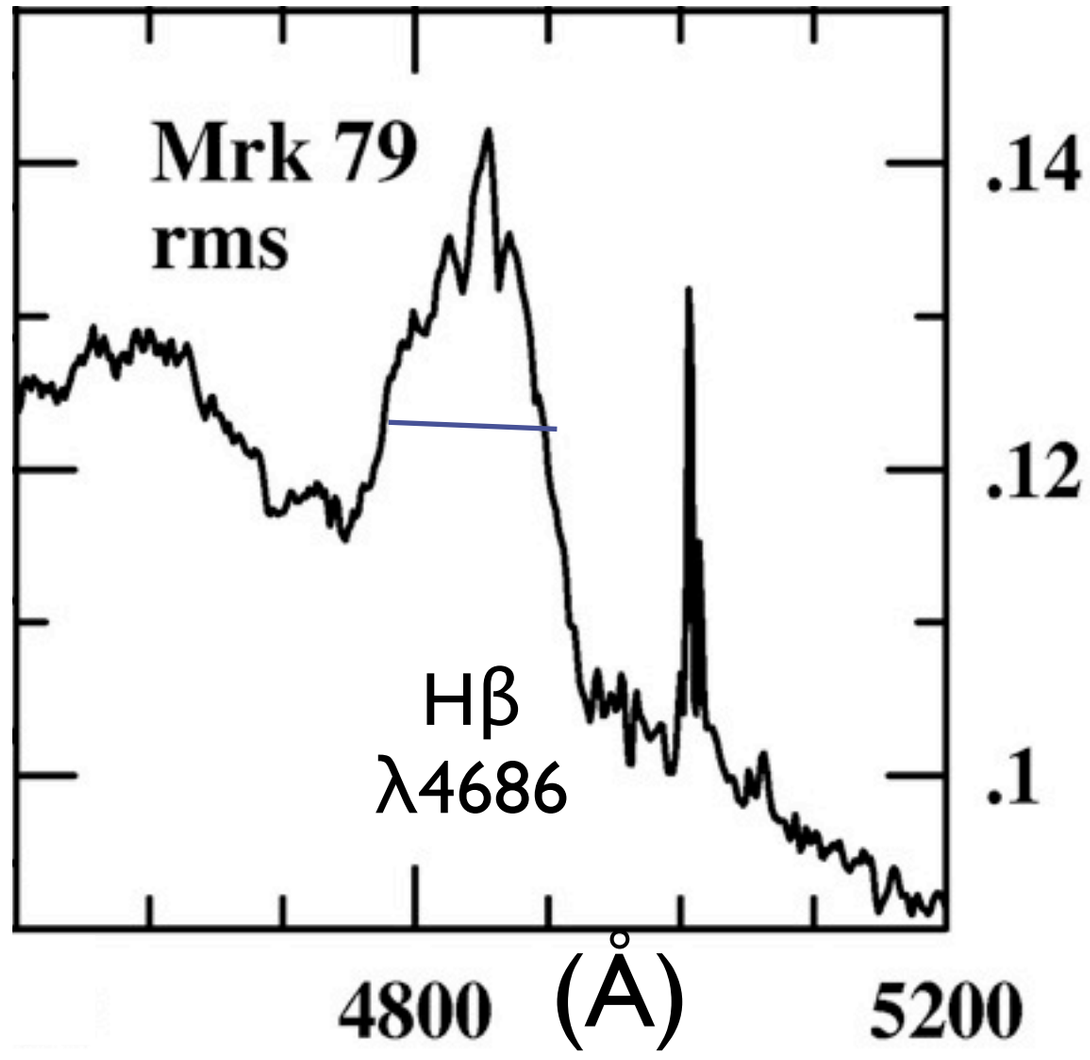

$$M_{BH} = f\, R_{BLR}\, \upsilon^2 / G$$

Now derive R from L.

Summary

Massive galaxies always make a central supermassive black hole. The situation remains unclear for lower-mass systems that sometimes but not always, host black holes.

We are building a strong case that these central massive dark objects are real black holes.

There are tight correlations between black hole mass and bulge properties.

But how tight are they? And how do the scaling relations depend on mass? What is the most massive black hole? What is the importance of galaxy morphology?

Can we see AGN feedback in action?

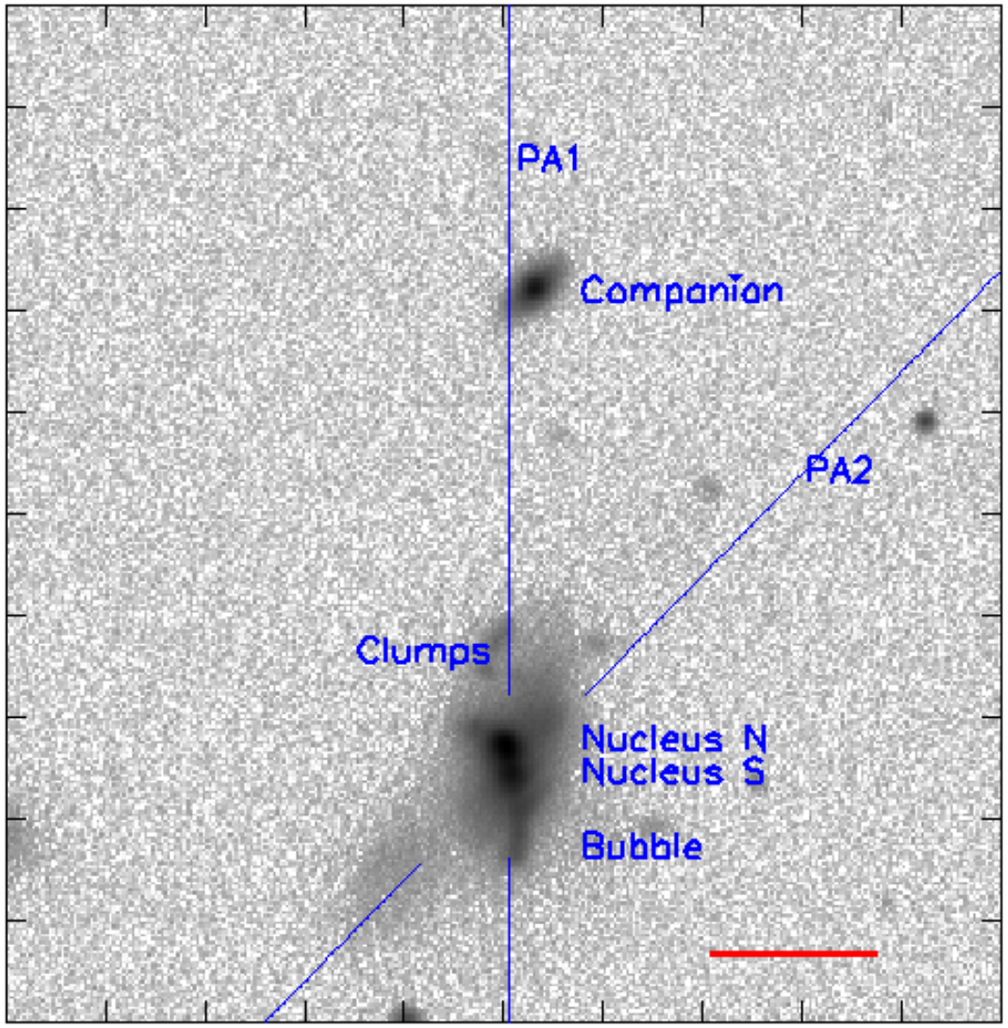

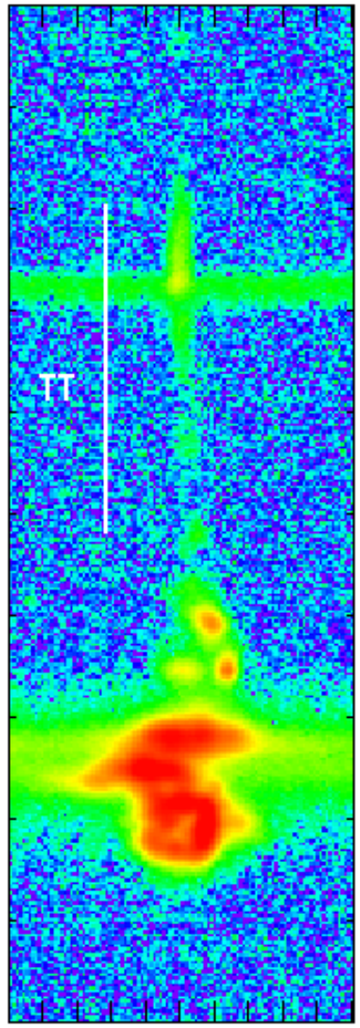

Greene, Zakamska, Smith 2012

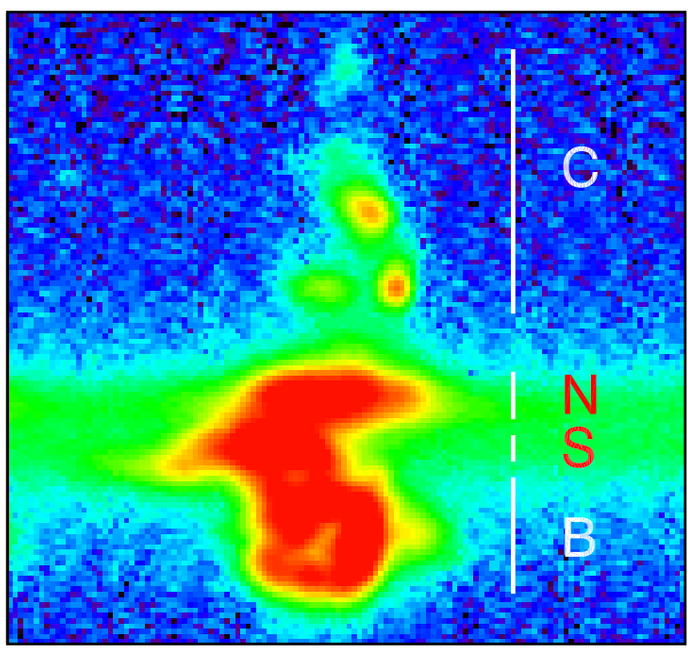

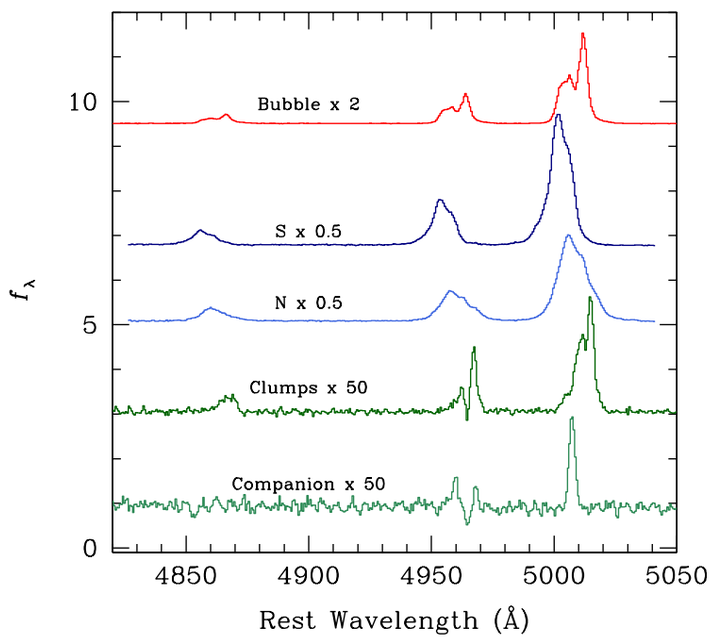

Energetics suggest $10^{45\text{-}46}$ erg/s kinetic luminosity. Very hard to achieve with the measured upper limit on the star formation rate.

This source has no radio jet. We argue it is the long-sought example of AGN feedback.

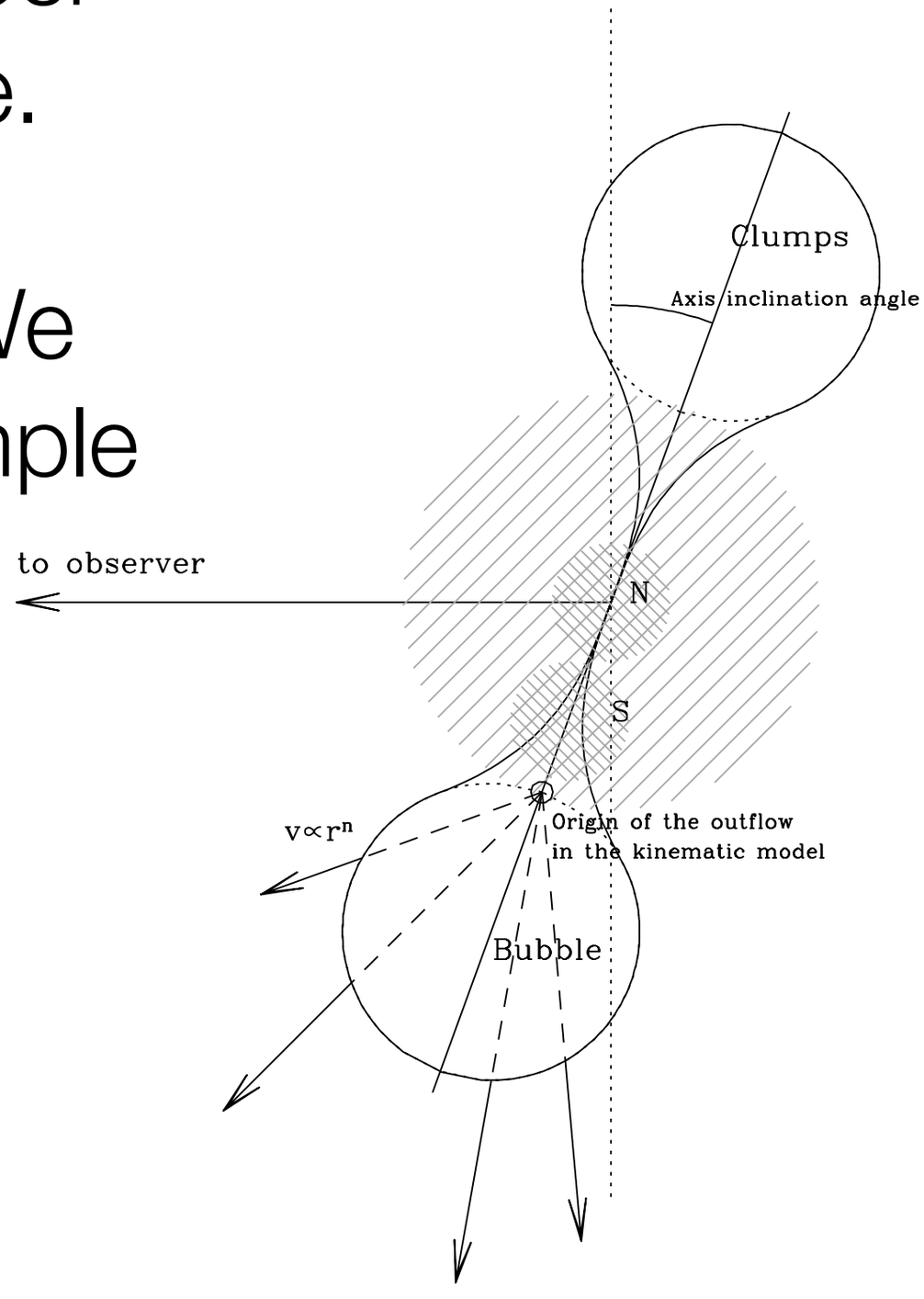

AGN Feedback?

At low z and low luminosity, only radio-jets are known to drive massive outflows (e.g., Stockton & Mackenty 1987).

We have finally found 20kpc outflows in z~0.5 obscured radio-quiet QSOs.

With GMT+NIR IFU+AO we can study the kinematics of ionized gas outflows in obscured and unobscured QSOs that are x100 more luminous at z~2 where all the action is. Actually test whether accreting black holes play a role in galaxy evolution.

Zakamska et al. in prep

Images in [OIII] emission line at different velocities:
-250 km/sec peak of [OIII] +250 km/sec

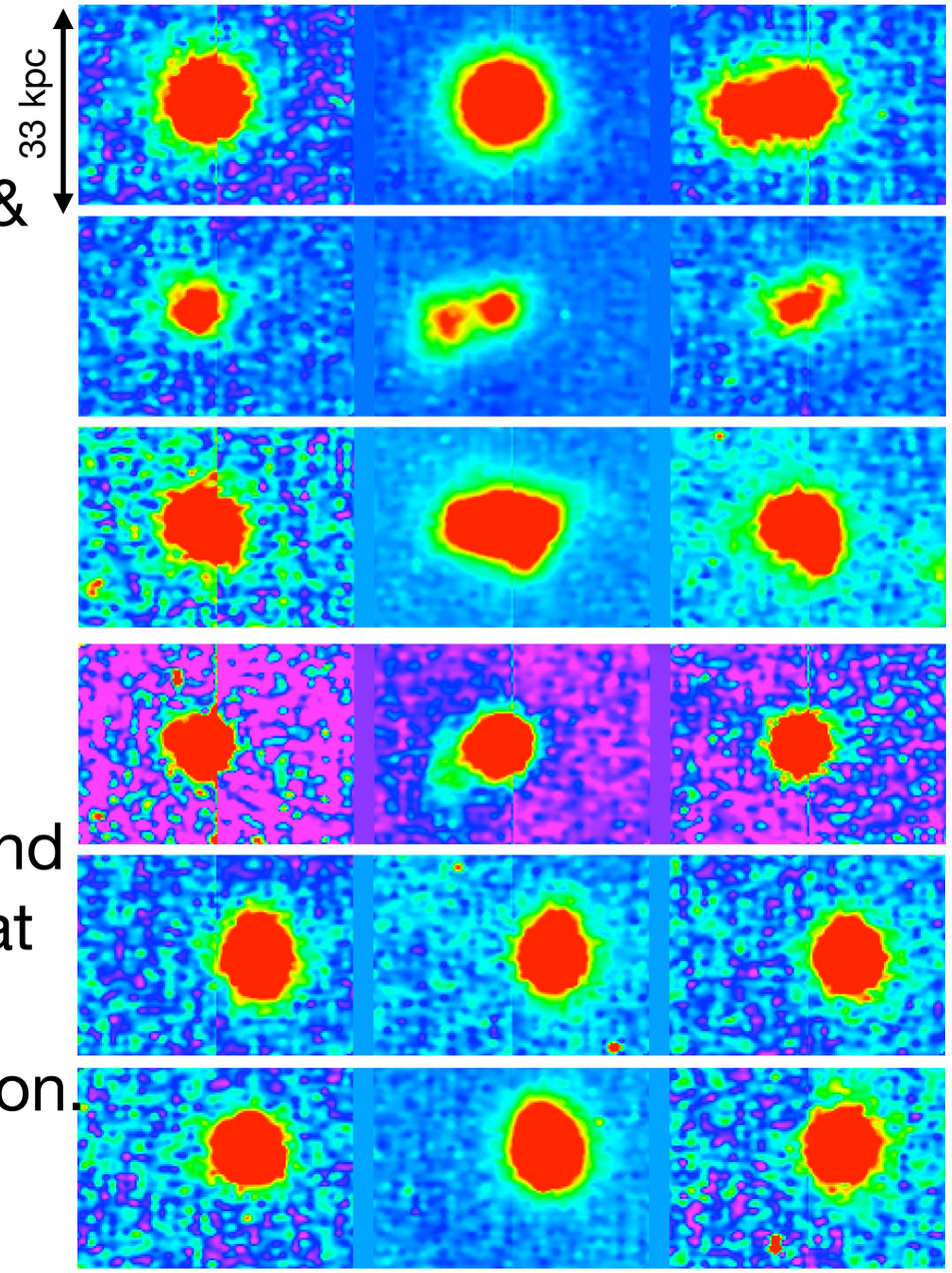

- Preliminary reductions
- Observed 14 z=0.5 quasars with GMOS IFU (Gemini-N), including 2 radio galaxies
- Extended ionized gas observed in every case
- In cases where emission is kinematically organized (e.g., symmetric around the nucleus) outflows are likely

Summary

Massive galaxies always make a central supermassive black hole. The situation remains unclear for lower-mass systems that sometimes but not always, host black holes.

We are building a strong case that these central massive dark objects are real black holes.

There are tight correlations between black hole mass and bulge properties.

But how tight are they? And how do the scaling relations depend on mass? What is the most massive black hole? What is the importance of galaxy morphology?